Numerische Mathematik (2019) 142:465–523
https://doi.org/10.1007/s00211-019-01044-8

Numerische Mathematik

Mesh and model adaptivity for frictional contact problems

Andreas Rademacher[1]

Received: 9 September 2015 / Revised: 6 December 2018 / Published online: 15 May 2019

Abstract
The article focuses on adaptive finite element methods for frictional contact problems. The approach is based on a reformulation of the mixed form of the underlying Signorini problem with friction as a nonlinear variational equation using nonlinear complimentarity functions. The usual dual weighted residual framework for a posteriori error estimation is applied. However, we have to take into account the nonsmoothness of the problem formulation. Error identities for measuring the discretization as well as the model error with respect to a model hierarchy of friction laws are derived and a method for the numerical evaluation of them is proposed. The estimates are utilized in an adaptive framework, which balances the discretization and the model error. Several numerical examples substantiate the accuracy of the proposed estimates and the efficiency of the adaptive method.

Mathematics Subject Classification 65N15 · 65N30 · 74G15 · 74S05 · 35J86

1 Introduction

In the modelling of many physical or engineering processes, contact problems with friction frequently occur, see, for instance, [22,37]. Hence, the development of efficient and accurate numerical solution techniques for frictional contact problems has been of special interest in the last decades. One main ingredient is given by efficient solution algorithms for the arising discrete problems. Furthermore, adaptive algorithms lead to an optimal convergence behavior of the discretizations, which cannot be achieved by uniform methods due to the missing regularity of frictional contact problems. They are based on accurate a posteriori error estimators, which should control the error in user-defined quantities of interest involving in our case the contact and frictional forces.

✉ Andreas Rademacher
andreas.rademacher@tu-dortmund.de

[1] Chair of Scientific Computing, Technische Universität Dortmund, Vogelpothsweg 87, 44227 Dortmund, Germany

In literature, the obstacle problem, as model contact problem, is frequently studied. A posteriori error estimates in the energy norm are derived, for instance, in [2,4,17,20,32,35,42,59] using different techniques. Even the convergence of adaptive algorithms in the context of obstacle problems is proven in [18,19,55]. Signorini's problem is studied, e.g., in [21,30,40,51,61], where a posteriori error estimates in the energy norm are discussed. Moreover, multibody contact problems are in the focus of [38,62]. The dual weighted residual (DWR) method, see, e.g., [3,5] is a popular approach to derive a posteriori error estimates, which control the error in user-defined quantities of interest. The approach is based on the representation of the quantity of interest by the solution of a so-called dual problem. Similar arguments are used in [45,46]. The DWR framework was applied to contact problems in [11,12] for the first time. The results are summarized in [58]. Here, a dual variational inequality is used to represent linear quantities of interest in the displacement. In [53], an alternative procedure is used, which is based on a linear dual problem representing also nonlinear quantities of interest in the displacement. It is extended to frictional contact problems and quantities of interest also in the Lagrange multiplier in [48]. There, a linear mixed dual problem, which does not depend on the primal problem, is used to represent the quantities of interest in the displacement as well as the Lagrange multiplier, which coincides with the contact forces. This approach also leads to an improved localization of the error estimate. In both approaches, the (frictional) contact conditions lead to extra additive terms in the estimates, which is some product of the dual solution and the error of the primal solution. However, the estimates do not directly measure the error in the (frictional) contact conditions and the accurate numerical approximation of the extra terms include several difficulties, which lead to involved and numerically costly algorithms. In [47], an approach is presented, which overcomes these drawbacks for Signorini's problem. Its starting point is a reformulation of Signorini's problem in mixed formulation as a nonlinear and nonsmooth variational equality based on a nonlinear complementarity (NCP) function, see, for instance, [31]. Here, the dual problem is also a linear mixed problem. However, it is determined by the active and inactive set of the primal problem. The usual error identities can be derived based on the DWR framework. However, the nonsmoothness of the underlying problem leads to remainder terms, which are of first order in the error of the discrete active set. Here, we extend this approach to frictional contact problems. The first step is the reformulation of the mixed problem using an NCP function as nonlinear variational equality, where we use the results presented in [33]. Since the NCP function for friction includes combinations of nonlinear functions in contrast to the one for contact, the derivation is more complex and leads to several remainder terms. The basic idea is to seperate the smooth and nonsmooth parts using fixed active sets. The results presented in this article can be applied on a wide range of discretization schemes. For mixed discretization schemes like [27,34], the application of the developed framework is straight forward. If semi-smooth Newton methods are used for solving the discrete contact problem, the dual problem coincide with the transposed system of the last Newton step. In displacement based discretization schemes like [9,39,64], an approximation to the Lagrange multiplier has to be calculated in a post processing step, cf., e.g., [17]. The derived error identities cannot be evaluated numerically. Thus, a numerical approximation scheme depending on the different discretization approaches has

to be realized. We exemplify such a strategy for the mixed discretization introduced in [27].

The performance of the solution algorithm of frictional contact problems depends on the chosen friction model. One can save a large amount of computation time and gain a more stable algorithm by choosing a different model. The idea is now to select the model out of a predefined model hierarchy based on an a posteriori error estimate corresponding to the desired accuracy. In literature, one finds only few contributions to model adaptive algorithms. Dimension adaptivity is considered in [1,8,13,56,57]. In these papers, volume elements are combined with shells or plates. The automatic selection of the local model is one subject in [43,44], where heterogeneous linear elastic models and their homogenization are included in the model hierarchy. The underlying a posteriori error estimates include the error in the energy norm as well as in linear quantities of interest. Models for different physical processes are adaptively coupled in [41] by means of problems from electrocardialogy. The basic DWR idea is extended to control modelling errors in [15]. Here, the model error is basically given by entering the solution to the coarse model into the fine one weighted by the dual solution. In [15], diffusion-reaction-equations with highly oscillating coeffients are considered. Further applications are given by time dependent problems in [16] as well as by problems from elasticity in [25]. In this article, we use the ideas from [15] to derive a posteriori estimates of the model error with respect to different friction laws, where the nonsmoothness of the underlying problems complicates the derivation. In the model adaptive algorithm, we globally balance the model and the discretization error, which cannot be done locally due to the structure of the problem.

The article is structured as follows: In Sect. 2, we introduce the strong and the mixed formulation of Signorini's problem with friction as well as the reformulation as a nonlinear variational equation. Furthermore, the assumptions on the model adaptive discretization are formulated. Section 3 focuses on the derivation of the error identities involving the model as well as the discretization error. At first, we consider the model and the discretization error, seperately. Afterwards, an identity for both is derived. In Sect. 4, we outline the ideas for the numerical approximation of the error identites and exemplify them for a concrete mixed discretization. Section 5 is devoted to numerical results, which substantiate the accuracy of the presented error estimates and the efficiency of the adaptive schemes. We conclude the article with a discussion of the results and an outlook on further tasks.

2 Problem formulation

In this section, we introduce the continuous problem formulation and a general model adaptive discretization.

2.1 Continuous problem formulation

We consider Signorini's problem with nonlinear friction laws on domains $\Omega \subset \mathbb{R}^d$, $d = 2, 3$ with sufficiently smooth boundary $\Gamma := \partial\Omega$. Homogeneous Dirichlet

boundary conditions are assumend on $\Gamma_D \subset \Gamma$, where Γ_D is closed with positive measure. The possible contact boundary is given by $\Gamma_C \subset \Gamma \backslash \Gamma_D$ with $\overline{\Gamma}_C \subsetneq \Gamma \backslash \Gamma_D$. Furthermore, we have the part $\Gamma_N = \Gamma \backslash (\Gamma_D \cup \Gamma_C)$, where Neumann boundary conditions are required. The usual Sobolev spaces are denoted by $L^2(\Omega)$, $H^l(\Omega)$ with $l \geq 1$, and $H^{1/2}(\Gamma_C)$. We set

$$H_D^1(\Omega) := \left\{ v \in H^1(\Omega) \,|\, \gamma(v) = 0 \text{ on } \Gamma_D \right\}$$

and $V := \left(H_D^1(\Omega)\right)^d$ with the trace operator γ. The topological dual space of $H^{1/2}(\Gamma_C)$ is given by $\tilde{H}^{-1/2}(\Gamma_C)$ with the norms $\|\cdot\|_{-1/2,\Gamma_C}$ and $\|\cdot\|_{1/2,\Gamma_C}$, respectively. The L^2-scalar products on $\omega \subset \Omega$ and $\Gamma' \subset \Gamma$ are denoted by $(\cdot,\cdot)_{0,\omega}$ and $(\cdot,\cdot)_{0,\Gamma'}$. The linear and bounded mapping $\gamma_C := \gamma_{|\Gamma_C} : H_D^1(\Omega) \to H^{1/2}(\Gamma_C)$ is surjective due to the assumptions on Γ_C, see [37, page 88]. We define $\mathbf{v}_n := \gamma_C(\mathbf{v})\mathbf{n}$ and $\mathbf{v}_{t,j} := \gamma_C(\mathbf{v})\mathbf{t}_j$, where $\mathbf{n}$ denotes the vector-valued function describing the outer unit normal vector with respect to Γ and $\mathbf{t}$ the $d \times (d-1)$-matrix-valued function containing an orthonormal basis of the tangential space. In the following, we use the inequality symbols $\geq$ and $\leq$ for functions in $L^2(\Gamma_C)$, where the symbols are defined as "almost everywhere". We set $H_+^{1/2}(\Gamma_C) := \left\{ v \in H^{1/2}(\Gamma_C) \middle| v \geq 0 \right\}$. The dual cone of $H_+^{1/2}(\Gamma_C)$ is

$$\Lambda_n := \left\{ \mu \in \tilde{H}^{-1/2}(\Gamma_C) \middle| \forall v \in H_+^{1/2}(\Gamma_C) : \ \langle \mu, v \rangle \geq 0 \right\}.$$

Furthermore, we set

$$\Lambda_t\left(\lambda_n^r\right) := \left\{ \mu \in \left(\tilde{H}^{-1/2}(\Gamma_C)\right)^{d-1} \middle| \langle \mu, v_t \rangle \leq \left\langle s^r\left(\lambda_n^r\right), |v_t| \right\rangle, \ v_t \in \left(H^{1/2}(\Gamma_C)\right)^{d-1} \right\}$$

with the euclidian norm $|\cdot|$. Here, $s^r : \Lambda_n \to \Lambda_n$ denotes the possible nonlinear friction law. The index r stands for reference friction law, its meaning will be clarified in the discussion of the model adaptive approach. For a given displacement field $\mathbf{v} \in V$, the linearized strain tensor is defined as $\boldsymbol{\varepsilon}(\mathbf{v}) := \frac{1}{2}\left(\nabla \mathbf{v} + (\nabla \mathbf{v})^\top\right)$ and the stress tensor as $\boldsymbol{\sigma}(\mathbf{v})_{ij} := \mathscr{C}_{ijkl}\boldsymbol{\varepsilon}(\mathbf{v})_{kl}$ describing a linear-elastic material law with $\mathscr{C}_{ijkl} \in L^\infty(\Omega)$, $\mathscr{C}_{ijkl} = \mathscr{C}_{jilk} = \mathscr{C}_{klij}$ and $\mathscr{C}_{ijkl}\boldsymbol{\tau}_{ij}\boldsymbol{\tau}_{kl} \geq \kappa \boldsymbol{\tau}_{ij}^2$ for $\boldsymbol{\tau} \in L^2(\Omega)^{d\times d}_{\text{sym}}$ and a $\kappa > 0$. We define $\boldsymbol{\sigma}_n := \boldsymbol{\sigma}\mathbf{n}$, $\boldsymbol{\sigma}_{nn} := \mathbf{n}^\top \boldsymbol{\sigma}\mathbf{n}$, $\boldsymbol{\sigma}_{nt,l} := \mathbf{t}_l^\top \boldsymbol{\sigma}\mathbf{n}$.

The strong formulation of Signorini's problem with friction is to find a displacement field $\mathbf{u}^r \in V \cap H^2(\Omega)$ such that

$$-\operatorname{div}\left(\boldsymbol{\sigma}\left(\mathbf{u}^r\right)\right) = \mathbf{f} \text{ in } \Omega, \quad \boldsymbol{\sigma}_n\left(\mathbf{u}^r\right) = \mathbf{b} \text{ on } \Gamma_N, \tag{1}$$

$$\mathbf{u}_n^r - g \leq 0, \ \boldsymbol{\sigma}_{nn}^r \leq 0, \ \boldsymbol{\sigma}_{nn}^r\left(\mathbf{u}_n^r - g\right) = 0 \text{ on } \Gamma_C, \tag{2}$$

$$\left|\boldsymbol{\sigma}_{nt}^r\right| \leq s^r\left(\boldsymbol{\sigma}_{nn}^r\right) \text{ with } \left\{ \begin{array}{l} \left|\boldsymbol{\sigma}_{nt}^r\right| < s^r\left(\boldsymbol{\sigma}_{nn}^r\right) \Rightarrow \mathbf{u}_t^r = 0 \\ \left|\boldsymbol{\sigma}_{nt}^r\right| = s^r\left(\boldsymbol{\sigma}_{nn}^r\right) \Rightarrow \exists \zeta \in \mathbb{R}_{\geq 0} : \mathbf{u}_t^r = -\zeta \boldsymbol{\sigma}_{nt}^r \end{array} \right\} \text{ on } \Gamma_C. \tag{3}$$

The equilibrium equation of linear elasticity is noted in (1), where the volume and surface loads are specified by $\mathbf{f}$ and $\mathbf{b}$. In the following weak formulation, we assume $\mathbf{f} \in \left(L^2(\Omega)\right)^d$, $\mathbf{b} \in \left(L^2(\Gamma_N)\right)^d$. The geometrical contact conditions are described in (2). The possible contact boundary Γ_C is parametrized by a sufficiently smooth function $\boldsymbol{\varphi} : \mathbb{R}^{d-1} \to \mathbb{R}$ such that, without loss of generality, the geometrical contact condition for a displacement field $\mathbf{v}$ in the d-th component is given by

$$\boldsymbol{\varphi}(\mathbf{x}) + \mathbf{v}_d(\mathbf{x}, \boldsymbol{\varphi}(\mathbf{x})) \leq \psi(\mathbf{x}_1 + \mathbf{v}_1(\mathbf{x}, \boldsymbol{\varphi}(\mathbf{x})), \ldots, \mathbf{x}_{d-1} + \mathbf{v}_{d-1}(\mathbf{x}, \boldsymbol{\varphi}(\mathbf{x})))$$

with $\mathbf{x} := (x_1, \ldots, x_{d-1}) \in \mathbb{R}^{d-1}$. The sufficiently smooth function ψ describes the surface of the rigid obstacle. The linearization, presented for instance in [37, Chapter 2], of this condition results in $\mathbf{v}_n \leq g$ in (2) with

$$g(x) := (\psi(\mathbf{x}) - \varphi(\mathbf{x}))(1 + (\nabla\boldsymbol{\varphi}(\mathbf{x}))^\top \nabla\boldsymbol{\varphi}(\mathbf{x}))^{-1/2}.$$

In the weak formulation, we assume $g \in H^{1/2}(\Gamma_C)$. The second condition, a sign condition on the outer normal stress, ensures that only pressure occurs. By the complementary condition in (2), we have either pressure or no contact. The frictional conditions are denoted in (3). They indicate that sticking occurs if the magnitude of the tangential forces is below a critical value given by the friction law s^r. If this critical value is reached, we obtain sliding, where the sliding direction corresponds to the negative direction of the tangential forces. Some examples of friction laws are given in Table 1, see, for instance, [65, Section 4.2]. They are illustrated in Fig. 1a. Let us briefly comment on the physical background of friction especially in the context of metal forming, cf. for instance [29, Section 3.2]. For Bowden and Tabor, the source of friction lies in adhesion forces between the contacting surfaces, see [14]. They postulate that s^r is proportional to the real contact surface ratio

$$\alpha_{\text{real}} = \frac{\text{meas}\,(A_{\text{real}})}{\text{meas}\,(A_0)}.$$

Here A_0 denotes the whole macroscopic contact surface neglecting microscopic effects like the surface roughness. On the other hand, the real microscopic contact surface is denoted by A_{real}. Due to surface roughness, A_{real} is smaller than A_0 and approaches A_0 for high contact pressure. Experimental investigations show that α_{real} depends linearly on the contact pressure $\boldsymbol{\sigma}^r_{nn}$, if $\boldsymbol{\sigma}^r_{nn}$ is small, leading to Coulomb's law s_2. Furthermore, α_{real} approaches 1 for large $\boldsymbol{\sigma}^r_{nn}$ leading to Tresca's friction law s_1 as limiting case. In [54], a smooth transition between these two cases is proposed. Using the ideas of [6], this behavior can be modeled by the friction law s_3 for instance. It is a mathematical approach to fit both limiting cases and the smooth transition demand. However, it has no physical basis. For our analysis, we assume that the considered friction laws are two times continuously differentiable w.r.t. $\boldsymbol{\sigma}^r_{nn}$. We have ordered the friction laws in Table 1 by there mathematical complexity and use this linear structure in the derivation of the a posteriori error estimates, where it is reasonable. However, as outlined before, the laws of Tresca and Coulomb are the two limiting cases of the one of Betten. From a model adaptive point of view, they should not be treated in

Table 1 Some examples of friction laws ordered by complexity

Formula	Name
$s_0(\boldsymbol{\sigma}_{nn}) = 0$	Frictionless contact
$s_1(\boldsymbol{\sigma}_{nn}) = C_T$	Tresca friction with a constant $C_T > 0$
$s_2(\boldsymbol{\sigma}_{nn}) = -\mathscr{F}\boldsymbol{\sigma}_{nn}$	Coulomb friction with a constant $\mathscr{F} > 0$
$s_3(\boldsymbol{\sigma}_{nn}) = C_T \sqrt[n]{\tanh\left(\left(\frac{-\mathscr{F}\boldsymbol{\sigma}_{nn}}{C_T}\right)^n\right)}$	Friction law of Betten with $n \in \mathbb{N}$

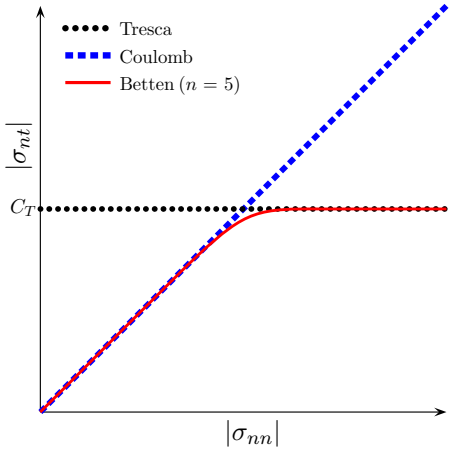

(a) Illustration of different friction laws

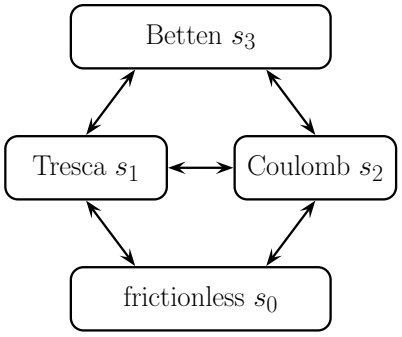

(b) Ordering of the different friction laws in the model adaptive algorithm

Fig. 1 Illustration of the considered friction laws and there ordering in the model adaptive algorithm

the proposed hierarchical way. It is more appropriate to used the structure presented in Fig. 1b. We consider three levels of models. The first level, the coarsest level, is given by frictionless contact. On level 2, the limiting cases of Tresca and Coulomb are collected, while level 3 contains the most general model of Betten. The details of the model adaptive algorithm are described in Sect. 5.3. However, it should be remarked that the hierarchy used for the a posteriori error estimation and the model adaptive algorithm may differ without causing any problems.

For the a posteriori error analysis, we use a mixed formulation of (1–3). The bilinear form of linear elasticity is given by $a(\mathbf{w}, \mathbf{v}) := (\boldsymbol{\sigma}(\mathbf{w}), \boldsymbol{\varepsilon}(\mathbf{v}))_0$ on $V \times V$, which is symmetric, continuous and due to Korn's inequality V-elliptic. The volume and surface loads are represented by $\langle \ell, \mathbf{v} \rangle := (\mathbf{f}, \mathbf{v})_0 + (\mathbf{b}, \mathbf{v})_{0,\Gamma_N}$. A function $\mathbf{w}^r := \left(\mathbf{u}^r, \lambda_n^r, \boldsymbol{\lambda}_t^r\right) \in V \times \Lambda_n \times \Lambda_t\left(\lambda_n^r\right)$ is a saddle point of the frictional contact problem (1–3) if and only if,

$$a\left(\mathbf{u}^r, \mathbf{v}\right) + \langle \lambda_n^r, \mathbf{v}_n \rangle + \left\langle \boldsymbol{\lambda}_t^r, \mathbf{v}_t \right\rangle = \langle \ell, \mathbf{v} \rangle, \tag{4}$$

$$\langle \mu_n - \lambda_n^r, \mathbf{u}_n^r - g \rangle + \left\langle \boldsymbol{\mu}_t - \boldsymbol{\lambda}_t^r, \mathbf{u}_t^r \right\rangle \leq 0, \tag{5}$$

for all $\mathbf{v} \in V$, all $\mu_n \in \Lambda_n$, and all $\boldsymbol{\mu}_t \in \Lambda_t$. If some smoothness assumptions are fulfilled, it holds $\lambda_n^r = -\boldsymbol{\sigma}_{nn}^r$ and $\boldsymbol{\lambda}_t^r = -\boldsymbol{\sigma}_{nt}^r$. The existence and uniqueness of the solution $\mathbf{w}^r$ depends on the chosen friction law s^r and its parameters. For Tresca's and Coulomb's friction law with $\mathscr{F}$ small enough, there exists a weak solution, which is uniquely determined in the case of Tresca friction. We refer to [23] for an overview on existence and uniqueness results.

We now reformulate the frictional contact conditions (5) in terms of two nonlinear equations. The geometrical contact conditions are equivalently expresed by

$$g - \mathbf{u}_n^r \in H_+^{1/2}(\Gamma_C), \quad \lambda_n^r \in \Lambda_n, \quad \left\langle \lambda_n^r, \mathbf{u}_n^r - g \right\rangle = 0. \tag{6}$$

Assuming $\lambda_n^r \in L^2(\Gamma_C)$, (6) simplifies to

$$g - \mathbf{u}_n^r \in H_+^{1/2}(\Gamma_C), \quad \lambda_n^r \geq 0 \text{ a.e. on } \Gamma_C, \quad \lambda_n^r \left(\mathbf{u}_n^r - g\right) = 0 \text{ a.e. on } \Gamma_C. \tag{7}$$

For geometrical contact problems, we have $\lambda_n^r \in L^2(\Gamma_C)$ for instance, if $g \in H^{5/2}(\Gamma_C)$ and $\mathscr{C}_{ijkl} \in W^{1,\infty}(\Omega)$, see [47]. The geometrical contact conditions (7) are equivalently reformulated as

$$\lambda_n^r - \max\left\{0, \lambda_n^r + \mathbf{u}_n^r - g\right\} = 0 \text{ a.e. on } \Gamma_C \tag{8}$$

by an NCP function, cf. [33, Chapter 4]. Multiplying with a test function $\mu_n \in L^2(\Gamma_C)$ leads to

$$C\left(\mathbf{w}^r\right)(\mu_n) := \left(\mu_n, \lambda_n^r - \max\left\{0, \lambda_n^r + \mathbf{u}_n^r - g\right\}\right)_{0,\Gamma_C} = 0.$$

However, the semilinear form C is not Fréchet differentiable in general.

If we require $\lambda_n^r \in L^2(\Gamma_C)$ and $\boldsymbol{\lambda}_t^r \in \left(L^2(\Gamma_C)\right)^{d-1}$, we obtain $s^r \in S$, where

$$S := \left\{ s : L^2(\Gamma_C) \to L_+^2(\Gamma_C) \,\middle|\, s \text{ continuously differentiable} \right\}$$

with $L_+^2(\Gamma_C) := \left\{ v \in L^2(\Gamma_C) \,\middle|\, v \geq 0 \text{ a.e.} \right\}$. Furthermore, Λ_t simplifies to

$$\Lambda_t\left(\lambda_n^r\right) = \left\{ \boldsymbol{\mu}_t \in \left(L^2(\Gamma_C)\right)^{d-1} \,\middle|\, \left|\boldsymbol{\mu}_t\right| \leq s^r\left(\lambda_n^r\right) \right\}.$$

The calculations in [33, Section 2.1] show that we obtain also the frictional conditions (3) a.e. Rewriting them with the help of a second NCP function, see [33, Chapter 5], gives us

$$\max\left\{s^r\left(\lambda_n^r\right), \left|\boldsymbol{\lambda}_t^r + \mathbf{u}_t^r\right|\right\} \boldsymbol{\lambda}_t^r - s^r\left(\lambda_n^r\right)\left(\boldsymbol{\lambda}_t^r + \mathbf{u}_t^r\right) = 0 \text{ a.e. on } \Gamma_C.$$

The multiplication with a test function $\boldsymbol{\mu}_t \in \left(L^2(\Gamma_C)\right)^{d-1}$ finally results in

$$D^r\left(\mathbf{w}^r\right)\left(\boldsymbol{\mu}_t\right) := \left(\boldsymbol{\mu}_t, \max\left\{s^r\left(\lambda_n^r\right), \left|\boldsymbol{\lambda}_t^r + \mathbf{u}_t^r\right|\right\} \boldsymbol{\lambda}_t^r - s^r\left(\lambda_n^r\right)\left(\boldsymbol{\lambda}_t^r + \mathbf{u}_t^r\right)\right)_{0,\Gamma_C} = 0.$$

In general, the semilinear form D is not Fréchet differentiable, too.

We define the semilinear form

$$A^r\left(\mathbf{w}^r\right)(\boldsymbol{\varphi}) := a\left(\mathbf{u}^r, \mathbf{v}\right) + \left(\lambda_n^r, \mathbf{v}_n\right)_{0,\Gamma_C} + \left(\boldsymbol{\lambda}_t^r, \mathbf{v}_t\right)_{0,\Gamma_C} - \langle \ell, \mathbf{v}\rangle + C\left(\mathbf{w}^r\right)(\mu_n) + D^r\left(\mathbf{w}^r\right)\left(\boldsymbol{\mu}_t\right)$$

with $\boldsymbol{\varphi} = \left(\mathbf{v}, \mu_n, \boldsymbol{\mu}_t\right) \in W := V \times L^2(\Gamma_C) \times \left(L^2(\Gamma_C)\right)^{d-1}$. Then Signorini's problem (4–5) is to find $\mathbf{w}^r \in W$ with

$$\forall \boldsymbol{\varphi} \in W: \qquad A^r\left(\mathbf{w}^r\right)(\boldsymbol{\varphi}) = 0.$$

2.2 Model adaptive discretization

The model adaptive discretization is carried out in two steps. At first, we specify a model adaptive friction law. To this end, we define a friction model hierarchy $\mathscr{H} := \{s_0, s_1, \ldots, s_M\}$. Here $s_M := s^r$ is the reference model, which is the most accurate or most general one. In general, the remaining models can be ordered by different criteria, for instance accuracy or mathematical complexity, which has no influence on the subsequent analysis. An example for a model hierarchy is given in Table 1, where the models are ordered by mathematical complexity. In this hierarchy, the reference model is the most general one. It can cope with all three different contact situations, for which the other frictional laws are specified, and some additional, which are not covered by the other ones. Finally, we compose a locally varying friction law $s \in S$ based on the different models in $\mathscr{H}$. Using the semilinear form

$$A(\mathbf{w})(\boldsymbol{\varphi}) := a(\mathbf{u}, \mathbf{v}) + (\lambda_n, \mathbf{v}_n)_{0,\Gamma_C} + (\boldsymbol{\lambda}_t, \mathbf{v}_t)_{0,\Gamma_C} - \langle \ell, \mathbf{v}\rangle + C(\mathbf{w})(\mu_n) + D(\mathbf{w})\left(\boldsymbol{\mu}_t\right)$$

with $\mathbf{w} = (\mathbf{u}, \lambda_n, \boldsymbol{\lambda}_t) \in W$, $\boldsymbol{\varphi} = \left(\mathbf{v}, \mu_n, \boldsymbol{\mu}_t\right) \in W$ and

$$D(\mathbf{w})\left(\boldsymbol{\mu}_t\right) := \left(\boldsymbol{\mu}_t, \max\left\{s(\lambda_n), |\boldsymbol{\lambda}_t + \mathbf{u}_t|\right\}\boldsymbol{\lambda}_t - s(\lambda_n)\left(\boldsymbol{\lambda}_t + \mathbf{u}_t\right)\right)_{0,\Gamma_C},$$

$\mathbf{w} \in W$ is a solution of Signorini's problem with a model adaptive friction law, if

$$\forall \boldsymbol{\varphi} \in W: A(\mathbf{w})(\boldsymbol{\varphi}) = 0.$$

We directly obtain a generalized Galerkin orthogonality relation

$$a\left(\mathbf{u}^r - \mathbf{u}, \mathbf{v}\right) + \left(\lambda_n^r - \lambda_n, \mathbf{v}_n\right)_{0,\Gamma_C} + \left(\boldsymbol{\lambda}_t^r - \boldsymbol{\lambda}_t, \mathbf{v}_t\right)_{0,\Gamma_C} = 0 \tag{9}$$

for all $\mathbf{v} \in V$.

The second step consists in the specification of the general discretization requirements, which ensure that the presented a posteriori error analysis applies to a wide range of techniques to calculate approximations $\mathbf{w}_h$ to $\mathbf{w}$. They have to fulfill the following assumption:

Assumption 1 Let $W_h := V_h \times \Lambda_{n,h} \times \Lambda_{t,h}$ be a finite dimensional subspace of W, which contains the discrete solution $\mathbf{w}_h$. Moreover, Eq. (4) has to hold for the discrete solution $\mathbf{w}_h$, i.e.

$$a(\mathbf{u}_h, \mathbf{v}_h) + \left(\lambda_{n,h}, \mathbf{v}_{h,n}\right)_{0,\Gamma_C} + \left(\boldsymbol{\lambda}_{t,h}, \mathbf{v}_{h,t}\right)_{0,\Gamma_C} = \langle l, \mathbf{v}_h \rangle \tag{10}$$

for all $\mathbf{v}_h \in V_h$.

Remark 1 From (10), a generalized Galerkin orthogonality follows, i.e.

$$a(\mathbf{u} - \mathbf{u}_h, \mathbf{v}_h) + \left(\lambda_n - \lambda_{n,h}, \mathbf{v}_{h,n}\right)_{0,\Gamma_C} + \left(\boldsymbol{\lambda}_t - \boldsymbol{\lambda}_{t,h}, \mathbf{v}_{h,t}\right)_{0,\Gamma_C} = 0 \tag{11}$$

for all $\mathbf{v}_h \in V_h$.

Remark 2 In Assumption 1, we require $\Lambda_{n,h} \subseteq L^2(\Gamma_C)$ and $\Lambda_{t,h}\left(\lambda_{n,h}\right) \subseteq \left(L^2(\Gamma_C)\right)^{d-1}$, only. We do not assume $\Lambda_{n,h} \subseteq \Lambda_n$ and $\Lambda_{t,h}\left(\lambda_{n,h}\right) \subseteq \Lambda_t\left(\lambda_{n,h}\right)$. Thus, we consider also nonconforming approximations of the Lagrange multiplier.

Remark 3 Our analysis applies to different discretization schemes. It includes methods, which are only based on the displacement. In this case, the Lagrange multipliers $\lambda_{n,h}$ and $\boldsymbol{\lambda}_{t,h}$ have to be determined in a post processing step, cf., for instance, [17]. It also applies to mixed discretizations like the one presented in [27], which we use in our numerical experiments, or Mortar methods, see, e.g., [63].

3 A posteriori error analysis

This section focuses on the derivation of an a posteriori error estimate in a user defined quantity of interest, where we employ the DWR method. Specifically, the error is estimated in a possibly nonlinear quantity of interest $J : W \to \mathbb{R}$, i.e. J can include the displacement $\mathbf{u}$ as well as the Lagrange multipliers λ_n and $\boldsymbol{\lambda}_t$ representing the contact and the frictional stress respectively.

3.1 Model error estimation

Initially, the model error $J(\mathbf{w}^r) - J(\mathbf{w})$ is treated. The first step in the derivation of the error identities is the definition of a suitable dual problem: Find $\mathbf{z}^r = \left(\mathbf{y}^r, \xi_n^r, \boldsymbol{\xi}_t^r\right) \in W$ with

$$a\left(\mathbf{v}, \mathbf{y}^r\right) - b_r^c\left(\xi_n^r, \mathbf{v}\right) + b_r^f\left(\boldsymbol{\xi}_t^r, \mathbf{v}\right) = J_{\mathbf{u}}'\left(\mathbf{w}^r\right)(\mathbf{v}), \tag{12}$$

$$\left(\mu_n, \mathbf{y}_n^r\right)_{0,\Gamma_C} + c_r^c\left(\xi_n^r, \mu_n\right) + c_r^f\left(\boldsymbol{\xi}_t^r, \mu_n\right) = J_{\lambda_n}'\left(\mathbf{w}^r\right)(\mu_n), \tag{13}$$

$$\left(\boldsymbol{\mu}_t, \mathbf{y}_t^r\right)_{0,\Gamma_C} + d_r^f\left(\boldsymbol{\xi}_t^r, \boldsymbol{\mu}_t\right) = J_{\boldsymbol{\lambda}_t}'\left(\mathbf{w}^r\right)\left(\boldsymbol{\mu}_t\right), \tag{14}$$

for all $(\mathbf{v}, \mu_n, \boldsymbol{\mu}_t) \in W$. Here, the bilinear forms $b_r^c : L^2(\Gamma_C) \times V \to \mathbb{R}$ and $c_r^c : L^2(\Gamma_C) \times L^2(\Gamma_C) \to \mathbb{R}$ are given by

$$b_r^c(\omega_n, \mathbf{v}) := \int_{\Gamma_C} \omega_n \chi_r^c \mathbf{v}_n \, do,$$
$$c_r^c(\omega_n, \mu_n) := \int_{\Gamma_C} \omega_n \left[1 - \chi_r^c\right] \mu_n \, do,$$

with

$$\chi_r^c(\mathbf{w}^r) := \begin{cases} 1, & \text{if } \lambda_n^r + \mathbf{u}_n^r - g > 0, \\ 0, & \text{if } \lambda_n^r + \mathbf{u}_n^r - g \leq 0. \end{cases}$$

We also write $\chi_r^c = \chi_r^c(\mathbf{w}^r)$. The bilinear forms b_r^c and c_r^c correspond to weighted L^2-scalar products on Γ_C, where the weight is given by the indicator function of the active and inactive geometrical contact set, respectively. Furthermore, we consider the bilinear forms $b_r^f : \left(L^2(\Gamma_C)\right)^{d-1} \times V \to \mathbb{R}$, $c_r^f : \left(L^2(\Gamma_C)\right)^{d-1} \times L^2(\Gamma_C) \to \mathbb{R}$, and $d_r^f : \left(L^2(\Gamma_C)\right)^{d-1} \times \left(L^2(\Gamma_C)\right)^{d-1} \to \mathbb{R}$ with

$$b_r^f(\boldsymbol{\omega}_t, \mathbf{v}) := \int_{\Gamma_C} \boldsymbol{\omega}_t \left[\chi_r^f \boldsymbol{\lambda}_t^r \left(n'(\mathbf{w}^r)\right)^\top - s^r(\lambda_n^r) I\right] \mathbf{v}_t \, do,$$
$$c_r^f(\boldsymbol{\omega}_t, \mu_n) := -\int_{\Gamma_C} \boldsymbol{\omega}_t \left(s^r\right)'(\lambda_n^r)(\mu_n) \left[\chi_r^f \boldsymbol{\lambda}_t^r + \mathbf{u}_t^r\right] do,$$
$$d_r^f(\boldsymbol{\omega}_t, \boldsymbol{\mu}_t) := \int_{\Gamma_C} \boldsymbol{\omega}_t \left[\max\left\{s^r(\lambda_n^r), n(\mathbf{w}^r)\right\} I - s^r(\lambda_n^r) I + \chi_r^f \boldsymbol{\lambda}_t^r \left(n'(\mathbf{w}^r)\right)^\top\right] \boldsymbol{\mu}_t \, do.$$

Here, we use the notation $n(\mathbf{w}^r) := \left|\boldsymbol{\lambda}_t^r + \mathbf{u}_t^r\right|$ and

$$n'(\mathbf{w}^r) = \begin{cases} \frac{\boldsymbol{\lambda}_t^r + \mathbf{u}_t^r}{n(\mathbf{w}^r)}, & \text{if } \mathbf{w} \neq 0, \\ 0, & \text{if } \mathbf{w} = 0. \end{cases}$$

However, the case $\mathbf{w} = 0$ does not occur because of the multiplication with the indicator function χ_r^f w.r.t. sliding and sticking, where

$$\chi_r^f(\mathbf{w}^r) := \begin{cases} 1, & \text{if } s^r(\lambda_n^r) < n(\mathbf{w}^r), \\ 0, & \text{if } s^r(\lambda_n^r) \geq n(\mathbf{w}^r). \end{cases}$$

The shorter notation $\chi_r^f := \chi_r^f(\mathbf{w}^r)$ is mostly used. We point out that, if the directional derivative $A'(\mathbf{w}^r)(\boldsymbol{\varphi}, \mathbf{z}^r)$ of A even in a generalized sense exists, the dual problem (12–14) matches

$$A'(\mathbf{w}^r)(\boldsymbol{\varphi}, \mathbf{z}^r) = J'(\mathbf{w}^r)(\boldsymbol{\varphi}).$$

Let us clarify the connection between $\max\left\{s^r\left(\lambda_n^r\right), n\left(\mathbf{w}^r\right)\right\}$ and the indicator function χ_r^f:

$$\begin{aligned} D^r\left(\mathbf{w}^r\right)\left(\boldsymbol{\mu}_t\right) &= \left(\boldsymbol{\mu}_t, \max\left\{s^r\left(\lambda_n^r\right), n\left(\mathbf{w}^r\right)\right\}\boldsymbol{\lambda}_t^r - s^r\left(\lambda_n^r\right)\left(\boldsymbol{\lambda}_t^r + \mathbf{u}_t^r\right)\right)_{0,\Gamma_C} \\ &= \left(\boldsymbol{\mu}_t, \chi_r^f n\left(\mathbf{w}^r\right)\boldsymbol{\lambda}_t^r + \left(1-\chi_r^f\right)s^r\left(\lambda_n^r\right)\boldsymbol{\lambda}_t^r - s^r\left(\lambda_n^r\right)\left(\boldsymbol{\lambda}_t^r + \mathbf{u}_t^r\right)\right)_{0,\Gamma_C} \\ &= \left(\boldsymbol{\mu}_t, \chi_r^f\left(n\left(\mathbf{w}^r\right)\boldsymbol{\lambda}_t^r - s^r\left(\lambda_n^r\right)\boldsymbol{\lambda}_t^r\right) - s^r\left(\lambda_n^r\right)\mathbf{u}_t^r\right)_{0,\Gamma_C} =: \bar{D}^r\left(\mathbf{w}^r\right)\left(\boldsymbol{\mu}_t\right). \end{aligned}$$

If we consider $\bar{D}^r$, we see χ_r^f as a fixed weighting function. Thus, the directional differentiability of $\bar{D}^r$ depends only on the smoothness of s^r. In the following results, if not otherwise stated, we assume that $\left(\mu_n, s^r\left(\lambda_n^r\right)\right)_{0,\Gamma_C}$ is three times directional differentiable w.r.t. λ_n^r. A short calculation now shows

$$\begin{aligned} &\left(\bar{D}^r\right)'\left(\mathbf{w}^r\right)\left(\delta\mathbf{w}, \boldsymbol{\mu}_t\right) \\ &\quad= \left(\bar{D}^r\right)'_{\mathbf{u}}\left(\mathbf{w}^r\right)\left(\delta\mathbf{u}, \boldsymbol{\mu}_t\right) + \left(\bar{D}^r\right)'_{\lambda_n}\left(\mathbf{w}^r\right)\left(\delta\lambda_n, \boldsymbol{\mu}_t\right) + \left(\bar{D}^r\right)'_{\boldsymbol{\lambda}_t}\left(\mathbf{w}^r\right)\left(\delta\boldsymbol{\lambda}_t, \boldsymbol{\mu}_t\right) \\ &\quad= \left(\boldsymbol{\mu}_t, \chi_r^f\left(\boldsymbol{\lambda}_t^r\left(n'\left(\mathbf{w}^r\right)\right)^\top\delta\mathbf{u}_t\right) - s^r\left(\lambda_n^r\right)\delta\mathbf{u}_t\right)_{0,\Gamma_C} \\ &\qquad- \left(\boldsymbol{\mu}_t, \chi_r^f\left(s^r\right)'\left(\lambda_n^r\right)\left(\delta\lambda_n\right)\boldsymbol{\lambda}_t^r + \left(s^r\right)'\left(\lambda_n^r\right)\left(\delta\lambda_n\right)\mathbf{u}_t^r\right)_{0,\Gamma_C} \\ &\qquad+ \left(\boldsymbol{\mu}_t, \chi_r^f\left(\boldsymbol{\lambda}_t^r\left(n'\left(\mathbf{w}^r\right)\right)^\top\delta\boldsymbol{\lambda}_t + n\left(\mathbf{w}^r\right)\delta\boldsymbol{\lambda}_t - s^r\left(\lambda_n^r\right)\delta\boldsymbol{\lambda}_t\right)\right)_{0,\Gamma_C} \\ &\quad= b_r^f\left(\boldsymbol{\mu}_t, \delta\mathbf{u}\right) + c_r^f\left(\boldsymbol{\mu}_t, \delta\lambda_n\right) + d_r^f\left(\boldsymbol{\mu}_t, \delta\boldsymbol{\lambda}_t\right). \end{aligned} \tag{15}$$

Analogously, we define the dual solution $\mathbf{z} = \left(\mathbf{y}, \xi_n, \boldsymbol{\xi}_t\right) \in W$ w.r.t. the model adaptive friction law s using the bilinear forms b^c, c^c, b^f, c^f, and d^f as well as the indicator functions χ^c and χ^f. Furthermore, we set

$$\bar{D}\left(\mathbf{w}\right)\left(\boldsymbol{\mu}_t\right) := \left(\boldsymbol{\mu}_t, \chi^f\left(n\left(\mathbf{w}\right)\boldsymbol{\lambda}_t - s\left(\lambda_n\right)\boldsymbol{\lambda}_t\right) - s\left(\lambda_n\right)\mathbf{u}_t\right)_{0,\Gamma_C} = D\left(\mathbf{w}\right)\left(\boldsymbol{\mu}_t\right)$$

and obtain

$$\bar{D}'\left(\mathbf{w}\right)\left(\delta\mathbf{w}, \boldsymbol{\mu}_t\right) = b^f\left(\boldsymbol{\mu}_t, \delta\mathbf{u}\right) + c^f\left(\boldsymbol{\mu}_t, \delta\lambda_n\right) + d^f\left(\boldsymbol{\mu}_t, \delta\boldsymbol{\lambda}_t\right). \tag{16}$$

We denote the model adaptive error w.r.t. the primal as well as to the dual solution by

$$\begin{aligned} e_{\mathbf{w}}^r &:= \left(e_{\mathbf{u}}^r, e_{\lambda_n}^r, e_{\boldsymbol{\lambda}_t}^r\right) := \left(\mathbf{u}^r - \mathbf{u}, \lambda_n^r - \lambda_n, \boldsymbol{\lambda}_t^r - \boldsymbol{\lambda}_t\right), \\ e_{\mathbf{z}}^r &:= \left(e_{\mathbf{y}}^r, e_{\xi_n}^r, e_{\boldsymbol{\xi}_t}^r\right) := \left(\mathbf{y}^r - \mathbf{y}, \xi_n^r - \xi_n, \boldsymbol{\xi}_t^r - \boldsymbol{\xi}_t\right), \end{aligned}$$

respectively. The error in the geometrical contact indicator function is given by $e_{\chi^c}^r := \chi_r^c\left(\mathbf{w}^r\right) - \chi^c\left(\mathbf{w}\right)$ and in the frictional indicator function by $e_{\chi^f}^r := \chi_r^f\left(\mathbf{w}^r\right) - \chi^f\left(\mathbf{w}\right)$.

In preparation of the main result, we study the bilinear forms in the dual problem concerning the contact conditions:

Lemma 1 *We obtain that*

$$\begin{aligned} &c_r^c\left(\xi_n^r, e_{\lambda_n}^r\right) - b_r^c\left(\xi_n^r, e_{\mathbf{u}}^r\right) + c^c\left(\xi_n, e_{\lambda_n}^r\right) - b^c\left(\xi_n, e_{\mathbf{u}}^r\right) \\ &\quad = \int_{\Gamma_C} e_{\chi^c}^r \left[e_{\xi_n}^r\left(\lambda_n + \mathbf{u}_n - g\right) - \xi_n\left(e_{\lambda_n}^r + e_{\mathbf{u},n}^r\right)\right] do =: 2\mathscr{R}_c^m \end{aligned}$$

holds.

Remark 4 The term $\mathscr{R}_c^m$ is the product of the error in the indicator function of the contact conditions and the model error. Thus it is of higher order.

Proof By the definition of the bilinear forms c_r^c, c^c, b_r^c, and b^c, we obtain using $C\left(\mathbf{w}^r\right)\left(\mu_n\right) = C\left(\mathbf{w}\right)\left(\mu_n\right) = 0$ for all $\mu_n \in L^2\left(\Gamma_C\right)$

$$\begin{aligned} &c_r^c\left(\xi_n^r, e_{\lambda_n}^r\right) - b_r^c\left(\xi_n^r, e_{\mathbf{u}}^r\right) + c^c\left(\xi_n, e_{\lambda_n}^r\right) - b^c\left(\xi_n, e_{\mathbf{u}}^r\right) \\ &\quad = \int_{\Gamma_C} \xi_n^r\left[1 - \chi_r^c\right] e_{\lambda_n}^r \, do - \int_{\Gamma_C} \xi_n^r \chi_r^c e_{\mathbf{u},n}^r \, do \\ &\qquad + \int_{\Gamma_C} \xi_n\left[1 - \chi^c\right] e_{\lambda_n}^r \, do - \int_{\Gamma_C} \xi_n \chi^c e_{\mathbf{u},n}^r \, do \\ &\quad = \int_{\Gamma_C} \xi_n^r\left[e_{\lambda_n}^r - \chi_r^c\left(e_{\lambda_n}^r + e_{\mathbf{u},n}^r\right)\right] do + \int_{\Gamma_C} \xi_n\left[e_{\lambda_n}^r - \chi^c\left(e_{\lambda_n}^r + e_{\mathbf{u},n}^r\right)\right] do \\ &\quad = \int_{\Gamma_C} \xi_n^r\left[\lambda_n^r - \chi_r^c\left(\lambda_n^r + \mathbf{u}_n^r - g\right)\right] do - \int_{\Gamma_C} \xi_n^r\left[\lambda_n - \chi_r^c\left(\lambda_n + \mathbf{u}_n - g\right)\right] do \\ &\qquad + \int_{\Gamma_C} \xi_n\left[\lambda_n^r - \chi^c\left(\lambda_n^r + \mathbf{u}_n^r - g\right)\right] do - \int_{\Gamma_C} \xi_n\left[\lambda_n - \chi^c\left(\lambda_n + \mathbf{u}_n - g\right)\right] do \\ &\quad = -\int_{\Gamma_C} \xi_n^r\left[\lambda_n - \chi_r^c\left(\lambda_n + \mathbf{u}_n - g\right)\right] do + \int_{\Gamma_C} \xi_n^r\left[\lambda_n - \chi^c\left(\lambda_n + \mathbf{u}_n - g\right)\right] do \\ &\qquad - \int_{\Gamma_C} \xi_n\left[\lambda_n^r - \chi_r^c\left(\lambda_n^r + \mathbf{u}_n^r - g\right)\right] do + \int_{\Gamma_C} \xi_n\left[\lambda_n^r - \chi^c\left(\lambda_n^r + \mathbf{u}_n^r - g\right)\right] do \\ &\quad = \int_{\Gamma_C} \xi_n^r e_{\chi^c}^r\left(\lambda_n + \mathbf{u}_n - g\right) do - \int_{\Gamma_C} \xi_n e_{\chi^c}^r\left(\lambda_n^r + \mathbf{u}_n^r - g\right) do \\ &\quad = \int_{\Gamma_C} e_{\chi^c}^r\left[\xi_n^r\left(\lambda_n + \mathbf{u}_n - g\right) - \xi_n\left(\lambda_n^r + \mathbf{u}_n^r - g\right)\right] do \\ &\quad = \int_{\Gamma_C} e_{\chi^c}^r\left[e_{\xi_n}^r\left(\lambda_n + \mathbf{u}_n - g\right) - \xi_n\left(e_{\lambda_n}^r + e_{\mathbf{u},n}^r\right)\right] do = 2\mathscr{R}_c^m. \end{aligned}$$

□

We define the semilinear form $\Delta\left(w\right)\left(\mu_t\right) := D^r\left(w\right)\left(\mu_t\right) - D\left(w\right)\left(\mu_t\right)$ and obtain

$$A\left(w\right)\left(\varphi\right) + \Delta\left(w\right)\left(\mu_t\right) = A^r\left(w\right)\left(\varphi\right).$$

Furthermore, we set $\bar{\Delta}\left(\omega, \varphi\right) := \left(\bar{D}^r\right)'\left(w\right)\left(\omega, \varphi\right)$. The second step is now to consider the bilinear form in the dual problems concerning the frictional conditions:

Lemma 2 *With the remainder term*

$$\mathscr{R}_f^m = \mathscr{R}_{\chi,1}^m + \mathscr{R}_{\chi,2}^m + \mathscr{R}_Q^m$$

including the frictional conditions, where

$$\begin{aligned}
\mathscr{R}_{\chi,1}^m &= -\left(\boldsymbol{\xi}_t^r, \left(\chi_r^f\left(\mathbf{w}^r\right) - \chi_r^f\left(\mathbf{w}\right)\right)\left(n\left(\mathbf{w}\right)\boldsymbol{\lambda}_t - s^r\left(\lambda_n\right)\boldsymbol{\lambda}_t\right)\right)_{0,\Gamma_C},\\
\mathscr{R}_{\chi,2}^m &= -\frac{1}{2}\left[\left(\bar{D}^r\right)'\left(\mathbf{w}\right)\left(e_{\mathbf{w}}^r, \boldsymbol{\xi}_t\right) - \bar{D}'\left(\mathbf{w}\right)\left(e_{\mathbf{w}}^r, \boldsymbol{\xi}_t\right)\right],\\
\mathscr{R}_Q^m &= \frac{1}{2}\int_0^1 \left(\bar{D}^r\right)'''\left(\mathbf{w} + s e_{\mathbf{w}}^r\right)\left(e_{\mathbf{w}}^r, e_{\mathbf{w}}^r, e_{\mathbf{w}}^r, \boldsymbol{\xi}_t^r\right) s(s-1)\, ds,
\end{aligned}$$

it holds

$$\begin{aligned}
&b_r^f\left(\boldsymbol{\xi}_t^r, e_{\mathbf{u}}^r\right) + c_r^f\left(\boldsymbol{\xi}_t^r, e_{\lambda_n}^r\right) + d_r^f\left(\boldsymbol{\xi}_t^r, e_{\boldsymbol{\lambda}_t}^r\right) + b^f\left(\boldsymbol{\xi}_t, e_{\mathbf{u}}^r\right) + c^f\left(\boldsymbol{\xi}_t, e_{\lambda_n}^r\right) + d^f\left(\boldsymbol{\xi}_t, e_{\boldsymbol{\lambda}_t}^r\right)\\
&\quad = -2\Delta\left(\mathbf{w}\right)\left(\boldsymbol{\xi}_t\right) - 2\Delta\left(\mathbf{w}\right)\left(e_{\boldsymbol{\xi}_t}^r\right) - \bar{\Delta}\left(e_{\mathbf{w}}^r, e_{\boldsymbol{\xi}_t}^r\right) + 2\mathscr{R}_f^m.
\end{aligned}$$

Remark 5 The remainder $\mathscr{R}_f^m$ is dominated by $\mathscr{R}_{\chi,1}^m$, which consists mainly of the error in the indicator function of the sticking and the sliping region. The other parts are of second and third order in the error, respectively.

Proof At first, we notice using the definition of $\bar{D}^r$ and $D\left(\mathbf{w}\right)\left(\boldsymbol{\mu}_t\right) = 0$

$$\begin{aligned}
&\bar{D}^r\left(\mathbf{w}\right)\left(\boldsymbol{\xi}_t^r\right)\\
&\quad = \left(\boldsymbol{\xi}_t^r, \chi_r^f\left(n\left(\mathbf{w}\right)\boldsymbol{\lambda}_t - s^r\left(\lambda_n\right)\boldsymbol{\lambda}_t\right) - s^r\left(\lambda_n\right)\mathbf{u}_t\right)_{0,\Gamma_C}\\
&\quad = \left(\boldsymbol{\xi}_t^r, \left(\chi_r^f\left(\mathbf{w}^r\right) - \chi_r^f\left(\mathbf{w}\right)\right)\left(n\left(\mathbf{w}\right)\boldsymbol{\lambda}_t - s^r\left(\lambda_n\right)\boldsymbol{\lambda}_t\right)\right)_{0,\Gamma_C}\\
&\qquad + \left(\boldsymbol{\xi}_t^r, \chi_r^f\left(\mathbf{w}\right)\left(n\left(\mathbf{w}\right)\boldsymbol{\lambda}_t - s^r\left(\lambda_n\right)\boldsymbol{\lambda}_t\right) - s^r\left(\lambda_n\right)\mathbf{u}_t\right)_{0,\Gamma_C}\\
&\quad = -\mathscr{R}_{\chi,1}^m + D^r\left(\mathbf{w}\right)\left(\boldsymbol{\xi}_t^r\right) = D^r\left(\mathbf{w}\right)\left(\boldsymbol{\xi}_t^r - \boldsymbol{\xi}_t\right) + D^r\left(\mathbf{w}\right)\left(\boldsymbol{\xi}_t\right) - \mathscr{R}_{\chi,1}^m\\
&\quad = D^r\left(\mathbf{w}\right)\left(\boldsymbol{\xi}_t^r - \boldsymbol{\xi}_t\right) - D\left(\mathbf{w}\right)\left(\boldsymbol{\xi}_t^r - \boldsymbol{\xi}_t\right) + D^r\left(\mathbf{w}\right)\left(\boldsymbol{\xi}_t\right) - D\left(\mathbf{w}\right)\left(\boldsymbol{\xi}_t\right) - \mathscr{R}_{\chi,1}^m\\
&\quad = \Delta\left(\mathbf{w}\right)\left(e_{\boldsymbol{\xi}_t}^r\right) + \Delta\left(\mathbf{w}\right)\left(\boldsymbol{\xi}_t\right) - \mathscr{R}_{\chi,1}^m.
\end{aligned}$$

The trapezoidal rule with its remainder term together with

$$\bar{D}^r\left(\mathbf{w}^r\right)\left(\boldsymbol{\mu}_t\right) = D^r\left(\mathbf{w}^r\right)\left(\boldsymbol{\mu}_t\right) = 0$$

and the preceding calculations lead to

$$\begin{aligned}
&-\Delta\left(\mathbf{w}\right)\left(e_{\boldsymbol{\xi}_t}^r\right) - \Delta\left(\mathbf{w}\right)\left(\boldsymbol{\xi}_t\right) + \mathscr{R}_{\chi,1}^m\\
&\quad = \bar{D}^r\left(\mathbf{w}^r\right)\left(\boldsymbol{\xi}_t^r\right) - \bar{D}^r\left(\mathbf{w}\right)\left(\boldsymbol{\xi}_t^r\right)
\end{aligned}$$

$$= \int_0^1 \left(\bar{D}^r\right)' \left(\mathbf{w} + s e^r_{\mathbf{w}}\right) \left(e^r_{\mathbf{w}}, \boldsymbol{\xi}^r_t\right) ds$$
$$= \frac{1}{2} \left(\bar{D}^r\right)' (\mathbf{w}) \left(e^r_{\mathbf{w}}, \boldsymbol{\xi}^r_t\right) + \frac{1}{2} \left(\bar{D}^r\right)' \left(\mathbf{w}^r\right) \left(e^r_{\mathbf{w}}, \boldsymbol{\xi}^r_t\right) - \mathscr{R}^m_Q.$$

From (15), (16) and

$$\begin{aligned}
&\left(\bar{D}^r\right)' (\mathbf{w}) \left(e^r_{\mathbf{w}}, \boldsymbol{\xi}^r_t\right) \\
&= \left(\bar{D}^r\right)' (\mathbf{w}) \left(e^r_{\mathbf{w}}, e^r_{\boldsymbol{\xi}_t}\right) + \left(\bar{D}^r\right)' (\mathbf{w}) \left(e^r_{\mathbf{w}}, \boldsymbol{\xi}_t\right) - \bar{D}' (\mathbf{w}) \left(e^r_{\mathbf{w}}, \boldsymbol{\xi}_t\right) + \bar{D}' (\mathbf{w}) \left(e^r_{\mathbf{w}}, \boldsymbol{\xi}_t\right) \\
&= \bar{\Delta} \left(e^r_{\mathbf{w}}, e^r_{\boldsymbol{\xi}_t}\right) - 2\mathscr{R}^m_{\chi,2} + b^f \left(\boldsymbol{\xi}_t, e^r_{\mathbf{u}}\right) + c^f \left(\boldsymbol{\xi}_t, e^r_{\lambda_n}\right) + d^f \left(\boldsymbol{\xi}_t, e^r_{\boldsymbol{\lambda}_t}\right),
\end{aligned}$$

we deduce the assertion by rearranging the single terms. □

Combining Lemmas 1 and 2, we obtain the following proposition concerning the model error:

Proposition 1 *Let the third directional derivative of J, $J''' : W \to \mathscr{L}(W, \mathscr{L}(W, W^*))$, exist. Then, the error identity*

$$J\left(\mathbf{w}^r\right) - J(\mathbf{w}) = -\Delta(\mathbf{w}) \left(\boldsymbol{\xi}_t\right) - \Delta(\mathbf{w}) \left(e^r_{\boldsymbol{\xi}_t}\right) - \frac{1}{2} \bar{\Delta} \left(e^r_{\mathbf{w}}, e^r_{\boldsymbol{\xi}_t}\right) + \mathscr{R}^m_J + \mathscr{R}^m_c + \mathscr{R}^m_f \tag{17}$$

holds for the model error in the quantity of interest with the remainder terms

$$\mathscr{R}^m_J = \frac{1}{2} \int_0^1 J''' \left(\mathbf{w} + s e^r_{\mathbf{w}}\right) \left(e^r_{\mathbf{w}}, e^r_{\mathbf{w}}, e^r_{\mathbf{w}}\right) s(s-1)\, ds$$

w.r.t. the quantity of interest J, $\mathscr{R}^m_c$ from Lemma 1 and $\mathscr{R}^m_f$ from Lemma 2.

Remark 6 The remainder $\mathscr{R}^m_J$ is of third order in the error. Consequently, the remainder terms are dominated by $\mathscr{R}^m_{\chi,1}$.

Proof The trapezoidal quadrature rule with its remainder term leads to

$$J\left(\mathbf{w}^r\right) - J(\mathbf{w}) = \int_0^1 J' \left(\mathbf{w} + s e^r_{\mathbf{w}}\right) \left(e^r_{\mathbf{w}}\right) ds = \frac{1}{2} J' (\mathbf{w}) \left(e^r_{\mathbf{w}}\right) + \frac{1}{2} J' \left(\mathbf{w}^r\right) \left(e^r_{\mathbf{w}}\right) + \mathscr{R}^m_J.$$

From the definition of the dual problems together with the generalized Galerkin orthogonality (9), we deduce

$$\begin{aligned}
J' \left(\mathbf{w}^r\right) \left(e^r_{\mathbf{w}}\right) &= a \left(e^r_{\mathbf{u}}, \mathbf{y}^r\right) - b^c_r \left(\xi^r_n, e^r_{\mathbf{u}}\right) + b^f_r \left(\boldsymbol{\xi}^r_t, e^r_{\mathbf{u}}\right) + \left(e^r_{\lambda_n}, \mathbf{y}^r_n\right)_{0,\Gamma_C} \\
&\quad + c^c_r \left(\xi^r_n, e^r_{\lambda_n}\right) + c^f_r \left(\boldsymbol{\xi}^r_t, e^r_{\lambda_n}\right) + \left(e^r_{\boldsymbol{\lambda}_t}, \mathbf{y}^r_t\right)_{0,\Gamma_C} + d^f_r \left(\boldsymbol{\xi}^r_t, e^r_{\boldsymbol{\lambda}_t}\right) \\
&= -b^c_r \left(\xi^r_n, e^r_{\mathbf{u}}\right) + b^f_r \left(\boldsymbol{\xi}^r_t, e^r_{\mathbf{u}}\right) + c^c_r \left(\xi^r_n, e^r_{\lambda_n}\right) + c^f_r \left(\boldsymbol{\xi}^r_t, e^r_{\lambda_n}\right) + d^f_r \left(\boldsymbol{\xi}^r_t, e^r_{\boldsymbol{\lambda}_t}\right)
\end{aligned}$$

and

$$
\begin{aligned}
J'(\mathbf{w})\left(e_{\mathbf{w}}^r\right) &= a\left(e_{\mathbf{u}}^r, \mathbf{y}\right) - b^c\left(\xi_n, e_{\mathbf{u}}^r\right) + b^f\left(\boldsymbol{\xi}_t, e_{\mathbf{u}}^r\right) + \left(e_{\lambda_n}^r, \mathbf{y}_n\right)_{0,\Gamma_C} \\
&\quad + c^c\left(\xi_n, e_{\lambda_n}^r\right) + c^f\left(\boldsymbol{\xi}_t, e_{\lambda_n}^r\right) + \left(e_{\boldsymbol{\lambda}_t}^r, \mathbf{y}_t\right)_{0,\Gamma_C} + d^f\left(\boldsymbol{\xi}_t, e_{\boldsymbol{\lambda}_t}^r\right) \\
&= -b^c\left(\xi_n, e_{\mathbf{u}}^r\right) + b^f\left(\boldsymbol{\xi}_t, e_{\mathbf{u}}^r\right) + c^c\left(\xi_n, e_{\lambda_n}^r\right) + c^f\left(\boldsymbol{\xi}_t, e_{\lambda_n}^r\right) + d^f\left(\boldsymbol{\xi}_t, e_{\boldsymbol{\lambda}_t}^r\right).
\end{aligned}
$$

Lemmas 1 and 2 together with the calculations above lead to

$$
\begin{aligned}
&J\left(\mathbf{w}^r\right) - J(\mathbf{w}) \\
&= \frac{1}{2} J'(\mathbf{w})\left(e_{\mathbf{w}}^r\right) + \frac{1}{2} J'\left(\mathbf{w}^r\right)\left(e_{\mathbf{w}}^r\right) + \mathscr{R}_J^m \\
&= \frac{1}{2}\left[-b_r^c\left(\xi_n^r, e_{\mathbf{u}}^r\right) + b_r^f\left(\boldsymbol{\xi}_t^r, e_{\mathbf{u}}^r\right) + c_r^c\left(\xi_n^r, e_{\lambda_n}^r\right) + c_r^f\left(\boldsymbol{\xi}_t^r, e_{\lambda_n}^r\right) + d_r^f\left(\boldsymbol{\xi}_t^r, e_{\boldsymbol{\lambda}_t}^r\right)\right] \\
&\quad + \frac{1}{2}\left[-b^c\left(\xi_n, e_{\mathbf{u}}^r\right) + b^f\left(\boldsymbol{\xi}_t, e_{\mathbf{u}}^r\right) + c^c\left(\xi_n, e_{\lambda_n}^r\right) + c^f\left(\boldsymbol{\xi}_t, e_{\lambda_n}^r\right) + d^f\left(\boldsymbol{\xi}_t, e_{\boldsymbol{\lambda}_t}^r\right)\right] + \mathscr{R}_J^m \\
&= -\Delta(\mathbf{w})\left(\boldsymbol{\xi}_t\right) - \Delta(\mathbf{w})\left(e_{\boldsymbol{\xi}_t}^r\right) - \frac{1}{2}\left(\bar{D}^r\right)'(\mathbf{w})\left(e_{\mathbf{w}}^r, e_{\boldsymbol{\xi}_t}^r\right) + \mathscr{R}_c^m + \mathscr{R}_f^m + \mathscr{R}_J^m,
\end{aligned}
$$

the assertion. □

3.2 Discretization error estimation

In this section, we consider the discretization error $J(\mathbf{w}) - J(\mathbf{w}_h)$ between the model adaptive solution $\mathbf{w}$ and its approximation $\mathbf{w}_h$. To this end, we need a discrete approximation $\mathbf{z}_h = \left(\mathbf{y}_h, \xi_{n,h}, \boldsymbol{\xi}_{t,h}\right) \in W_h$ to $\mathbf{z}$, which does not have to fulfill any further assumptions. We denote by $e_{\mathbf{w}}$ and $e_{\mathbf{z}}$ the discretization error, i.e.

$$
\begin{aligned}
e_{\mathbf{w}} &= \left(e_{\mathbf{u}}, e_{\lambda_n}, e_{\boldsymbol{\lambda}_t}\right) = \left(\mathbf{u} - \mathbf{u}_h, \lambda_n - \lambda_{n,h}, \boldsymbol{\lambda}_t - \boldsymbol{\lambda}_{t,h}\right), \\
e_{\mathbf{z}} &= \left(e_{\mathbf{y}}, e_{\xi_n}, e_{\boldsymbol{\xi}_t}\right) = \left(\mathbf{y} - \mathbf{y}_h, \xi_n - \xi_{n,h}, \boldsymbol{\xi}_t - \boldsymbol{\xi}_{t,h}\right).
\end{aligned}
$$

Furthermore, we define

$$
\begin{aligned}
\bar{D}_h(\mathbf{w}_h)\left(\boldsymbol{\mu}_{t,h}\right) &:= \left(\boldsymbol{\mu}_{t,h}, \chi_h^f\left(n(\mathbf{w}_h)\boldsymbol{\lambda}_{t,h} - s\left(\lambda_{n,h}\right)\boldsymbol{\lambda}_{t,h}\right) - s\left(\lambda_{n,h}\right)\mathbf{u}_{h,t}\right)_{0,\Gamma_C} \\
&= D_h(\mathbf{w}_h)\left(\boldsymbol{\mu}_{t,h}\right)
\end{aligned}
$$

and notice

$$
\bar{D}_h'(\mathbf{w}_h)\left(\delta\mathbf{w}, \boldsymbol{\mu}_t\right) = b_h^f\left(\boldsymbol{\mu}_t, \delta\mathbf{u}\right) + c_h^f\left(\boldsymbol{\mu}_t, \delta\lambda_n\right) + d_h^f\left(\boldsymbol{\mu}_t, \delta\boldsymbol{\lambda}_t\right) \tag{18}
$$

with the bilinear forms $b_h^f : \Lambda_{t,h} \times V_h \to \mathbb{R}$, $c_h^f : \Lambda_{t,h} \times \Lambda_{n,h} \to \mathbb{R}$, and $d_h^f : \Lambda_{t,h} \times \Lambda_{t,h} \to \mathbb{R}$ concerning the frictional conditions,

$$
b_h^f(\boldsymbol{\omega}_t, \mathbf{v}) := \int_{\Gamma_C} \boldsymbol{\omega}_t \left[\chi_h^f \boldsymbol{\lambda}_{t,h}\left(n'(\mathbf{w}_h)\right)^\top - s(\mathbf{w}_h) I\right] \mathbf{v}_t \, do,
$$

$$c_h^f(\boldsymbol{\omega}_t, \mu_n) := -\int_{\Gamma_C} \boldsymbol{\omega}_t s'\left(\lambda_{n,h}\right)(\mu_n)\left[\chi_h^f \boldsymbol{\lambda}_{t,h} + \mathbf{u}_{h,t}\right] do,$$

$$d_h^f\left(\boldsymbol{\omega}_t, \boldsymbol{\mu}_t\right) := \int_{\Gamma_C} \boldsymbol{\omega}_t \left[\max\left\{s\left(\lambda_{n,h}\right), n\left(\mathbf{w}_h\right)\right\} I - s\left(\lambda_{n,h}\right) I\right] \boldsymbol{\mu}_t \, do + \int_{\Gamma_C} \boldsymbol{\omega}_t \chi_h^f \boldsymbol{\lambda}_{t,h} \left(n'\left(\mathbf{w}_h\right)\right)^\top \boldsymbol{\mu}_t \, do,$$

and

$$\chi_h^f(w_h) := \begin{cases} 1, & \text{if } s\left(\lambda_{n,h}\right) < n\left(\mathbf{w}_h\right), \\ 0, & \text{if } s\left(\lambda_{n,h}\right) \geq n\left(\mathbf{w}_h\right). \end{cases}$$

The error in the frictional indicator function is $e_\chi^f = \chi^f - \chi_h^f$. First, we clarify the connection between the frictional part of the dual problem and the frictional conditions:

Lemma 3 *Let $(\mu_n, s(\lambda_n))_{0,\Gamma_C}$ for arbitrary $\mu_n \in L^2(\Gamma_C)$ be twice directional differentiable w.r.t. λ_n. Then we have the identity*

$$b^f\left(\boldsymbol{\xi}_t, e_{\mathbf{u}}\right) + c^f\left(\boldsymbol{\xi}_t, e_{\lambda_n}\right) + d^f\left(\boldsymbol{\xi}_t, e_{\boldsymbol{\lambda}_t}\right) = -D\left(\mathbf{w}_h\right)\left(e_{\boldsymbol{\xi}_t}\right) - D\left(\mathbf{w}_h\right)\left(\boldsymbol{\xi}_{t,h}\right) + \mathscr{R}_f^{(2)}.$$

The remainder term $\mathscr{R}_f^{(2)} = \mathscr{R}_\chi^{(2)} + \mathscr{R}_Q^{(2)}$ consists of

$$\mathscr{R}_\chi^{(2)} := -\left(\boldsymbol{\xi}_t, e_\chi^f\left(n\left(\mathbf{w}_h\right)\boldsymbol{\lambda}_{t,h} - s\left(\lambda_{n,h}\right)\boldsymbol{\lambda}_{t,h}\right)\right)_{0,\Gamma_C}$$

and

$$\mathscr{R}_Q^{(2)} := \int_0^1 \bar{D}''\left(\mathbf{w}_h + s e_{\mathbf{w}}\right)\left(e_{\mathbf{w}}, e_{\mathbf{w}}, \boldsymbol{\xi}_t\right) s \, ds.$$

Proof We obtain using the box quadrature rule with its remainder and (16)

$$\begin{aligned} \bar{D}\left(\mathbf{w}\right)\left(\boldsymbol{\xi}_t\right) - \bar{D}\left(\mathbf{w}_h\right)\left(\boldsymbol{\xi}_t\right) &= \int_0^1 \bar{D}'\left(\mathbf{w}_h + s e_{\mathbf{w}}\right)\left(e_{\mathbf{w}}, \boldsymbol{\xi}_t\right) ds \\ &= \bar{D}'\left(\mathbf{w}\right)\left(e_{\mathbf{w}}, \boldsymbol{\xi}_t\right) - \mathscr{R}_Q^{(2)} \\ &= b^f\left(\boldsymbol{\xi}_t, e_{\mathbf{u}}\right) + c^f\left(\boldsymbol{\xi}_t, e_{\lambda_n}\right) + d^f\left(\boldsymbol{\xi}_t, e_{\boldsymbol{\lambda}_t}\right) - \mathscr{R}_Q^{(2)}. \end{aligned}$$

The equation $\bar{D}\left(\mathbf{w}\right)\left(\boldsymbol{\xi}_t\right) = D\left(\mathbf{w}\right)\left(\boldsymbol{\xi}_t\right) = 0$ leads to

$$\begin{aligned} \bar{D}\left(\mathbf{w}\right)\left(\boldsymbol{\xi}_t\right) - \bar{D}\left(\mathbf{w}_h\right)\left(\boldsymbol{\xi}_t\right) &= -\bar{D}\left(\mathbf{w}_h\right)\left(\boldsymbol{\xi}_t\right) \\ &= -\bar{D}\left(\mathbf{w}_h\right)\left(\boldsymbol{\xi}_t\right) - \bar{D}_h\left(\mathbf{w}_h\right)\left(\boldsymbol{\xi}_t\right) + \bar{D}_h\left(\mathbf{w}_h\right)\left(\boldsymbol{\xi}_t\right) \\ &= -\left(\boldsymbol{\xi}_t, \chi^f\left(n\left(\mathbf{w}_h\right)\boldsymbol{\lambda}_{t,h} - s\left(\lambda_{n,h}\right)\boldsymbol{\lambda}_{t,h}\right) - s\left(\lambda_{n,h}\right)\mathbf{u}_{h,t}\right)_{0,\Gamma_C} \end{aligned}$$

$$
\begin{aligned}
&+\left(\boldsymbol{\xi}_t, \chi_h^f \left(n\left(\mathbf{w}_h\right)\boldsymbol{\lambda}_{t,h} - s\left(\lambda_{n,h}\right)\boldsymbol{\lambda}_{t,h}\right) - s\left(\lambda_{n,h}\right)\mathbf{u}_{h,t}\right)_{0,\Gamma_C} - D\left(\mathbf{w}_h\right)\left(\boldsymbol{\xi}_t\right)\\
&= -\left(\boldsymbol{\xi}_t, e_\chi^f \left(n\left(\mathbf{w}_h\right)\boldsymbol{\lambda}_{t,h} - s\left(\lambda_{n,h}\right)\boldsymbol{\lambda}_{t,h}\right)\right)_{0,\Gamma_C} - D\left(\mathbf{w}_h\right)\left(e_{\boldsymbol{\xi}_t}\right) - D\left(\mathbf{w}_h\right)\left(\boldsymbol{\xi}_{t,h}\right)\\
&= \mathscr{R}_\chi^{(2)} - D\left(\mathbf{w}_h\right)\left(e_{\boldsymbol{\xi}_t}\right) - D\left(\mathbf{w}_h\right)\left(\boldsymbol{\xi}_{t,h}\right).
\end{aligned}
$$

Rearranging the terms finishes the proof. □

Using only the primal residual, we get the following error identity.

Proposition 2 *If the second directional derivative of J, $J'' : W \to \mathscr{L}(W, W^*)$, exists as well as Assumption 1 and the assumptions of Lemma 3 hold, we obtain the error identity*

$$
\begin{aligned}
J\left(\mathbf{w}\right) - J\left(\mathbf{w}_h\right) = \rho\left(\mathbf{w}_h\right)\left(\mathbf{z} - \mathbf{z}_h\right) - C\left(\mathbf{w}_h\right)\left(\xi_{n,h}\right) - D\left(\mathbf{w}_h\right)\left(\boldsymbol{\xi}_{t,h}\right)\\
+ \mathscr{R}_J^{(2)} + \mathscr{R}_c^{(2)} + \mathscr{R}_f^{(2)},
\end{aligned}
\tag{19}
$$

with the primal residual

$$
\rho\left(\mathbf{w}_h\right)\left(\boldsymbol{\varphi}\right) := -A\left(\mathbf{w}_h\right)\left(\boldsymbol{\varphi}\right).
$$

The remainder term w.r.t. the quantity of interest, $\mathscr{R}_J^{(2)}$, is given by

$$
\mathscr{R}_J^{(2)} = -\int_0^1 J''\left(\mathbf{w}_h + s e_{\mathbf{w}}\right)\left(e_{\mathbf{w}}, e_{\mathbf{w}}\right) s\, ds.
$$

For the contact conditions, we have the remainder

$$
\mathscr{R}_c^{(2)} = \int_{\Gamma_C} \xi_n e_\chi^c \left[\lambda_{n,h} + \mathbf{u}_{h,n} - g\right] do,
$$

with $e_\chi^c = \chi^c - \chi_h^c$, and

$$
\chi_h^c := \begin{cases} 1, & \text{if } \lambda_{n,h} + \mathbf{u}_{h,n} - g > 0, \\ 0, & \text{if } \lambda_{n,h} + \mathbf{u}_{h,n} - g \leq 0. \end{cases}
$$

Remark 7 By $C\left(\mathbf{w}_h\right)\left(\xi_{n,h}\right)$, we measure the violation of the geometrical contact conditions (2). The term $D\left(\mathbf{w}_h\right)\left(\boldsymbol{\xi}_{t,h}\right)$ represents the error of the discrete solution concerning the frictional conditions (3).

Remark 8 The term $\mathscr{R}_J^{(2)}$ corresponds to the usual remainder of the DWR method for linear problems with nonlinear quantities of interest, cf. [3, Proposition 6.6]. It vanishes for linear quantities of interest J.

Remark 9 The remainder $\mathscr{R}_c^{(2)}$ w.r.t. the geometrical contact conditions becomes zero, if the analytic active set equals the discrete one. The frictional remainder term $\mathscr{R}_f^{(2)}$ has a higher order part of the same order as $\mathscr{R}_J^{(2)}$ and one in the indicator function of friction. The second part vanishes, if the sliding and sticking regions are exactly resolved. The remainder terms will be discussed in more detail in Sect. 4.

Proof We use the box quadrature rule with its remainder term to obtain

$$\begin{aligned} J(\mathbf{w}) - J(\mathbf{w}_h) &= \int_0^1 J'(\mathbf{w}_h + s e_{\mathbf{w}})(e_{\mathbf{w}})\, ds = J'(\mathbf{w})(e_{\mathbf{w}}) + \mathscr{R}_J^{(2)} \\ &= J'_{\mathbf{u}}(\mathbf{w})(e_{\mathbf{u}}) + J'_{\lambda_n}(\mathbf{w})\left(e_{\lambda_n}\right) + J'_{\boldsymbol{\lambda}_t}(\mathbf{w})\left(e_{\boldsymbol{\lambda}_t}\right) + \mathscr{R}_J^{(2)}. \end{aligned}$$

From the definition of the continuous dual problem, cf. (12–14), we conclude

$$\begin{aligned} &J'_{\mathbf{u}}(\mathbf{w})(e_{\mathbf{u}}) + J'_{\lambda_n}(\mathbf{w})\left(e_{\lambda_n}\right) + J'_{\boldsymbol{\lambda}_t}(\mathbf{w})\left(e_{\boldsymbol{\lambda}_t}\right) \\ &\quad = a(e_{\mathbf{u}}, \mathbf{y}) - b^c(\xi_n, e_{\mathbf{u}}) + b^f\left(\boldsymbol{\xi}_t, e_{\mathbf{u}}\right) + \left(e_{\lambda_n}, \mathbf{y}_n\right)_{0,\Gamma_C} + c^c\left(\xi_n, e_{\lambda_n}\right) + c^f\left(\boldsymbol{\xi}_t, e_{\lambda_n}\right) \\ &\qquad + \left(e_{\boldsymbol{\lambda}_t}, \mathbf{y}_t\right)_{0,\Gamma_C} + d^f\left(\boldsymbol{\xi}_t, e_{\boldsymbol{\lambda}_t}\right). \end{aligned}$$

The Galerkin orthogonality (11) leads to

$$\begin{aligned} &a(e_{\mathbf{u}}, \mathbf{y}) + \left(e_{\lambda_n}, \mathbf{y}_n\right)_{0,\Gamma_C} + \left(e_{\boldsymbol{\lambda}_t}, \mathbf{y}_t\right)_{0,\Gamma_C} = a\left(e_{\mathbf{u}}, e_{\mathbf{y}}\right) + \left(e_{\lambda_n}, e_{\mathbf{y},n}\right)_{0,\Gamma_C} + \left(e_{\boldsymbol{\lambda}_t}, e_{\mathbf{y},t}\right)_{0,\Gamma_C} \\ &\quad = \langle l, e_{\mathbf{y}}\rangle - a\left(\mathbf{u}_h, e_{\mathbf{y}}\right) - \left(\lambda_{n,h}, e_{\mathbf{y},n}\right)_{0,\Gamma_C} - \left(\boldsymbol{\lambda}_{t,h}, e_{\mathbf{y},t}\right)_{0,\Gamma_C}. \end{aligned}$$

From the proof of Proposition 3.1 in [47], we know

$$c^c\left(\xi_n, e_{\lambda_n}\right) - b^c(\xi_n, e_{\mathbf{u}}) = -C(\mathbf{w}_h)\left(e_{\xi_n}\right) - C(\mathbf{w}_h)\left(\xi_{n,h}\right) + \mathscr{R}_c^{(2)}$$

and from Lemma 3

$$b^f\left(\boldsymbol{\xi}_t, e_{\mathbf{u}}\right) + c^f\left(\boldsymbol{\xi}_t, e_{\lambda_n}\right) + d^f\left(\boldsymbol{\xi}_t, e_{\boldsymbol{\lambda}_t}\right) = -D(\mathbf{w}_h)\left(e_{\boldsymbol{\xi}_t}\right) - D(\mathbf{w}_h)\left(\boldsymbol{\xi}_{t,h}\right) + \mathscr{R}_f^{(2)}.$$

In summary, we obtain

$$\begin{aligned} &J(\mathbf{w}) - J(\mathbf{w}_h) \\ &\quad = a(e_{\mathbf{u}}, \mathbf{y}) - b^c(\xi_n, e_{\mathbf{u}}) + b^f\left(\boldsymbol{\xi}_t, e_{\mathbf{u}}\right) + \left(e_{\lambda_n}, \mathbf{y}_n\right)_{0,\Gamma_C} + c^c\left(\xi_n, e_{\lambda_n}\right) + c^f\left(\boldsymbol{\xi}_t, e_{\lambda_n}\right) \\ &\qquad + \left(e_{\boldsymbol{\lambda}_t}, \mathbf{y}_t\right)_{0,\Gamma_C} + d^f\left(\boldsymbol{\xi}_t, e_{\boldsymbol{\lambda}_t}\right) + \mathscr{R}_J^{(2)} \\ &\quad = \langle l, e_{\mathbf{y}}\rangle - a\left(\mathbf{u}_h, e_{\mathbf{y}}\right) - \left(\lambda_{n,h}, e_{\mathbf{y},n}\right)_{0,\Gamma_C} - \left(\boldsymbol{\lambda}_{t,h}, e_{\mathbf{y},t}\right)_{0,\Gamma_C} - C(\mathbf{w}_h)\left(e_{\xi_n}\right) \\ &\qquad - D(\mathbf{w}_h)\left(e_{\boldsymbol{\xi}_t}\right) - C(\mathbf{w}_h)\left(\xi_{n,h}\right) - D(\mathbf{w}_h)\left(\boldsymbol{\xi}_{t,h}\right) + \mathscr{R}_J^{(2)} + \mathscr{R}_c^{(2)} + \mathscr{R}_f^{(2)} \\ &\quad = \rho(\mathbf{w}_h)(\mathbf{z} - \mathbf{z}_h) - C(\mathbf{w}_h)\left(\xi_{n,h}\right) - D(\mathbf{w}_h)\left(\boldsymbol{\xi}_{t,h}\right) + \mathscr{R}_J^{(2)} + \mathscr{R}_c^{(2)} + \mathscr{R}_f^{(2)}, \end{aligned}$$

which is the assertion. □

Now, we study the error identity involving the dual residual. To this end, we need to apply the following lemma:

Lemma 4 *Under the general assumptions of this section, we obtain the identity*

$$\begin{aligned} &b^f\left(\boldsymbol{\xi}_t, e_{\mathbf{u}}\right) + c^f\left(\boldsymbol{\xi}_t, e_{\lambda_n}\right) + d^f\left(\boldsymbol{\xi}_t, e_{\boldsymbol{\lambda}_t}\right) \\ &\quad + b_h^f\left(\boldsymbol{\xi}_{t,h}, e_{\mathbf{u}}\right) + c_h^f\left(\boldsymbol{\xi}_{t,h}, e_{\lambda_n}\right) + d_h^f\left(\boldsymbol{\xi}_{t,h}, e_{\boldsymbol{\lambda}_t}\right) \\ &= -D\left(\mathbf{w}_h\right)\left(e_{\boldsymbol{\xi}_t}\right) - 2D\left(\mathbf{w}_h\right)\left(\boldsymbol{\xi}_{t,h}\right) + 2\mathscr{R}_f^{(3)}. \end{aligned}$$

The remainder term $\mathscr{R}_f^{(3)} = \mathscr{R}_\chi^{(2)} + \mathscr{R}_\chi^{(3)} + \mathscr{R}_D^{(3)} + \mathscr{R}_Q^{(3)}$ *is given by a remainder in the frictional indicator function* $\mathscr{R}_\chi^{(3)} = \mathscr{R}_{\chi,1}^{(3)} + \mathscr{R}_{\chi,2}^{(3)}$ *with*

$$\begin{aligned} \mathscr{R}_{\chi,1}^{(3)} &= -\frac{1}{2}\left[\bar{D}'\left(\mathbf{w}_h\right)\left(e_{\mathbf{w}}, \boldsymbol{\xi}_{t,h}\right) - \bar{D}_h'\left(\mathbf{w}_h\right)\left(e_{\mathbf{w}}, \boldsymbol{\xi}_{t,h}\right)\right], \\ \mathscr{R}_{\chi,2}^{(3)} &= -\frac{1}{2}\left[\bar{D}\left(\mathbf{w}_h\right)\left(e_{\boldsymbol{\xi}_t}\right) - \bar{D}_h\left(\mathbf{w}_h\right)\left(e_{\boldsymbol{\xi}_t}\right)\right], \end{aligned}$$

a cubic remainder

$$\mathscr{R}_D^{(3)} = \frac{1}{2}\int_0^1 \bar{D}''\left(\mathbf{w}_h + s e_{\mathbf{w}}\right)\left(e_{\mathbf{w}}, e_{\mathbf{w}}, e_{\boldsymbol{\xi}_t}\right) s\, ds$$

in $e_{\mathbf{w}}$ *and* $e_{\boldsymbol{\xi}_t}$*, as well as a quadrature remainder*

$$\mathscr{R}_Q^{(3)} = \frac{1}{2}\int_0^1 \bar{D}'''\left(\mathbf{w}_h + s e_{\mathbf{w}}\right)\left(e_{\mathbf{w}}, e_{\mathbf{w}}, e_{\mathbf{w}}, \boldsymbol{\xi}_t\right) s(s-1)\, ds,$$

which is of third order in the error $e_{\mathbf{w}}$*.*

Remark 10 The remainder term $\mathscr{R}_f^{(3)}$ is dominated by the remainder $\mathscr{R}_\chi^{(2)}$, all other parts are of higher order in the error.

Proof Using Lemma 3 and the trapezoidal rule with its remainder term, we obtain

$$\begin{aligned} &-2D\left(\mathbf{w}_h\right)\left(e_{\boldsymbol{\xi}_t}\right) - 2D\left(\mathbf{w}_h\right)\left(\boldsymbol{\xi}_{t,h}\right) + 2\mathscr{R}_\chi^{(2)} \\ &= 2\left[\bar{D}\left(\mathbf{w}\right)\left(\boldsymbol{\xi}_t\right) - \bar{D}\left(\mathbf{w}_h\right)\left(\boldsymbol{\xi}_t\right)\right] = 2\int_0^1 \bar{D}'\left(\mathbf{w}_h + s e_{\mathbf{w}}\right)\left(e_{\mathbf{w}}, \boldsymbol{\xi}_t\right) ds \\ &= \bar{D}'\left(\mathbf{w}\right)\left(e_{\mathbf{w}}, \boldsymbol{\xi}_t\right) + \bar{D}'\left(\mathbf{w}_h\right)\left(e_{\mathbf{w}}, \boldsymbol{\xi}_t\right) - 2\mathscr{R}_Q^{(3)} \\ &= b^f\left(\boldsymbol{\xi}_t, e_{\mathbf{u}}\right) + c^f\left(\boldsymbol{\xi}_t, e_{\lambda_n}\right) + d^f\left(\boldsymbol{\xi}_t, e_{\boldsymbol{\lambda}_t}\right) + \bar{D}'\left(\mathbf{w}_h\right)\left(e_{\mathbf{w}}, \boldsymbol{\xi}_t\right) - 2\mathscr{R}_Q^{(3)}. \end{aligned}$$

Studying $\bar{D}'\left(\mathbf{w}_h\right)\left(e_{\mathbf{w}}, \boldsymbol{\xi}_t\right)$ in more detail leads to

$$\bar{D}'\left(\mathbf{w}_h\right)\left(e_{\mathbf{w}}, \boldsymbol{\xi}_t\right)$$

$$
\begin{aligned}
&= \bar{D}'(\mathbf{w}_h)\left(e_{\mathbf{w}}, e_{\boldsymbol{\xi}_t}\right) + \bar{D}'(\mathbf{w}_h)\left(e_{\mathbf{w}}, \boldsymbol{\xi}_{t,h}\right) \\
&= \bar{D}'(\mathbf{w}_h)\left(e_{\mathbf{w}}, e_{\boldsymbol{\xi}_t}\right) + \bar{D}'(\mathbf{w}_h)\left(e_{\mathbf{w}}, \boldsymbol{\xi}_{t,h}\right) - \bar{D}_h'(\mathbf{w}_h)\left(e_{\mathbf{w}}, \boldsymbol{\xi}_{t,h}\right) + \bar{D}_h'(\mathbf{w}_h)\left(e_{\mathbf{w}}, \boldsymbol{\xi}_{t,h}\right) \\
&= \bar{D}'(\mathbf{w}_h)\left(e_{\mathbf{w}}, e_{\boldsymbol{\xi}_t}\right) - 2\mathscr{R}_{\chi,1}^{(3)} + b_h^f\left(\boldsymbol{\xi}_{t,h}, e_{\mathbf{u}}\right) + c_h^f\left(\boldsymbol{\xi}_{t,h}, e_{\lambda_n}\right) + d_h^f\left(\boldsymbol{\xi}_{t,h}, e_{\boldsymbol{\lambda}_t}\right).
\end{aligned}
$$

To finish the proof, we use the box quadrature rule and obtain

$$
\begin{aligned}
&\bar{D}'(\mathbf{w}_h)\left(e_{\mathbf{w}}, e_{\boldsymbol{\xi}_t}\right) \\
&= \int_0^1 \bar{D}'(\mathbf{w}_h + s e_{\mathbf{w}})\left(e_{\mathbf{w}}, e_{\boldsymbol{\xi}_t}\right) ds - 2\mathscr{R}_D^{(3)} \\
&= \bar{D}(\mathbf{w})\left(e_{\boldsymbol{\xi}_t}\right) - \bar{D}(\mathbf{w}_h)\left(e_{\boldsymbol{\xi}_t}\right) - 2\mathscr{R}_D^{(3)} \\
&= -\bar{D}(\mathbf{w}_h)\left(e_{\boldsymbol{\xi}_t}\right) + \bar{D}_h(\mathbf{w}_h)\left(e_{\boldsymbol{\xi}_t}\right) - \bar{D}_h(\mathbf{w}_h)\left(e_{\boldsymbol{\xi}_t}\right) - 2\mathscr{R}_D^{(3)} \\
&= -D(\mathbf{w}_h)\left(e_{\boldsymbol{\xi}_t}\right) - 2\mathscr{R}_{\chi,2}^{(3)} - 2\mathscr{R}_D^{(3)},
\end{aligned}
$$

the assertion. □

The bilinear forms $b_h^c : \Lambda_{n,h} \times V_h \to \mathbb{R}$ and $c_h^c : \Lambda_{n,h} \times \Lambda_{n,h} \to \mathbb{R}$ w.r.t. the geometrical contact conditions are given by

$$
\begin{aligned}
b_h^c(\omega_n, \mathbf{v}) &:= \int_{\Gamma_C} \omega_n \chi_h^c \mathbf{v}_n \, do, \\
c_h^c(\omega_n, \mu_n) &:= \int_{\Gamma_C} \omega_n \left[1 - \chi_h^c\right] \mu_n \, do.
\end{aligned}
$$

Using the presented lemma above, we obtain the error representation:

Proposition 3 *We assume that the third directional derivative of J,*

$$
J''' : W \to \mathscr{L}(W, \mathscr{L}(W, W^*)),
$$

exists and that Assumption 1 hold. Then the error representation

$$
\begin{aligned}
J(\mathbf{w}) - J(\mathbf{w}_h) = \frac{1}{2}\rho(\mathbf{w}_h)(e_{\mathbf{z}}) + \frac{1}{2}\rho^*(\mathbf{w}_h, \mathbf{z}_h)(e_{\mathbf{w}}) - C(\mathbf{w}_h)\left(\xi_{n,h}\right) \\
- D(\mathbf{w}_h)\left(\boldsymbol{\xi}_{t,h}\right) + \mathscr{R}_J^{(3)} + \mathscr{R}_c^{(3)} + \mathscr{R}_f^{(3)}
\end{aligned} \tag{20}
$$

is valid. Here, the dual residual ρ^* is defined as

$$
\begin{aligned}
\rho^*(\mathbf{w}_h, \mathbf{z}_h)(\boldsymbol{\varphi}) := J'(\mathbf{w}_h)(\boldsymbol{\varphi}) - a(\mathbf{v}, \mathbf{y}_h) + b_h^c\left(\xi_{n,h}, \mathbf{v}\right) \\
- b_h^f\left(\boldsymbol{\xi}_{t,h}, \mathbf{v}\right) - \left(\mu_n, \mathbf{y}_{h,n}\right)_{0,\Gamma_C} \\
- c_h^c\left(\xi_{n,h}, \mu_n\right) - c_h^f\left(\boldsymbol{\xi}_{t,h}, \mu_n\right) - \left(\boldsymbol{\mu}_t, \mathbf{y}_{h,t}\right)_{0,\Gamma_C} - d_h^f\left(\boldsymbol{\xi}_{t,h}, \boldsymbol{\mu}_t\right).
\end{aligned}
$$

For the remainder $\mathscr{R}_J^{(3)}$ w.r.t. the quantity of interest, it holds

$$\mathscr{R}_J^{(3)} = \frac{1}{2}\int_0^1 J'''\left(\mathbf{w}_h + s e_{\mathbf{w}}\right)\left(e_{\mathbf{w}}, e_{\mathbf{w}}, e_{\mathbf{w}}\right) s(s-1)\, ds$$

and for the remainder $\mathscr{R}_c^{(3)}$ concerning the geometrical contact conditions

$$\mathscr{R}_c^{(3)} = \frac{1}{2}\int_{\Gamma_C} e_\chi^c \left\{\xi_n\left[\lambda_{n,h} + \mathbf{u}_{h,n} - g\right] + \xi_{n,h}\left[\lambda_n + \mathbf{u}_n - g\right]\right\} do.$$

Remark 11 The remainder $\mathscr{R}_J^{(3)}$ is also obtained, if the DWR method is applied on other types of problems, see [3, Proposition 6.2] and compare Remark 8. It vanishes, if J is linear or quadratic in $\mathbf{w}$.

Remark 12 The remainder terms $\mathscr{R}_c^{(3)}$ and $\mathscr{R}_f^{(3)}$ are of the same order in the error e_χ^c and e_χ^f as $\mathscr{R}_c^{(2)}$ and $\mathscr{R}_f^{(2)}$ because of the nonsmoothness of C and D.

Proof By applying the Trapezoidal quadrature rule with its remainder term, we obtain

$$\begin{aligned} J(\mathbf{w}) - J(\mathbf{w}_h) &= \int_0^1 J'\left(\mathbf{w}_h + s e_{\mathbf{w}}\right)\left(e_{\mathbf{w}}\right) ds = \frac{1}{2}J'\left(\mathbf{w}_h\right)\left(e_{\mathbf{w}}\right) + \frac{1}{2}J'\left(\mathbf{w}\right)\left(e_{\mathbf{w}}\right) + \mathscr{R}_J^{(3)} \\ &= \frac{1}{2}J'_{\mathbf{u}}\left(\mathbf{w}\right)\left(e_{\mathbf{u}}\right) + \frac{1}{2}J'_{\lambda_n}\left(\mathbf{w}\right)\left(e_{\lambda_n}\right) + \frac{1}{2}J'_{\boldsymbol{\lambda}_t}\left(\mathbf{w}\right)\left(e_{\boldsymbol{\lambda}_t}\right) + \frac{1}{2}J'_{\mathbf{u}}\left(\mathbf{w}_h\right)\left(e_{\mathbf{u}}\right) \\ &\quad + \frac{1}{2}J'_{\lambda_n}\left(\mathbf{w}_h\right)\left(e_{\lambda_n}\right) + \frac{1}{2}J'_{\boldsymbol{\lambda}_t}\left(\mathbf{w}_h\right)\left(e_{\boldsymbol{\lambda}_t}\right) + \mathscr{R}_J^{(3)}. \end{aligned}$$

We know from the proofs of Proposition 3.1 and 3.2 in [47] that

$$\begin{aligned} &c^c\left(\xi_n, e_{\lambda_n}\right) - b^c\left(\xi_n, e_{\mathbf{u}}\right) + c_h^c\left(\xi_{n,h}, e_{\lambda_n}\right) - b_h^c\left(\xi_{n,h}, e_{\mathbf{u}}\right) \\ &\quad = -C\left(\mathbf{w}_h\right)\left(e_{\xi_n}\right) - 2C\left(\mathbf{w}_h\right)\left(\xi_{n,h}\right) + 2\mathscr{R}_c^{(3)}. \end{aligned}$$

From the proof of Proposition 2 together with Lemma 4 and the preceding equations, we deduce

$$\begin{aligned} &J'_{\mathbf{u}}\left(\mathbf{w}\right)\left(e_{\mathbf{u}}\right) + J'_{\lambda_n}\left(\mathbf{w}\right)\left(e_{\lambda_n}\right) + J'_{\boldsymbol{\lambda}_t}\left(\mathbf{w}\right)\left(e_{\boldsymbol{\lambda}_t}\right) \\ &\quad = \left\langle l, e_{\mathbf{y}}\right\rangle - a\left(\mathbf{u}_h, e_{\mathbf{y}}\right) - \left(\lambda_{n,h}, e_{\mathbf{y},n}\right)_{0,\Gamma_C} - \left(\boldsymbol{\lambda}_{t,h}, e_{\mathbf{y},t}\right)_{0,\Gamma_C} - b^c\left(\xi_n, e_{\mathbf{u}}\right) + b^f\left(\boldsymbol{\xi}_t, e_{\mathbf{u}}\right) \\ &\qquad + c^c\left(\xi_n, e_{\lambda_n}\right) + c^f\left(\boldsymbol{\xi}_t, e_{\lambda_n}\right) + d^f\left(\boldsymbol{\xi}_t, e_{\boldsymbol{\lambda}_t}\right) \\ &\quad = \left\langle l, e_{\mathbf{y}}\right\rangle - a\left(\mathbf{u}_h, e_{\mathbf{y}}\right) - \left(\lambda_{n,h}, e_{\mathbf{y},n}\right)_{0,\Gamma_C} - \left(\boldsymbol{\lambda}_{t,h}, e_{\mathbf{y},t}\right)_{0,\Gamma_C} - c_h^c\left(\xi_{n,h}, e_{\lambda_n}\right) + b_h^c\left(\xi_{n,h}, e_{\mathbf{u}}\right) \\ &\qquad - C\left(\mathbf{w}_h\right)\left(\xi_n - \xi_{n,h}\right) - 2C\left(\mathbf{w}_h\right)\left(\xi_{n,h}\right) + 2\mathscr{R}_c^{(3)} - b_h^f\left(\boldsymbol{\xi}_{t,h}, e_{\mathbf{u}}\right) - c_h^f\left(\boldsymbol{\xi}_{t,h}, e_{\lambda_n}\right) \\ &\qquad - d_h^f\left(\boldsymbol{\xi}_{t,h}, e_{\boldsymbol{\lambda}_t}\right) - D\left(\mathbf{w}_h\right)\left(\boldsymbol{\xi}_t - \boldsymbol{\xi}_{t,h}\right) - 2D\left(\mathbf{w}_h\right)\left(\boldsymbol{\xi}_{t,h}\right) + 2\mathscr{R}_f^{(3)} \\ &\quad = \rho\left(\mathbf{w}_h\right)\left(\mathbf{z} - \mathbf{z}_h\right) - c_h^c\left(\xi_{n,h}, e_{\lambda_n}\right) + b_h^c\left(\xi_{n,h}, e_{\mathbf{u}}\right) - b_h^f\left(\boldsymbol{\xi}_{t,h}, e_{\mathbf{u}}\right) - c_h^f\left(\boldsymbol{\xi}_{t,h}, e_{\lambda_n}\right) \\ &\qquad - d_h^f\left(\boldsymbol{\xi}_{t,h}, e_{\boldsymbol{\lambda}_t}\right) - 2C\left(\mathbf{w}_h\right)\left(\xi_{n,h}\right) - 2D\left(\mathbf{w}_h\right)\left(\boldsymbol{\xi}_{t,h}\right) + 2\mathscr{R}_c^{(3)} + 2\mathscr{R}_f^{(3)}. \end{aligned}$$

Inserting the Galerkin orthogonality (11) and the definition of the dual residual ρ^* leads to

$$\begin{aligned}
&J(\mathbf{w}) - J(\mathbf{w}_h) \\
&= \frac{1}{2}\rho(\mathbf{w}_h)(\mathbf{z}-\mathbf{z}_h) + \frac{1}{2}J'_{\mathbf{u}}(\mathbf{w}_h)(e_{\mathbf{u}}) + \frac{1}{2}J'_{\lambda_n}(\mathbf{w}_h)\left(e_{\lambda_n}\right) + \frac{1}{2}J'_{\boldsymbol{\lambda}_t}(\mathbf{w}_h)\left(e_{\boldsymbol{\lambda}_t}\right) \\
&\quad - \frac{1}{2}a(e_{\mathbf{u}}, \mathbf{y}_h) - \frac{1}{2}\left(e_{\lambda_n}, \mathbf{y}_{h,n}\right)_{0,\Gamma_C} - \frac{1}{2}\left(e_{\boldsymbol{\lambda}_t}, \mathbf{y}_{h,t}\right)_{0,\Gamma_C} - \frac{1}{2}c_h^c\left(\xi_{n,h}, e_{\lambda_n}\right) \\
&\quad + \frac{1}{2}b_h^c\left(\xi_{n,h}, e_{\mathbf{u}}\right) - \frac{1}{2}b_h^f\left(\boldsymbol{\xi}_{t,h}, e_{\mathbf{u}}\right) - \frac{1}{2}c_h^f\left(\boldsymbol{\xi}_{t,h}, e_{\lambda_n}\right) - \frac{1}{2}d_h^f\left(\boldsymbol{\xi}_{t,h}, e_{\boldsymbol{\lambda}_t}\right) \\
&\quad - C(\mathbf{w}_h)\left(\xi_{n,h}\right) - D(\mathbf{w}_h)\left(\boldsymbol{\xi}_{t,h}\right) + \mathscr{R}_c^{(3)} + \mathscr{R}_f^{(3)} + \mathscr{R}_J^{(3)} \\
&= \frac{1}{2}\rho(\mathbf{w}_h)(\mathbf{z}-\mathbf{z}_h) + \frac{1}{2}\rho^*(\mathbf{w}_h, \mathbf{z}_h)(\mathbf{w}-\mathbf{w}_h) - C(\mathbf{w}_h)\left(\xi_{n,h}\right) - D(\mathbf{w}_h)\left(\boldsymbol{\xi}_{t,h}\right) \\
&\quad + \mathscr{R}_c^{(3)} + \mathscr{R}_f^{(3)} + \mathscr{R}_J^{(3)},
\end{aligned}$$

which finishes the proof. □

The comparison of primal and dual residual leads to

Proposition 4 *If the second directional derivative of J, $J'' : W \to \mathscr{L}(W, W^*)$, exists and Assumption 1 holds, we obtain for the difference between the primal residual ρ and the dual residual $\rho^\star$*

$$\rho^\star(\mathbf{w}_h, \mathbf{z}_h)(\mathbf{w}-\mathbf{w}_h) = \rho(\mathbf{w}_h)(\mathbf{z}-\mathbf{z}_h) + \Delta J + \Delta C + \Delta D,$$

where

$$\begin{aligned}
\Delta J &= -\int_0^1 J''(\mathbf{w}_h + s e_{\mathbf{w}})(e_{\mathbf{w}}, e_{\mathbf{w}})\, ds, \\
\Delta C &= \int_{\Gamma_C} e_\chi^c \left\{ e_{\xi_n}\left[\lambda_n + \mathbf{u}_n - g\right] - \xi_n\left[e_{\lambda_n} + e_{dis,n}\right]\right\} do, \\
\Delta D &= \sum_{i=1}^4 \Delta D_i, \\
\Delta D_1 &= \int_0^1 \bar{D}''(\mathbf{w}_h + s e_{\mathbf{w}})\left(e_{\mathbf{w}}, e_{\mathbf{w}}, \boldsymbol{\xi}_t\right) ds, \\
\Delta D_2 &= \int_0^1 \bar{D}''(\mathbf{w}_h + s e_{\mathbf{w}})\left(e_{\mathbf{w}}, e_{\mathbf{w}}, e_{\boldsymbol{\xi}_t}\right) s\, ds, \\
\Delta D_3 &= D(\mathbf{w}_h)\left(e_{\boldsymbol{\xi}_t}\right) - \bar{D}(\mathbf{w}_h)\left(e_{\boldsymbol{\xi}_t}\right), \\
\Delta D_4 &= \bar{D}'(\mathbf{w}_h)\left(e_{\mathbf{w}}, \boldsymbol{\xi}_{t,h}\right) - \bar{D}'_h(\mathbf{w}_h)\left(e_{\mathbf{w}}, \boldsymbol{\xi}_{t,h}\right).
\end{aligned}$$

Remark 13 From Proposition 4 we learn that the difference between the primal and the dual residual is of higher order in the error than the remainder terms $\mathscr{R}_c^{(2)}, \mathscr{R}_f^{(2)}, \mathscr{R}_c^{(3)}$,

and $\mathscr{R}_f^{(3)}$. Thus, the difference between the primal and dual residual is no estimate for the remainders $\mathscr{R}_c^{(2)}$ and $\mathscr{R}_f^{(2)}$ in contrast to smooth nonlinear problems, cf. [3, Proposition 6.6 and Remark 6.7].

Remark 14 The term ΔJ equals zero, if the quantity of interest J is linear in $\mathbf{w}$.

Proof The definition of the dual residual ρ^*, the continuous dual problem, and the definition of the primal residual lead to

$$
\begin{aligned}
&\rho^\star\left(\mathbf{w}_h, \mathbf{z}_h\right)\left(e_{\mathbf{w}}\right)\\
&\quad= J'\left(\mathbf{w}_h\right)\left(e_{\mathbf{w}}\right) - a\left(e_{\mathbf{u}}, \mathbf{y}_h\right) + b_h^c\left(\xi_{n,h}, e_{\mathbf{u}}\right) - b_h^f\left(\boldsymbol{\xi}_{t,h}, e_{\mathbf{u}}\right) - \left(e_{\lambda_n}, \mathbf{y}_{h,n}\right)_{0,\Gamma_C}\\
&\qquad- c_h^c\left(\xi_{n,h}, e_{\lambda_n}\right) - c_h^f\left(\boldsymbol{\xi}_{t,h}, e_{\lambda_n}\right) - \left(e_{\boldsymbol{\lambda}_t}, \mathbf{y}_{h,t}\right)_{0,\Gamma_C} - d_h^f\left(\boldsymbol{\xi}_{t,h}, e_{\boldsymbol{\lambda}_t}\right)\\
&\quad= J'\left(\mathbf{w}_h\right)\left(e_{\mathbf{w}}\right) - a\left(e_{\mathbf{u}}, \mathbf{y}_h\right) + b_h^c\left(\xi_{n,h}, e_{\mathbf{u}}\right) - b_h^f\left(\boldsymbol{\xi}_{t,h}, e_{\mathbf{u}}\right) - \left(e_{\lambda_n}, \mathbf{y}_{h,n}\right)_{0,\Gamma_C}\\
&\qquad- c_h^c\left(\xi_{n,h}, e_{\lambda_n}\right) - c_h^f\left(\boldsymbol{\xi}_{t,h}, e_{\lambda_n}\right) - \left(e_{\boldsymbol{\lambda}_t}, \mathbf{y}_{h,t}\right)_{0,\Gamma_C} - d_h^f\left(\boldsymbol{\xi}_{t,h}, e_{\boldsymbol{\lambda}_t}\right) - J'\left(\mathbf{w}\right)\left(e_{\mathbf{w}}\right)\\
&\qquad+ a\left(e_{\mathbf{u}}, \mathbf{y}\right) - b^c\left(\xi_n, e_{\mathbf{u}}\right) + b^f\left(\boldsymbol{\xi}_t, e_{\mathbf{u}}\right) + \left(e_{\lambda_n}, \mathbf{y}_n\right)_{0,\Gamma_C} + c^c\left(\xi_n, e_{\lambda_n}\right)\\
&\qquad+ c^f\left(\boldsymbol{\xi}_t, e_{\lambda_n}\right) + \left(e_{\boldsymbol{\lambda}_t}, \mathbf{y}_t\right)_{0,\Gamma_C} + d^f\left(\boldsymbol{\xi}_t, e_{\boldsymbol{\lambda}_t}\right)\\
&\quad= -\int_0^1 J''\left(\mathbf{w}_h + s e_{\mathbf{w}}\right)\left(e_{\mathbf{w}}, e_{\mathbf{w}}\right)\, ds + a\left(e_{\mathbf{u}}, e_{\mathbf{y}}\right) + \left(e_{\lambda_n}, e_{\mathbf{y},n}\right)_{0,\Gamma_C} + \left(e_{\boldsymbol{\lambda}_t}, e_{\mathbf{y},t}\right)_{0,\Gamma_C}\\
&\qquad+ b_h^c\left(\xi_{n,h}, e_{\mathbf{u}}\right) - b^c\left(\xi_n, e_{\mathbf{u}}\right) - c_h^c\left(\xi_{n,h}, e_{\lambda_n}\right) + c^c\left(\xi_n, e_{\lambda_n}\right) - b_h^f\left(\boldsymbol{\xi}_{t,h}, e_{\mathbf{u}}\right)\\
&\qquad+ b^f\left(\boldsymbol{\xi}_t, e_{\mathbf{u}}\right) - c_h^f\left(\boldsymbol{\xi}_{t,h}, e_{\lambda_n}\right) + c^f\left(\boldsymbol{\xi}_t, e_{\lambda_n}\right) - d_h^f\left(\boldsymbol{\xi}_{t,h}, e_{\boldsymbol{\lambda}_t}\right) + d^f\left(\boldsymbol{\xi}_t, e_{\boldsymbol{\lambda}_t}\right)\\
&\quad= \Delta J + \rho\left(\mathbf{w}_h\right)\left(\mathbf{z} - \mathbf{z}_h\right) + C\left(\mathbf{w}_h\right)\left(e_{\xi_n}\right) + D\left(\mathbf{w}_h\right)\left(e_{\boldsymbol{\xi}_t}\right) - c_h^c\left(\xi_{n,h}, e_{\lambda_n}\right)\\
&\qquad+ b_h^c\left(\xi_{n,h}, e_{\mathbf{u}}\right) + c^c\left(\xi_n, e_{\lambda_n}\right) - b^c\left(\xi_n, e_{\mathbf{u}}\right) - b_h^f\left(\boldsymbol{\xi}_{t,h}, e_{\mathbf{u}}\right) - c_h^f\left(\boldsymbol{\xi}_{t,h}, e_{\boldsymbol{\lambda}_t}\right)\\
&\qquad- d_h^f\left(\boldsymbol{\xi}_{t,h}, e_{\boldsymbol{\lambda}_t}\right) + b^f\left(\boldsymbol{\xi}_t, e_{\mathbf{u}}\right) + c^f\left(\boldsymbol{\xi}_t, e_{\lambda_n}\right) + d^f\left(\boldsymbol{\xi}_t, e_{\boldsymbol{\lambda}_t}\right).
\end{aligned}
$$

From Proposition 3.3 in [47] we know

$$
C\left(\mathbf{w}_h\right)\left(e_{\xi_n}\right) - \left[c_h^c\left(\xi_{n,h}, e_{\lambda_n}\right) - b_h^c\left(\xi_{n,h}, e_{\mathbf{u}}\right)\right] + c^c\left(\xi_n, e_{\lambda_n}\right) - b^c\left(\xi_n, e_{\mathbf{u}}\right) = \Delta C.
$$

The Eqs. (16) and (18) imply

$$
\begin{aligned}
&D\left(\mathbf{w}_h\right)\left(e_{\boldsymbol{\xi}_t}\right) + b^f\left(\boldsymbol{\xi}_t, e_{\mathbf{u}}\right) + c^f\left(\boldsymbol{\xi}_t, e_{\lambda_n}\right) + d^f\left(\boldsymbol{\xi}_t, e_{\boldsymbol{\lambda}_t}\right)\\
&\qquad- \left[b_h^f\left(\boldsymbol{\xi}_{t,h}, e_{\mathbf{u}}\right) + c_h^f\left(\boldsymbol{\xi}_{t,h}, e_{\boldsymbol{\lambda}_t}\right) + d_h^f\left(\boldsymbol{\xi}_{t,h}, e_{\boldsymbol{\lambda}_t}\right)\right]\\
&\quad= D\left(\mathbf{w}_h\right)\left(e_{\boldsymbol{\xi}_t}\right) + \bar{D}'\left(\mathbf{w}\right)\left(e_{\mathbf{w}}, \boldsymbol{\xi}_t\right) - \bar{D}_h'\left(\mathbf{w}_h\right)\left(e_{\mathbf{w}}, \boldsymbol{\xi}_{t,h}\right)\\
&\quad= D\left(\mathbf{w}_h\right)\left(e_{\boldsymbol{\xi}_t}\right) + \bar{D}'\left(\mathbf{w}\right)\left(e_{\mathbf{w}}, \boldsymbol{\xi}_t\right) - \bar{D}'\left(\mathbf{w}_h\right)\left(e_{\mathbf{w}}, \boldsymbol{\xi}_t\right) + \bar{D}'\left(\mathbf{w}_h\right)\left(e_{\mathbf{w}}, \boldsymbol{\xi}_t\right)\\
&\qquad- \bar{D}_h'\left(\mathbf{w}_h\right)\left(e_{\mathbf{w}}, \boldsymbol{\xi}_{t,h}\right)\\
&\quad= D\left(\mathbf{w}_h\right)\left(e_{\boldsymbol{\xi}_t}\right) + \int_0^1 \bar{D}''\left(\mathbf{w}_h + s e_{\mathbf{w}}\right)\left(e_{\mathbf{w}}, e_{\mathbf{w}}, \boldsymbol{\xi}_t\right)\, ds + \bar{D}'\left(\mathbf{w}_h\right)\left(e_{\mathbf{w}}, \boldsymbol{\xi}_t\right)\\
&\qquad- \bar{D}_h'\left(\mathbf{w}_h\right)\left(e_{\mathbf{w}}, \boldsymbol{\xi}_{t,h}\right)
\end{aligned}
$$

$$= D(\mathbf{w}_h)\left(e_{\xi_t}\right) + \Delta D_1 + \bar{D}'(\mathbf{w}_h)\left(e_{\mathbf{w}}, \boldsymbol{\xi}_t\right) - \bar{D}'_h(\mathbf{w}_h)\left(e_{\mathbf{w}}, \boldsymbol{\xi}_{t,h}\right).$$

Furthermore, we find using $D(\mathbf{w})\left(e_{\xi_t}\right) = \bar{D}(\mathbf{w})\left(e_{\xi_t}\right) = 0$ and the box quadrature rule with its remainder that

$$\begin{aligned}
&D(\mathbf{w}_h)\left(e_{\xi_t}\right) + \bar{D}'(\mathbf{w}_h)\left(e_{\mathbf{w}}, \boldsymbol{\xi}_t\right) - \bar{D}'_h(\mathbf{w}_h)\left(e_{\mathbf{w}}, \boldsymbol{\xi}_{t,h}\right) + \Delta D_1 \\
&= D(\mathbf{w}_h)\left(e_{\xi_t}\right) + \bar{D}'(\mathbf{w}_h)\left(e_{\mathbf{w}}, e_{\xi_t}\right) + \bar{D}'(\mathbf{w}_h)\left(e_{\mathbf{w}}, \boldsymbol{\xi}_{t,h}\right) - \bar{D}'_h(\mathbf{w}_h)\left(e_{\mathbf{w}}, \boldsymbol{\xi}_{t,h}\right) + \Delta D_1 \\
&= \bar{D}(\mathbf{w}_h)\left(e_{\xi_t}\right) - \bar{D}(\mathbf{w})\left(e_{\xi_t}\right) + \bar{D}'(\mathbf{w}_h)\left(e_{\mathbf{w}}, e_{\xi_t}\right) - \bar{D}(\mathbf{w}_h)\left(e_{\xi_t}\right) + D(\mathbf{w}_h)\left(e_{\xi_t}\right) \\
&\quad + \Delta D_1 + \Delta D_4 \\
&= -\int_0^1 \bar{D}'(\mathbf{w}_h + s e_{\mathbf{w}})\left(e_{\mathbf{w}}, e_{\xi_t}\right) ds + \bar{D}'(\mathbf{w}_h)\left(e_{\mathbf{w}}, e_{\xi_t}\right) + \Delta D_1 + \Delta D_3 + \Delta D_4 \\
&= \int_0^1 \bar{D}''(\mathbf{w}_h + s e_{\mathbf{w}})\left(e_{\mathbf{w}}, e_{\mathbf{w}}, e_{\xi_t}\right) s\, ds + \Delta D_1 + \Delta D_3 + \Delta D_4 \\
&= \Delta D_1 + \Delta D_2 + \Delta D_3 + \Delta D_4 = \Delta D.
\end{aligned}$$

Combining the different parts, we get the assertion. □

3.3 Estimation of model and discretization error

As last result in this section, we estimate the error $J(\mathbf{w}^r) - J(\mathbf{w}_h)$ including the modeling as well as the discretization error in the quantity of interest. We define

$$\begin{aligned}
e_{\mathbf{w}}^{r,h} &= \left(e_{\mathbf{u}}^{r,h}, e_{\lambda_n}^{r,h}, e_{\boldsymbol{\lambda}_t}^{r,h}\right) = \left(\mathbf{u}^r - \mathbf{u}_h, \lambda_n^r - \lambda_{n,h}, \boldsymbol{\lambda}_t^r - \boldsymbol{\lambda}_{t,h}\right), \\
e_{\mathbf{z}}^{r,h} &= \left(e_{\mathbf{y}}^{r,h}, e_{\xi_n}^{r,h}, e_{\boldsymbol{\xi}_t}^{r,h}\right) = \left(\mathbf{y}^r - \mathbf{y}_h, \xi_n^r - \xi_{n,h}, \boldsymbol{\xi}_t^r - \boldsymbol{\xi}_{t,h}\right).
\end{aligned}$$

Furthermore, we set $e_{\chi^c}^{r,h} := \chi_r^c - \chi_h^c$ and $e_{\chi^f}^{r,h} := \chi_r^f - \chi_h^f$. In addition, we need an analogous result to Lemma 2:

Lemma 5 *It holds*

$$\begin{aligned}
&b_h^f\left(\boldsymbol{\xi}_{t,h}, e_{\mathbf{u}}^{r,h}\right) + c_h^f\left(\boldsymbol{\xi}_{t,h}, e_{\lambda_n}^{r,h}\right) + d_h^f\left(\boldsymbol{\xi}_{t,h}, e_{\boldsymbol{\lambda}_t}^{r,h}\right) \\
&\quad + b_r^f\left(\boldsymbol{\xi}_t^r, e_{\mathbf{u}}^{r,h}\right) + c_r^f\left(\boldsymbol{\xi}_t^r, e_{\lambda_n}^{r,h}\right) + d_r^f\left(\boldsymbol{\xi}_t^r, e_{\boldsymbol{\lambda}_t}^{r,h}\right) + D(\mathbf{w}_h)\left(e_{\boldsymbol{\xi}_t}^{r,h}\right) \\
&= -2D(\mathbf{w}_h)\left(\boldsymbol{\xi}_{t,h}\right) - 2\Delta(\mathbf{w}_h)\left(\boldsymbol{\xi}_{t,h}\right) - 2\Delta(\mathbf{w}_h)\left(e_{\mathbf{z}}^{r,h}\right) - \bar{\Delta}\left(e_{\mathbf{w}}^{r,h}, e_{\mathbf{z}}^{r,h}\right) + 2\mathscr{R}_f^{m,h}
\end{aligned}$$

with the remainder term $\mathscr{R}_f^{m,h} = \mathscr{R}_{\chi,1}^{m,h} + \mathscr{R}_{\chi,2}^{m,h} + \mathscr{R}_Q^{m,h}$,

$$\begin{aligned}
\mathscr{R}_{\chi,1}^{m,h} &= -\left(\boldsymbol{\xi}_t^r, \left(\chi_r^f(\mathbf{w}^r) - \chi_r^f(\mathbf{w}_h)\right)\left(n(\mathbf{w}_h)\boldsymbol{\lambda}_{t,h} - s^r(\lambda_{n,h})\boldsymbol{\lambda}_{t,h}\right)\right)_{0,\Gamma_C}, \\
\mathscr{R}_{\chi,2}^{m,h} &= -\frac{1}{2}\left[\left(\bar{D}^r\right)'(\mathbf{w}_h)\left(e_{\mathbf{w}}^{r,h}, \boldsymbol{\xi}_{t,h}\right) - \bar{D}'_h(\mathbf{w}_h)\left(e_{\mathbf{w}}^{r,h}, \boldsymbol{\xi}_{t,h}\right)\right]
\end{aligned}$$

$$\mathscr{R}_Q^{m,h} = \frac{1}{2}\int_0^1 \left(\bar{D}^r\right)''' \left(\mathbf{w} + s e_{\mathbf{w}}^{r,h}\right)\left(e_{\mathbf{w}}^{r,h}, e_{\mathbf{w}}^{r,h}, e_{\mathbf{w}}^{r,h}, \boldsymbol{\xi}_t^r\right) s(s-1)\, ds,$$

Proof The definition of $\bar{D}^r$ leads to

$$\begin{aligned}
&\bar{D}^r\left(\mathbf{w}_h\right)\left(\boldsymbol{\xi}_t^r\right)\\
&= \left(\boldsymbol{\xi}_t^r, \chi_r^f\left(n\left(\mathbf{w}_h\right)\boldsymbol{\lambda}_{t,h} - s^r\left(\lambda_{n,h}\right)\boldsymbol{\lambda}_{t,h}\right) - s^r\left(\lambda_{n,h}\right)\mathbf{u}_{h,t}\right)_{0,\Gamma_C}\\
&= \left(\boldsymbol{\xi}_t^r, \left(\chi_r^f\left(\mathbf{w}^r\right) - \chi_r^f\left(\mathbf{w}_h\right)\right)\left(n\left(\mathbf{w}_h\right)\boldsymbol{\lambda}_{t,h} - s^r\left(\lambda_{n,h}\right)\boldsymbol{\lambda}_{t,h}\right)\right)_{0,\Gamma_C}\\
&\quad + \left(\boldsymbol{\xi}_t^r, \chi_r^f\left(\mathbf{w}_h\right)\left(n\left(\mathbf{w}_h\right)\boldsymbol{\lambda}_{t,h} - s^r\left(\lambda_{n,h}\right)\boldsymbol{\lambda}_{t,h}\right) - s^r\left(\lambda_{n,h}\right)\mathbf{u}_{h,t}\right)_{0,\Gamma_C}\\
&= -\mathscr{R}_{\chi,1}^{m,h} + D^r\left(\mathbf{w}_h\right)\left(\boldsymbol{\xi}_t^r\right) = D^r\left(\mathbf{w}_h\right)\left(e_{\boldsymbol{\xi}_t}^{r,h}\right) + D^r\left(\mathbf{w}_h\right)\left(\boldsymbol{\xi}_{t,h}\right) - \mathscr{R}_{\chi,1}^{m,h}\\
&= D^r\left(\mathbf{w}_h\right)\left(e_{\boldsymbol{\xi}_t}^{r,h}\right) - D\left(\mathbf{w}_h\right)\left(e_{\boldsymbol{\xi}_t}^{r,h}\right) + D^r\left(\mathbf{w}_h\right)\left(\boldsymbol{\xi}_{t,h}\right) - D\left(\mathbf{w}_h\right)\left(\boldsymbol{\xi}_{t,h}\right)\\
&\quad + D\left(\mathbf{w}_h\right)\left(e_{\boldsymbol{\xi}_t}^{r,h}\right) + D\left(\mathbf{w}_h\right)\left(\boldsymbol{\xi}_{t,h}\right) - \mathscr{R}_{\chi,1}^{m,h}\\
&= \Delta\left(\mathbf{w}_h\right)\left(e_{\boldsymbol{\xi}_t}^{r,h}\right) + \Delta\left(\mathbf{w}_h\right)\left(\boldsymbol{\xi}_{t,h}\right) + D\left(\mathbf{w}_h\right)\left(e_{\boldsymbol{\xi}_t}^{r,h}\right) + D\left(\mathbf{w}_h\right)\left(\boldsymbol{\xi}_{t,h}\right) - \mathscr{R}_{\chi,1}^{m,h}.
\end{aligned}$$

The trapezoidal rule with its remainder term together with

$$\bar{D}^r\left(\mathbf{w}^r\right)\left(\boldsymbol{\mu}_t\right) = D^r\left(\mathbf{w}^r\right)\left(\boldsymbol{\mu}_t\right) = 0$$

and the preceding calculations lead to

$$\begin{aligned}
&-\Delta\left(\mathbf{w}_h\right)\left(e_{\boldsymbol{\xi}_t}^{r,h}\right) - \Delta\left(\mathbf{w}_h\right)\left(\boldsymbol{\xi}_{t,h}\right) - D\left(\mathbf{w}_h\right)\left(e_{\boldsymbol{\xi}_t}^{r,h}\right) - D\left(\mathbf{w}_h\right)\left(\boldsymbol{\xi}_{t,h}\right) + \mathscr{R}_{\chi,1}^{m,h}\\
&= \bar{D}^r\left(\mathbf{w}^r\right)\left(\boldsymbol{\xi}_t^r\right) - \bar{D}^r\left(\mathbf{w}_h\right)\left(\boldsymbol{\xi}_t^r\right)\\
&= \int_0^1 \left(\bar{D}^r\right)'\left(\mathbf{w}_h + s e_{\mathbf{w}}^{r,h}\right)\left(e_{\mathbf{w}}^{r,h}, \boldsymbol{\xi}_t^r\right) ds\\
&= \frac{1}{2}\left(\bar{D}^r\right)'\left(\mathbf{w}_h\right)\left(e_{\mathbf{w}}^{r,h}, \boldsymbol{\xi}_t^r\right) + \frac{1}{2}\left(\bar{D}^r\right)'\left(\mathbf{w}^r\right)\left(e_{\mathbf{w}}^{r,h}, \boldsymbol{\xi}_t^r\right) - \mathscr{R}_Q^{m,h}.
\end{aligned}$$

We use Eq. (15) and

$$\begin{aligned}
&\left(\bar{D}^r\right)'\left(\mathbf{w}_h\right)\left(e_{\mathbf{w}}^{r,h}, \boldsymbol{\xi}_t^r\right)\\
&= \left(\bar{D}^r\right)'\left(\mathbf{w}_h\right)\left(e_{\mathbf{w}}^{r,h}, e_{\boldsymbol{\xi}_t}^{r,h}\right) + \left(\bar{D}^r\right)'\left(\mathbf{w}_h\right)\left(e_{\mathbf{w}}^{r,h}, \boldsymbol{\xi}_{t,h}\right) - \bar{D}_h'\left(\mathbf{w}_h\right)\left(e_{\mathbf{w}}^{r,h}, \boldsymbol{\xi}_{t,h}\right)\\
&\quad + \bar{D}_h'\left(\mathbf{w}_h\right)\left(e_{\mathbf{w}}^{r,h}, \boldsymbol{\xi}_{t,h}\right)\\
&= \bar{\Delta}\left(e_{\mathbf{w}}^{r,h}, e_{\boldsymbol{\xi}_t}^{r,h}\right) - 2\mathscr{R}_{\chi,2}^{m,h} + b_h^f\left(\boldsymbol{\xi}_{t,h}, e_{\mathbf{u}}^{r,h}\right) + c_h^f\left(\boldsymbol{\xi}_{t,h}, e_{\lambda_n}^{r,h}\right) + d_h^f\left(\boldsymbol{\xi}_{t,h}, e_{\boldsymbol{\lambda}_t}^{r,h}\right),
\end{aligned}$$

apply (18) to deduce the assertion by combining the single terms. □

Applying the above presented lemma, we obtain the following error identity for the error w.r.t. modeling and discretization:

Proposition 5 *We assume that the third directional derivative of J,*

$$J''' : W \to \mathscr{L}(W, \mathscr{L}(W, W^*)),$$

exist and that Assumption 1 holds. Then, the error identity

$$\begin{aligned} &J\left(\mathbf{w}^r\right) - J\left(\mathbf{w}_h\right) \\ &\quad = -\Delta\left(\mathbf{w}_h\right)\left(\mathbf{z}_h\right) + \frac{1}{2}\rho\left(\mathbf{w}_h\right)\left(e_{\mathbf{z}}\right) + \frac{1}{2}\rho^*\left(\mathbf{w}_h, \mathbf{z}_h\right)\left(e_{\mathbf{w}}\right) - C\left(\mathbf{w}_h\right)\left(\xi_{n,h}\right) \\ &\qquad - D\left(\mathbf{w}_h\right)\left(\boldsymbol{\xi}_{t,h}\right) - \Delta\left(\mathbf{w}_h\right)\left(e_{\mathbf{z}}^{r,h}\right) - \frac{1}{2}\bar{\Delta}\left(e_{\mathbf{w}}^{r,h}, e_{\mathbf{z}}^{r,h}\right) + \mathscr{R}_J^{m,h} + \mathscr{R}_c^{m,h} + \mathscr{R}_f^{m,h} \end{aligned} \tag{21}$$

holds for the model and discretization error in the quantity of interest. Here, the remainder terms are given by

$$\mathscr{R}_J^{m,h} = \frac{1}{2}\int_0^1 J'''\left(\mathbf{w}_h + s e_{\mathbf{w}}^{r,h}\right)\left(e_{\mathbf{w}}^{r,h}, e_{\mathbf{w}}^{r,h}, e_{\mathbf{w}}^{r,h}\right) s(s-1)\, ds$$

w.r.t. the quantity of interest J,

$$\mathscr{R}_c^{m,h} = \frac{1}{2}\int_{\Gamma_C} \xi_n^r e_\chi^{c,r}\left[\lambda_{n,h} + \mathbf{u}_{h,n} - g\right] + \xi_{n,h} e_\chi^{c,r}\left[\lambda_n^r + \mathbf{u}_n^r - g\right] do$$

and $\mathscr{R}_f^m$ from Lemma 2.

Remark 15 The remainder $\mathscr{R}_J^{m,h}$ is of third order in the error $e_{\mathbf{w}}^{r,h}$ and equals mainly the remainders $\mathscr{R}_J^m$ from Propositon 1 and $\mathscr{R}_J^{(3)}$ from Proposition 3. The remainder $\mathscr{R}_c^{m,h}$ is of the same structure as $\mathscr{R}_c^{(3)}$ in Proposition 3.

Proof The starting point is again the application of the trapezoidal rule with its remainder leading to

$$\begin{aligned} J\left(\mathbf{w}^r\right) - J\left(\mathbf{w}_h\right) &= \int_0^1 J'\left(\mathbf{w}_h + s e_{\mathbf{w}}^{r,h}\right)\left(e_{\mathbf{w}}^{r,h}\right) ds \\ &= \frac{1}{2}J'\left(\mathbf{w}_h\right)\left(e_{\mathbf{w}}^{r,h}\right) + \frac{1}{2}J'\left(\mathbf{w}^r\right)\left(e_{\mathbf{w}}^{r,h}\right) + \mathscr{R}_J^{m,h}. \end{aligned}$$

We now proceed as in the proof of Proposition 1. However, we have to take into account that (11) holds instead of (9). Thus, we obtain by (11)

$$\begin{aligned} &a\left(e_{\mathbf{u}}^{r,h}, \mathbf{y}^r\right) + \left(e_{\lambda_n}^{r,h}, \mathbf{y}_n^r\right)_{0,\Gamma_C} + \left(e_{\boldsymbol{\lambda}_t}^{r,h}, \mathbf{y}_t^r\right)_{0,\Gamma_C} \\ &\quad = a\left(e_{\mathbf{u}}^{r,h}, e_{\mathbf{y}}^{r,h}\right) + \left(e_{\lambda_n}^{r,h}, e_{\mathbf{y},n}^{r,h}\right)_{0,\Gamma_C} + \left(e_{\boldsymbol{\lambda}_t}^{r,h}, e_{\mathbf{y},t}^{r,h}\right)_{0,\Gamma_C} \end{aligned}$$

$$= \rho\left(\mathbf{w}_h\right)\left(e_{\mathbf{z}}^{r,h}\right) + C\left(\mathbf{w}_h\right)\left(e_{\xi_n}^{r}\right) + D\left(\mathbf{w}_h\right)\left(e_{\boldsymbol{\xi}_t}^{r}\right).$$

The defintions of the continuous dual problem (12–14) and the preceding calculation imply

$$\begin{aligned}
J'\left(\mathbf{w}^r\right)\left(e_{\mathbf{w}}^{r,h}\right) &= a\left(e_{\mathbf{u}}^{r,h}, \mathbf{y}^r\right) - b_r^c\left(\xi_n^r, e_{\mathbf{u}}^{r,h}\right) + b_r^f\left(\boldsymbol{\xi}_t^r, e_{\mathbf{u}}^{r,h}\right) + \left(e_{\lambda_n}^{r,h}, \mathbf{y}_n^r\right)_{0,\Gamma_C} \\
&\quad + c_r^c\left(\xi_n^r, e_{\lambda_n}^{r,h}\right) + c_r^f\left(\boldsymbol{\xi}_t^r, e_{\lambda_n}^{r,h}\right) + \left(e_{\boldsymbol{\lambda}_t}^{r,h}, \mathbf{y}_t^r\right)_{0,\Gamma_C} + d_r^f\left(\boldsymbol{\xi}_t^r, e_{\boldsymbol{\lambda}_t}^{r,h}\right) \\
&= \rho\left(\mathbf{w}_h\right)\left(e_{\mathbf{z}}^{r,h}\right) + C\left(\mathbf{w}_h\right)\left(e_{\xi_n}^{r,h}\right) + D\left(\mathbf{w}_h\right)\left(e_{\boldsymbol{\xi}_t}^{r,h}\right) - b_r^c\left(\xi_n^r, e_{\mathbf{u}}^{r,h}\right) \\
&\quad + b_r^f\left(\boldsymbol{\xi}_t^r, e_{\mathbf{u}}^{r,h}\right) + c_r^c\left(\xi_n^r, e_{\lambda_n}^{r,h}\right) + c_r^f\left(\boldsymbol{\xi}_t^r, e_{\lambda_n}^{r,h}\right) + d_r^f\left(\boldsymbol{\xi}_t^r, e_{\boldsymbol{\lambda}_t}^{r,h}\right).
\end{aligned}$$

By (11) and the definition of the dual residual ρ^*, we deduce

$$\begin{aligned}
&J'\left(\mathbf{w}^r\right)\left(e_{\mathbf{w}}^{r,h}\right) \\
&= J'\left(\mathbf{w}^r\right)\left(e_{\mathbf{w}}^{r,h}\right) - a\left(e_{\mathbf{u}}^{r,h}, \mathbf{y}_h\right) - \left(e_{\lambda_n}^{r,h}, \mathbf{y}_{h,n}\right)_{0,\Gamma_C} - \left(e_{\boldsymbol{\lambda}_t}^{r,h}, \mathbf{y}_{h,t}\right)_{0,\Gamma_C} \\
&\quad + b_h^c\left(\xi_{n,h}, e_{\mathbf{u}}^{r,h}\right) - b_h^f\left(\boldsymbol{\xi}_{t,h}, e_{\mathbf{u}}^{r,h}\right) - c_h^c\left(\xi_{n,h}, e_{\lambda_n}^{r,h}\right) \\
&\quad - c_h^f\left(\boldsymbol{\xi}_{t,h}, e_{\lambda_n}^{r,h}\right) - d_h^f\left(\boldsymbol{\xi}_{t,h}, e_{\boldsymbol{\lambda}_t}^{r,h}\right) \\
&\quad - b_h^c\left(\xi_{n,h}, e_{\mathbf{u}}^{r,h}\right) + b_h^f\left(\boldsymbol{\xi}_{t,h}, e_{\mathbf{u}}^{r,h}\right) + c_h^c\left(\xi_{n,h}, e_{\lambda_n}^{r,h}\right) \\
&\quad + c_h^f\left(\boldsymbol{\xi}_{t,h}, e_{\lambda_n}^{r,h}\right) + d_h^f\left(\boldsymbol{\xi}_{t,h}, e_{\boldsymbol{\lambda}_t}^{r,h}\right) \\
&= -b_h^c\left(\xi_{n,h}, e_{\mathbf{u}}^{r,h}\right) + b_h^f\left(\boldsymbol{\xi}_{t,h}, e_{\mathbf{u}}^{r,h}\right) + c_h^c\left(\xi_{n,h}, e_{\lambda_n}^{r,h}\right) + c_h^f\left(\boldsymbol{\xi}_{t,h}, e_{\lambda_n}^{r,h}\right) \\
&\quad + d_h^f\left(\boldsymbol{\xi}_{t,h}, e_{\boldsymbol{\lambda}_t}^{r,h}\right) + \rho^*\left(\mathbf{w}_h, \mathbf{z}_h\right)\left(e_{\mathbf{w}}^{r,h}\right)
\end{aligned}$$

By the same technique as in the proofs of Propositions 3.1 and 3.2 in [47], we obtain

$$\begin{aligned}
&c_r^c\left(\xi_n^r, e_{\lambda_n}^{r,h}\right) - b_r^c\left(\xi_n^r, e_{\mathbf{u}}^{r,h}\right) + c_h^c\left(\xi_{n,h}, e_{\lambda_n}^{r,h}\right) - b_h^c\left(\xi_{n,h}, e_{\mathbf{u}}^{r,h}\right) + C\left(\mathbf{w}_h\right)\left(e_{\xi_n}^{r,h}\right) \\
&= c_r^c\left(\xi_n^r, e_{\lambda_n}^{r,h}\right) - b_r^c\left(\xi_n^r, e_{\mathbf{u}}^{r,h}\right) + C\left(\mathbf{w}_h\right)\left(\xi_n^r\right) \\
&\quad + c_h^c\left(\xi_{n,h}, e_{\lambda_n}^{r,h}\right) - b_h^c\left(\xi_{n,h}, e_{\mathbf{u}}^{r,h}\right) + C\left(\mathbf{w}_h\right)\left(\xi_{n,h}\right) - 2C\left(\mathbf{w}_h\right)\left(\xi_{n,h}\right) \\
&= \int_{\Gamma_C} \xi_n^r e_{\chi^c}^{r,h}\left[\lambda_{n,h} + \mathbf{u}_{h,n} - g\right] + \xi_{n,h} e_{\chi^c}^{r,h}\left[\lambda_n^r + \mathbf{u}_n^r - g\right] do - 2C\left(\mathbf{w}_h\right)\left(\xi_{n,h}\right) \\
&= 2\mathscr{R}_c^{m,h} - 2C\left(\mathbf{w}_h\right)\left(\xi_{n,h}\right).
\end{aligned}$$

All in all, we deduce applying Lemma 5

$$
\begin{aligned}
&2\left(J\left(\mathbf{w}^r\right)-J\left(\mathbf{w}_h\right)\right)\\
&\quad=J'\left(\mathbf{w}_h\right)\left(e_{\mathbf{w}}^{r,h}\right)+J'\left(\mathbf{w}^r\right)\left(e_{\mathbf{w}}^{r,h}\right)+2\mathscr{R}_J^{m,h}\\
&\quad=\rho\left(\mathbf{w}_h\right)\left(e_{\mathbf{z}}^{r,h}\right)+\rho^*\left(\mathbf{w}_h,\mathbf{z}_h\right)\left(e_{\mathbf{w}}^{r,h}\right)+2\mathscr{R}_J^{m,h}\\
&\qquad+c_r^c\left(\xi_n^r,e_{\lambda_n}^{r,h}\right)-b_r^c\left(\xi_n^r,e_{\mathbf{u}}^{r,h}\right)+c_h^c\left(\xi_{n,h},e_{\lambda_n}^{r,h}\right)\\
&\qquad-b_h^c\left(\xi_{n,h},e_{\mathbf{u}}^{r,h}\right)+C\left(\mathbf{w}_h\right)\left(e_{\xi_n}^{r,h}\right)\\
&\qquad+b_h^f\left(\boldsymbol{\xi}_{t,h},e_{\mathbf{u}}^{r,h}\right)+c_h^f\left(\boldsymbol{\xi}_{t,h},e_{\lambda_n}^{r,h}\right)+d_h^f\left(\boldsymbol{\xi}_{t,h},e_{\boldsymbol{\lambda}_t}^{r,h}\right)\\
&\qquad+b_r^f\left(\boldsymbol{\xi}_t^r,e_{\mathbf{u}}^{r,h}\right)+c_r^f\left(\boldsymbol{\xi}_t^r,e_{\lambda_n}^{r,h}\right)+d_r^f\left(\boldsymbol{\xi}_t^r,e_{\boldsymbol{\lambda}_t}^{r,h}\right)+D\left(\mathbf{w}_h\right)\left(e_{\boldsymbol{\xi}_t}^{r,h}\right)\\
&\quad=\rho\left(\mathbf{w}_h\right)\left(e_{\mathbf{z}}^{r,h}\right)+\rho^*\left(\mathbf{w}_h,\mathbf{z}_h\right)\left(e_{\mathbf{w}}^{r,h}\right)+2\mathscr{R}_J^{m,h}+2\mathscr{R}_c^{m,h}-2C\left(\mathbf{w}_h\right)\left(\xi_{n,h}\right)\\
&\qquad-2D\left(\mathbf{w}_h\right)\left(\boldsymbol{\xi}_{t,h}\right)-2\Delta\left(\mathbf{w}_h\right)\left(\boldsymbol{\xi}_{t,h}\right)-2\Delta\left(\mathbf{w}_h\right)\left(e_{\mathbf{z}}^{r,h}\right)-\bar{\Delta}\left(e_{\mathbf{w}}^{r,h},e_{\mathbf{z}}^{r,h}\right)+2\mathscr{R}_f^{m,h}.
\end{aligned}
$$

Division by 2 then gives the assertion. □

4 Numerical evaluation of the error identities

The error identities (19), (20), and (21) from Propositions 2, 3 and 5 cannot be evaluated numerically, because they involve the analytic solutions $\mathbf{w}$ and $\mathbf{z}$ as well as the unknown remainder terms. The remainder terms $\mathscr{R}_J^{(2)}$, $\mathscr{R}_J^{(3)}$, and $\mathscr{R}_J^{m,h}$ are of second and third order in the error, respectively, which implies that they are of higher order and negligible. The remainder terms with respect to the geometrical contact conditions, $\mathscr{R}_c^{(2)}$, $\mathscr{R}_c^{(3)}$ and $\mathscr{R}_c^{m,h}$, are of first order in the error of the active set. Numerical examples substantiate that they are decreasing fast. However, a strict analysis of there convergence properties is missing and strongly depends on the chosen discretization. The remainder terms $\mathscr{R}_f^{(2)}$, $\mathscr{R}_f^{(3)}$ and $\mathscr{R}_f^{m,h}$ with respect to the friction conditions consist of terms which are of first order in the error of the frictional active set and ones which are of higher order in the error. While it is clear that the second ones can be neglected, the same is not true for the first ones. However, the remarks for the remainder terms $\mathscr{R}_c^{(2)}$, $\mathscr{R}_c^{(3)}$ and $\mathscr{R}_c^{m,h}$ also hold here. The remaining terms $\Delta\left(\mathbf{w}_h\right)\left(e_{\mathbf{z}}^{r,h}\right)$ and $\frac{1}{2}\bar{\Delta}\left(e_{\mathbf{w}}^{r,h},e_{\mathbf{z}}^{r,h}\right)$, which arise in the estimation of the model error, are of second as well as third order in the error and are neglected. The numerical results in Sect. 5 substantiate that neglecting the remainder terms is feasible. Beside the remainder terms, the error identities also include the analytic primal and dual solution, which have to be numerically approximated. The corresponding discretization dependent operator is denoted by $\mathscr{A}$. We refer to [3, Section 4.1 and Section 5.2] for an overview of possible choices and their mathematical justification under strong smoothness assumptions.

All in all, we obtain the primal error estimator

$$
J\left(\mathbf{w}\right)-J\left(\mathbf{w}_h\right)\approx\eta_p:=\rho\left(\mathbf{w}_h\right)\left(\mathscr{A}\left(\mathbf{z}_h\right)-\mathbf{z}_h\right)-C\left(\mathbf{w}_h\right)\left(\xi_{n,h}\right)-D\left(\mathbf{w}_h\right)\left(\boldsymbol{\xi}_{t,h}\right),
$$

the primal dual one

$$J(\mathbf{w}) - J(\mathbf{w}_h) \approx \eta := \frac{1}{2}\rho(\mathbf{w}_h)(\mathscr{A}(\mathbf{z}_h) - \mathbf{z}_h) + \frac{1}{2}\rho^*(\mathbf{w}_h, \mathbf{z}_h)(\mathscr{A}(\mathbf{w}_h) - \mathbf{w}_h) - C(\mathbf{w}_h)\left(\xi_{n,h}\right) - D(\mathbf{w}_h)\left(\boldsymbol{\xi}_{t,h}\right),$$

and the model as well as discretization error estimator

$$J\left(\mathbf{w}^r\right) - J(\mathbf{w}_h) \approx -\Delta(\mathbf{w}_h)(\mathbf{z}_h) + \eta = \eta_m + \eta.$$

Up to this point, we have not specified any further assumptions on the discretization. Henceforth, we carry out further steps to obtain concrete error estimators for a mixed discretization. It was first proposed for geometrical contact problems in [26] and extended to frictional contact problems in [27,28] as well as higher order methods in [52]. In the aforementioned references, a Schur-complement ansatz is used to solve the discrete problems. Here, we use a primal-dual-active-set-strategy, which was developed for this discretization approach in [10]. We outline the discretization in more detail here: Let $\mathscr{T}_h$ be a finite element mesh of Ω with mesh size h and let $\mathscr{E}_C$ be a finite element mesh of Γ_C with mesh size H, respectively. The number of mesh elements in $\mathscr{T}_h$ is denoted by M_Ω and in $\mathscr{E}_C$ by M_C. We use line segments, quadrangles or hexahedrons to define $\mathscr{T}_h$ or $\mathscr{E}_C$. But this is not a restriction, triangles and tetrahedrons are also possible. Furthermore, let $\boldsymbol{\Psi}_T : [-1,1]^d \to T \in \mathscr{T}_h$ and $\boldsymbol{\Phi}_E : [-1,1]^{d-1} \to E \in \mathscr{E}_C$ be affine and d-linear transformations. We define

$$\begin{aligned}
V_h &:= \left\{ \mathbf{v} \in V \;\middle|\; \forall T \in \mathscr{T}_h : \; \mathbf{v}_{|T} \circ \boldsymbol{\Psi}_T \in Q_1^d \right\}, \\
\Lambda_H &:= \left\{ \mu \in L^2(\Gamma_C) \;\middle|\; \forall E \in \mathscr{E}_C : \; \mu_{|E} \circ \boldsymbol{\Phi}_E \in \mathbb{P}_0 \right\}, \\
\Lambda_{n,H} &:= \left\{ \mu_n \in \Lambda_H \,|\; \forall E \in \mathscr{E}_C : \; \mu_{n|E} \geq 0 \right\}, \\
\Lambda_{t,H}\left(\lambda_{n,H}\right) &:= \left\{ \boldsymbol{\mu}_t \in \Lambda_H^{d-1} \;\middle|\; \forall E \in \mathscr{E}_C : \; \boldsymbol{\mu}_{t|E} \leq \frac{1}{|E|}\int_E s\left(\lambda_{n,H}\right) do \right\},
\end{aligned}$$

where Q_1 is the set of d-linear functions on $[-1,1]^d$ and $\mathbb{P}_0$ the set of piecewise constant basis functions for the Lagrange Multiplier on $[-1,1]^{d-1}$. The discrete saddle point problem is to find $\left(\mathbf{u}_h, \lambda_{n,H}, \boldsymbol{\lambda}_{t,H}\right) \in V_h \times \Lambda_{n,H} \times \Lambda_{t,H}$ such that

$$a(\mathbf{u}_h, \mathbf{v}_h) + \left(\lambda_{n,H}, \mathbf{v}_{h,n}\right)_{0,\Gamma_C} + \left(\boldsymbol{\lambda}_{t,H}, \mathbf{v}_{h,t}\right)_{0,\Gamma_C} = \langle l, \mathbf{v}_h \rangle, \tag{22}$$

$$\left(\mu_{n,H} - \lambda_{n,H}, \mathbf{u}_{h,n} - g\right)_{0,\Gamma_C} + \left(\boldsymbol{\mu}_{t,H} - \boldsymbol{\lambda}_{t,H}, \mathbf{u}_{h,t}\right)_{0,\Gamma_C} \leq 0, \tag{23}$$

holds for all $\mathbf{v}_h \in V_h$, all $\mu_{n,H} \in \Lambda_{n,H}$, and all $\boldsymbol{\mu}_{t,H} \in \Lambda_{t,H}$. It is well-known that we obtain a stable discretization if a discrete inf-sup condition is fulfilled. In the case of quasi-uniform meshes the discrete inf-sup condition holds if the quotient of the mesh sizes h/H is sufficiently small, cf., for instance, [52]. If different mesh sizes h and H are used, the Lagrange multiplier has to be defined on a coarser mesh leading to a higher implementational complexity than using a surface mesh $\mathscr{E}_C$ inherited from

the interior mesh $\mathscr{T}_h$. In our numerical experiments, we observe oscillating Lagrange multipliers for $h = H$ and stable schmes for $H = 2h$, which corresponds to the results in the mentioned reference. Consequently, the numerical experiments in Sect. 5 are based on meshes with $H = 2h$.

Our definition of the discrete dual solution is motivated by the primal-dual-active-set-strategy to solve the discrete problem (22–23) outlined in [10, Section 5.4]. There, the active and inactive sets are based on the surface mesh $\mathscr{E}_C$. Consequently, we define the following discrete indicator functions for $E \in \mathscr{E}_C$:

$$\chi_E^c(\mathbf{w}_h) := \begin{cases} 1, & \text{if } \int_E \lambda_{n,H} + \mathbf{u}_{h,n} - g \, do > 0, \\ 0, & \text{if } \int_E \lambda_{n,H} + \mathbf{u}_{h,n} - g \, do \le 0, \end{cases}$$

$$\chi_E^f(\mathbf{w}_h) := \begin{cases} 1, & \text{if } \int_E s\left(\lambda_{n,H}\right) - \left|\boldsymbol{\lambda}_{t,H} + \mathbf{u}_{h,t}\right| \, do < 0, \\ 0, & \text{if } \int_E s\left(\lambda_{n,H}\right) - \left|\boldsymbol{\lambda}_{t,H} + \mathbf{u}_{h,t}\right| \, do \ge 0. \end{cases}$$

The discrete bilinear forms are then given by

$$\begin{aligned}
\bar{b}_h^c(\omega_n, \mathbf{v}) &:= \sum_{E \in \mathscr{E}_C} \int_E \omega_n \chi_E^c \mathbf{v}_n \, do, \\
\bar{c}_h^c(\omega_n, \mu_n) &:= \sum_{E \in \mathscr{E}_C} \int_{\Gamma_C} \omega_n \left[1 - \chi_E^c\right] \mu_n \, do, \\
\bar{b}_h^f(\boldsymbol{\omega}_t, \mathbf{v}) &:= \sum_{E \in \mathscr{E}_C} \int_E \boldsymbol{\omega}_t \left[\chi_E^f \boldsymbol{\lambda}_{t,H} \left(n'(\mathbf{w}_h)\right)^\top - s\left(\lambda_{n,H}\right) I\right] \mathbf{v}_t \, do, \\
\bar{c}_h^f(\boldsymbol{\omega}_t, \mu_n) &:= -\sum_{E \in \mathscr{E}_C} \int_E \boldsymbol{\omega}_t \, (s)'\left(\lambda_{n,H}\right)(\mu_n) \left[\chi_E^f \boldsymbol{\lambda}_{t,H} + \mathbf{u}_{h,t}\right] do, \\
\bar{d}_h^f(\boldsymbol{\omega}_t, \boldsymbol{\mu}_t) &:= \sum_{E \in \mathscr{E}_C} \int_E \boldsymbol{\omega}_t \left[\max\left\{s\left(\lambda_{n,H}\right), n(\mathbf{w}_h)\right\} I - s\left(\lambda_{n,H}\right) I\right] \boldsymbol{\mu}_t \, do \\
&\quad + \sum_{E \in \mathscr{E}_C} \int_E \boldsymbol{\omega}_t \chi_E^f \boldsymbol{\lambda}_{t,H} \left(n'(\mathbf{w}_h)\right)^\top \boldsymbol{\mu}_t \, do.
\end{aligned}$$

The discrete dual problem is to find a dual solution $\mathbf{z}_h = \left(\mathbf{y}_h, \xi_{n,H}, \boldsymbol{\xi}_{t,H}\right) \in V_h \times \Lambda_H \times \Lambda_H^{d-1}$ with

$$\begin{aligned}
a(\mathbf{v}_h, \mathbf{y}_h) - \bar{b}_h^c\left(\xi_{n,H}, \mathbf{v}_h\right) + \bar{b}_h^f\left(\boldsymbol{\xi}_{t,H}, \mathbf{v}_h\right) &= J_{\mathbf{u}}'(\mathbf{w}_h)(\mathbf{v}_h), \\
\left(\mu_{n,H}, \mathbf{y}_{h,n}\right)_{0,\Gamma_C} + \bar{c}_h^c\left(\xi_{n,H}, \mu_{n,H}\right) + \bar{c}_h^f\left(\boldsymbol{\xi}_{t,H}, \mu_{n,H}\right) &= J_{\lambda_n}'(\mathbf{w}_h)\left(\mu_{n,H}\right), \\
\left(\boldsymbol{\mu}_{t,H}, \mathbf{y}_{h,t}\right)_{0,\Gamma_C} + \bar{d}_h^f\left(\boldsymbol{\xi}_{t,H}, \boldsymbol{\mu}_{t,H}\right) &= J_{\boldsymbol{\lambda}_t}'(\mathbf{w}_h)\left(\boldsymbol{\mu}_{t,H}\right),
\end{aligned}$$

for all $\left(\mathbf{v}_h, \mu_{n,H}, \boldsymbol{\mu}_{t,H}\right) \in V_h \times \Lambda_H \times \Lambda_H^{d-1}$. We should remark that we use the bilinear forms $\bar{b}_h^c$, $\bar{b}_h^f$, $\bar{c}_h^c$, $\bar{c}_h^f$, and $\bar{d}_h^h$ instead of b_h^c, b_h^f, c_h^c, c_h^f, and d_h^h, since the dual problem using b_h^c, b_h^f, c_h^c, c_h^f, and d_h^h is not necessaryly well posed.

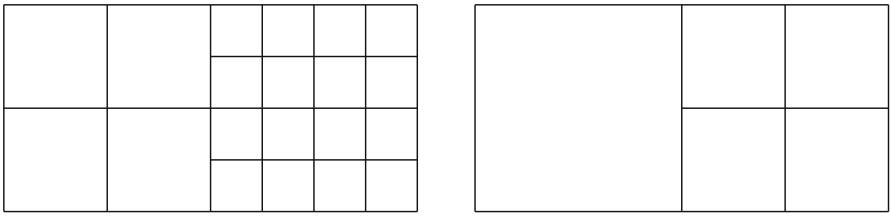

(a) Mesh with patch structure **(b)** Corresponding patch mesh

Fig. 2 Illustration of the patch structure of the finite element mesh

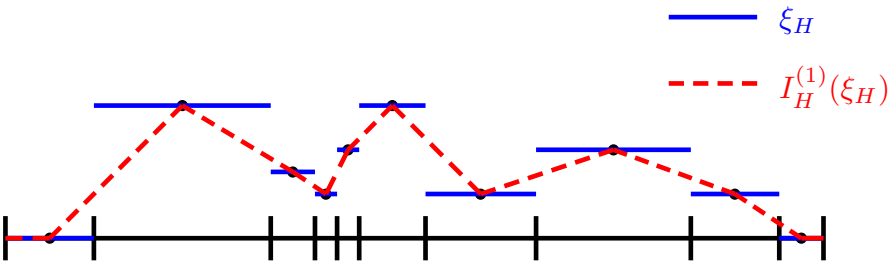

Fig. 3 Illustration of $I_H^{(1)}$

In this article, we use higher order reconstructions of the discrete solutions for the approximation of $\mathbf{w}$ and $\mathbf{z}$, because this procedure is computationally cheaper than the calculation of higher order solutions or extrapolation techniques. The primal and dual displacement $\mathbf{u}$ and $\mathbf{y}$ are approximated using patchwise d-quadratic reconstruction, cf., e.g., [3, Section 4.1] for this well known procedure. Let $I_{2h}^{(2)}$ be the corresponding interpolation operator. For the evaluation of $I_{2h}^{(2)}$, we require a special structure of the adaptively refined finite element mesh. This so-called patch-structure is obtained through the refinement of all children of a refined element, provided that one of these children is actually marked for refinement. This property is illustrated in Fig. 2. For the higher order reconstruction of the Lagrange multipliers, we use a patchwise linear interpolation $I_H^{(1)}$, it is illustrated in Fig. 3. We define $\mathscr{A}^I\left(\left(\mathbf{v}_h, \mu_{n,H}, \boldsymbol{\mu}_{t,H}\right)\right) := \left(I_{2h}^{(2)}\mathbf{v}_h, I_H^{(1)}\mu_{n,H}, I_H^{(1)}\boldsymbol{\mu}_{t,H}\right)$ and obtain the error estimators

$$\begin{aligned}\eta_p &:= \rho\left(\mathbf{w}_h\right)\left(\mathscr{A}^I\left(\mathbf{z}_h\right) - \mathbf{z}_h\right) - C\left(\mathbf{w}_h\right)\left(\xi_{n,h}\right) - D\left(\mathbf{w}_h\right)\left(\boldsymbol{\xi}_{t,H}\right),\\ \eta &:= \frac{1}{2}\rho\left(\mathbf{w}_h\right)\left(\mathscr{A}^I\left(\mathbf{z}_h\right) - \mathbf{z}_h\right) + \frac{1}{2}\rho^*\left(\mathbf{w}_h, \mathbf{z}_h\right)\left(\mathscr{A}^I\left(\mathbf{w}_h\right) - \mathbf{w}_h\right)\\ &\quad -C\left(\mathbf{w}_h\right)\left(\xi_{n,h}\right) - D\left(\mathbf{w}_h\right)\left(\boldsymbol{\xi}_{t,H}\right).\end{aligned}$$

In [3, Section 5.2] the approximation of the weights by higher order reconstruction is justified for Poisson's equation with smooth solutions on uniform meshes, where the considerations rely on an asymptotic expansion of the error in the nodal points of the mesh. However, there exists no analysis on the one hand for nei-

ther nonsmooth nor nonlinear problems as well as on the other hand for adaptively refined meshes. In our case, we require similar properties also of the Lagrange multipliers, i.e. some superconvergence properties in the midpoints of the elements.

If we consider usual nonlinear partial differential equations with standard finite element discretizations, the formulation of the dual problem would be standard and it would depend on the discretization by the chosen discrete trial and test spaces solely. Yet, the situation is even more complex in our case, because the formulation of the dual problem involves the discrete solution in a nonsmooth manner via the discrete active set. Due to the lack of an appropriate analysis, we can substantiate the replacement of the analytic terms in the weights by the higher order reconstruction only by numerical experiments, which will be discussed in the next section, where we consider some challenging examples. More detailed numerical experiments on this topic can also be found in [48].

To utilize the error estimators η_p and η in an adaptive refinement strategy, we have to localize the error contributions given by the residuals with respect to the single mesh elements $T \in \mathcal{T}_h$ leading to local error indicators η_T . Here, the filtering technique developed in [15] is applied, which implies less implementational effort than the standard approach using integration by parts outlined for instance in [3]. An alternative localization method was recently proposed in [49]. The terms connected to C and D are added to the adjacent volume cells to the boundary cells.

5 Numerical results

This section is devoted to numerical tests of the presented error estimator. At first, we consider an example with known analytical solution in order to check the accuracy. Afterwards, we apply the estimator on an example, where the Lagrange multipliers are not in $L^2(\Gamma_C)$ and show the efficiency of the mesh adaptive algorithm. Finally, we test the model adaptive approach. For model adaptive results concerning 3D examples from sheet-bulk-metal-forming, we refer to [7,50]. Some results in the case of multibody contact problems are presented in [24, Chapter 5].

5.1 First example: Known analytical solution

At first, we consider a 2D Signorini problem with Tresca friction, whose analytical solution is known. It is a modified version of an example used in [47,48]. Let $\Omega := (-3, 0) \times (-1, 1)$ be the domain. We assume homogeneous Dirichlet boundary conditions on $\Gamma_D := \{-3\} \times [-1, 1]$ and homogeneous Neumann boundary conditions on $\Gamma_N := (-3, 0) \times \{-1, 1\}$. The possible contact boundary is denoted by $\Gamma_C := \{0\} \times [-1, 1]$. The material law is given by Hooke's law with Young's modulus $E := 10$ and Poisson number $\nu := 0.3$ using the plain strain assumption. The analytical solution is called $\mathbf{u}(x, y) := (u_1(x, y), u_2(x, y))^\top$, where

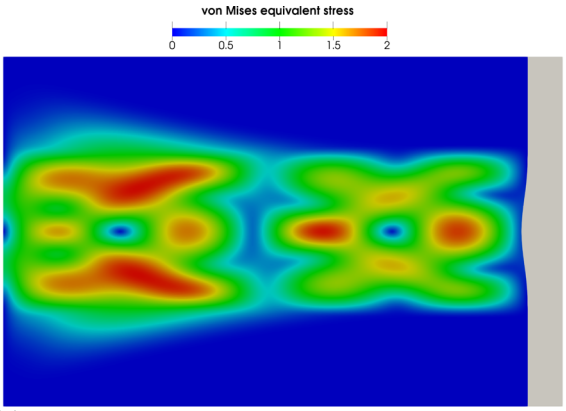

(a) Plot of the von Mises equivalent stress on the deformed con - figuration and the obstacle colored in grey on the right

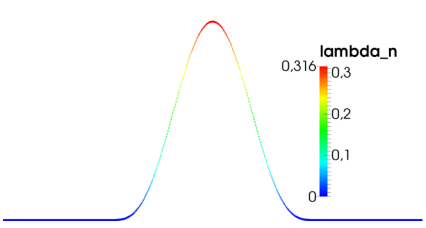

(b) Plot of $\lambda_{n,H}$

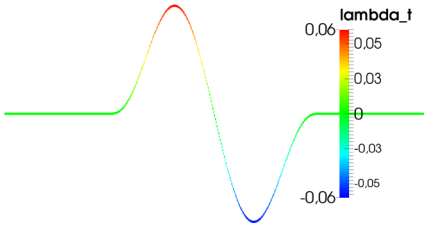

(c) Plot of $\lambda_{t,H}$

Fig. 4 Numerical solution of the first example for $M_\Omega = 1{,}572{,}864$ and $M_C = 1024$

$$u_1(x, y) := \begin{cases} -(x+3)^2 \left(y - \frac{x^2}{18} - \frac{1}{2}\right)^4 \left(y + \frac{x^2}{18} + \frac{1}{2}\right)^4, & |y| < \frac{x^2}{18} + \frac{1}{2}, \\ 0, & \text{else}, \end{cases}$$

$$u_2(x, y) := \begin{cases} \frac{24}{\pi} \sin\left(\frac{4\pi(x+3)}{3}\right) \left[\left(y - \frac{1}{2}\right)^3 \left(y + \frac{1}{2}\right)^4 + \left(y - \frac{1}{2}\right)^4 \left(y + \frac{1}{2}\right)^3\right], & |y| < \frac{1}{2}, \\ 0, & \text{else}. \end{cases}$$

The volume force is then given by $\mathbf{f} := -\mathrm{div}(\boldsymbol{\sigma}(\mathbf{u}))$ and the obstacle by $g(y) := u_1(0, y)$. The friction law is Tresca with $s = 0.1$. The analytic Lagrange multipliers are calculated by $\lambda_n = -\sigma_{nn}(\mathbf{u})$ and $\boldsymbol{\lambda}_t = -\sigma_{nt}(\mathbf{u})$ on Γ_C. The discrete solution $\mathbf{w}_h$ is illustrated in Fig. 4. Here, the von Mises equivalent stress is depicted. It is under the plain strain assumption given by

$$\sigma_{M,2}(\sigma, \sigma_e) := \frac{\sqrt{\left(\sigma_{11}^2 + \sigma_{22}^2\right)\left(\nu^2 - \nu + 1\right) + \sigma_{11}\sigma_{22}\left(2\nu^2 - 2\nu - 1\right) + 3\sigma_{21}^2}}{\sigma_e}, \tag{24}$$

see, for instance, [66, Section 3.3.2]. We set $\sigma_e := 1$. In this example, contact takes place on the whole contact boundary Γ_C. However, we observe large biactive sets

$$\Gamma_B^c := \{x \in \Gamma_C | \, \lambda_n(x) = u_n(x) - g(x) = 0\} \quad = [-1, -0.5] \cup [0.5, 1]$$
$$\Gamma_B^f := \{x \in \Gamma_C | \, \lambda_t(x) = u_t(x) = 0\} \quad = [-1, -0.5] \cup [0.5, 1]$$

with $|\Gamma_B^c|_{d-1} = |\Gamma_B^f|_{d-1} = 1$. Furthermore, it should be remarked that we have sticking on $[-0.5, 0.5]$.

We consider the quantities of interest

$$J_{a,1}(\mathbf{u}) := \int_\Omega \omega_1(x) \, |\mathbf{u}|^2 \, dx,$$
$$J_{a,2}(\boldsymbol{\lambda}_t) := \int_{-1}^{1} \omega_2(y) \boldsymbol{\lambda}_t^2(y) \, dy,$$

where $\omega_1(x) = 0.5 \left(\tanh(20(0.5 - |x - (-0.5, 0)^\top|)) + 1\right)$ is a cut off function w.r.t. the disc $B_{0.5}\left((-0.5, 0)^\top\right)$ and $\omega_2(y) = 0.5 \tanh(20(0.25 - |y - 0.125|)) + 0.5$ is one w.r.t. $\{0\} \times [-0.125, 0.375]$. The first quantity of interest was also considered in [48], where we observed that some approaches had difficulties to estimate the error in this cases accurately. Thus, it provides a good test for the presented estimator. The second quantity of interest focuses on the frictional Lagrange multiplier, where the error is even harder to estimate, since the error in $\boldsymbol{\lambda}_t$ is only of order h in the norm connected to Λ_t leading to relevant remainder terms. The relative discretization error w.r.t. the quantity of interest is given by

$$E_{\text{rel}}(J) := \frac{J(\mathbf{w}) - J(\mathbf{w}_h)}{J(\mathbf{w})},$$

and the effectivity index by

$$I_{\text{eff}}(J, \tilde{\eta}) := \frac{J(\mathbf{w}) - J(\mathbf{w}_h)}{\tilde{\eta}}.$$

In Table 2, the results for the quantity of interest $J_{a,1}$ are listed. Here, the number of uniform refinements based on a coarse initial triangulation is denoted by L. We found by analyzing the data that the effectivity indices seem to converge of order h^2 to 1 for η_p and η, which is almost optimal. When regarding $J_{a,2}$, see Table 3, we observe an almost constant effectivity index of 0.45 for η_p. In contrast to η_p, the effectivity index for η seems to converge to 1 with order better than h. The reason for the less accurate estimation by η_p lies in the remainder terms. We obtain here

$$\mathscr{R}_{J_{a,2}}^{(2)} = \int_{\Gamma_C} \omega_2(y)[\boldsymbol{\lambda}_t(y) - \boldsymbol{\lambda}_{t,H}(y)]^2 \, dy \qquad \text{and set} \qquad \widetilde{\mathscr{R}}_{J_{a,2}}^{(2)} := \frac{\mathscr{R}_{J_{a,2}}^{(2)}}{J_{a,2}(\mathbf{w})}.$$

Table 3 reveals that the relative remainder term $\widetilde{\mathscr{R}}_{J_{a,2}}^{(2)}$ is larger than the relative discretization error $E_{\text{rel}}\left(J_{a,2}\right)$ and of the same order in h. To improve the estimator η_p, we add an approximation of $\mathscr{R}_{J_{a,2}}^{(2)}$ to it, i.e. we set

Table 2 Results of the presented error estimators for $J_{a,1}$

M_Ω	L	$E_{\text{rel}}(J_{a,1})$	$I_{\text{eff}}(J_{a,1}, \eta_p)$	$I_{\text{eff}}(J_{a,1}, \eta)$
384	0	$1.64877 \cdot 10^{-2}$	0.75664	1.35182
1536	1	$1.23560 \cdot 10^{-2}$	1.32806	1.53448
6144	2	$3.34870 \cdot 10^{-3}$	1.02872	1.03228
24,576	3	$8.47788 \cdot 10^{-4}$	1.00476	1.00472
98,304	4	$2.12445 \cdot 10^{-4}$	1.00122	1.00121
393,216	5	$5.31427 \cdot 10^{-5}$	1.00032	1.00032
1,572,864	6	$1.32877 \cdot 10^{-5}$	1.00008	1.00009

Table 3 Results of the presented error estimators for $J_{a,2}$

M_Ω	L	$E_{\text{rel}}(J_{a,2})$	$I_{\text{eff}}(J_{a,2}, \eta_p)$	$I_{\text{eff}}(J_{a,2}, \eta)$	$\widetilde{\mathscr{R}}^{(2)}_{J_{a,2}}$	$I_{\text{eff}}\left(J_{a,2}, \eta_p^c\right)$
384	0	$5.52047 \cdot 10^{-1}$	−0.35125	−0.43657	$-1.47422 \cdot 10^{0}$	−0.27035
1536	1	$1.16762 \cdot 10^{-1}$	0.43169	0.55337	$-7.92715 \cdot 10^{-2}$	0.63643
6144	2	$1.92788 \cdot 10^{-2}$	0.44564	0.84072	$-2.07101 \cdot 10^{-2}$	0.91283
24,576	3	$4.44213 \cdot 10^{-3}$	0.45071	0.95411	$-5.25697 \cdot 10^{-3}$	0.98752
98,304	4	$1.09268 \cdot 10^{-3}$	0.45136	0.98472	$-1.31923 \cdot 10^{-3}$	0.99773
393,216	5	$2.72085 \cdot 10^{-4}$	0.45144	0.99441	$-3.30117 \cdot 10^{-4}$	0.99964
1,572,864	6	$6.79543 \cdot 10^{-5}$	0.45143	0.99773	$-8.25486 \cdot 10^{-5}$	0.99998

$$\eta_p^c := \eta_p + \int_{\Gamma_C} \omega_2(y)[I_H^{(1)}\boldsymbol{\lambda}_{t,H}(y) - \boldsymbol{\lambda}_{t,H}(y)]^2\, dy.$$

As shown in Table 3, the estimator η_p^c is very accurate and the effectivity index converges to 1 with an order greater than h^2. The results are surprisingly well. However, they rely on the smoothness of the discussed example. Since $\mathscr{R}^{(2)}_{J_{a,3}} = 0$ holds, we do not observe this problem for η. Furthermore, we have in this case $\Delta J_{a,2} = \mathscr{R}^{(2)}_{J_{a,2}}$ and therefore a large difference between primal and dual residual.

The numerical experiments in [48] show that integrals over Γ_C involving the Lagrange multipliers are not approximated of higher order by $I_H^{(1)}\lambda_{n,H}$ and $I_H^{(1)}\boldsymbol{\lambda}_{t,H}$. However, the contribution of the terms involving $I_H^{(1)}$ is very small compared to the other ones. Consequently, we do not see the missing order on the considered meshes. All in all, we do not obtain an asymptotically exact error estimator but a very accurate one. It is a main advantage of the presented error estimators that it suffices to work with the higher order reconstruction to obtain reasonable results.

Finally, we take a closer look on the remainder terms of the error estimation connected to the problem setting and not to the quantity of interest. To do so, we consider the quantity of interest

Table 4 Results of the presented error estimators for $J_{a,3}$

L	$E_{\text{rel}}(J_{a,3})$	$I_{\text{eff}}(J_{a,3},\eta_p)$	$I_{\text{eff}}(J_{a,3},\eta)$	$\widetilde{\mathscr{R}}_c^{(2)}$	$\int_{\Gamma_C} e_\chi^c\, do$	$\int_{\Gamma_C} e_\chi^f\, do$
0	$9.94687 \cdot 10^{-3}$	1.03616	1.07955	$1.45757 \cdot 10^{-3}$	0.50000	0.00000
1	$-1.41849 \cdot 10^{-1}$	0.86827	1.08739	$-1.19684 \cdot 10^{-4}$	0.06250	−0.25000
2	$-2.20741 \cdot 10^{-2}$	0.99269	0.99032	$-2.18998 \cdot 10^{-5}$	−0.40625	−0.50000
3	$-5.61951 \cdot 10^{-3}$	0.98023	0.97588	$-5.78284 \cdot 10^{-6}$	−0.50000	−0.50000
4	$-1.41387 \cdot 10^{-3}$	0.99380	0.99306	$-1.45473 \cdot 10^{-6}$	−0.53125	−0.53125
5	$-3.54307 \cdot 10^{-4}$	0.99798	0.99788	$-3.64523 \cdot 10^{-7}$	−0.51562	−0.51562
6	$-8.86368 \cdot 10^{-5}$	0.99929	0.99931	$-9.11908 \cdot 10^{-8}$	−0.52344	−0.52344

$$J_{a,3}(w) = \int_\Omega -\operatorname{div}(\sigma(y))u\, dx + \int_{\Gamma_C} \xi_n \lambda_n + \xi_t \lambda_t\, do.$$

Here, we set $y = (y_1, y_2)^\top$,

$$y_1(x_1, x_2) = 0.1 x_1^2 (x_1+3)^2 (x_2+1)^2 (x_2-1)^2,$$
$$\xi_n(x_2) = 1000 \begin{cases} (x_2-0.5)(x_2-1), & x_2 > 0.5, \\ (x_2+0.5)(x_2+1), & x_2 < -0.5, \\ 0, & \text{else}, \end{cases}$$

and $\xi_t = -2\xi_n$. Therefore, we obtain the analytic dual solution $z = (y, \xi_n, \xi_t)$. In particular, we are now able, to evaluate the remainder terms. In detail, we look on

$$\widetilde{\mathscr{R}}_c^{(2)} := \frac{\mathscr{R}_c^{(2)}}{J(w)}.$$

Due to the special structure of the example, it holds $\mathscr{R}_c^{(2)} = \mathscr{R}_c^{(3)}$. Hence, we do not discuss $\mathscr{R}_c^{(3)}$. Furthermore, the remainder terms with respect to friction are zero, since we use Tresca's law of friction and have sticking on $\Gamma_C \backslash \Gamma_B$. In Table 4, the results concerning the quantity of interest $J_{a,3}$ are listed. We found a very accurate error estimation as for $J_{a,1}$, cf. Table 2. Looking at the errors in the active sets with respect to the geometrical contact as well as to the friction, we observe that this error does not converge to zero. Numerical errors in the solution algorithm lead to this behavior on the biactive set Γ_B. The remainder $\widetilde{\mathscr{R}}_c^{(2)}$ and therefore $\mathscr{R}_c^{(2)}$ is of the same order as the error. However, it is three orders of magnitude smaller such that the missing higher order property does not disturb the error estimation in the calculations. These results substantiate that the presented error estimators are robust with respect to biactive sets.

If we change the obstacle g in such a way that $|\Gamma_B| = 0$ holds and the analytic solution is not modified, we obtain that the errors with respect to the active set are zero for sufficiently fine meshes and that the remainder terms are of higher order. We refer to [47, Section 5.1] for more details on this topic.

5.2 Second Example: Low regularity

In Sect. 2.1, we have assumed $\lambda_n \in L^2(\Gamma_C)$ and $\boldsymbol{\lambda}_t \in \left(L^2(\Gamma_C)\right)^{d-1}$ to derive the problem formulation, on which the a posteriori error estimate is based. Now, we test how the estimator works, if this assumption is violated. To this end, we modify an example, which has been analysed in [60, Section 4.2.1] and [47, Section 5.3] for the frictionless case. For the detailed mechanical background of this example, we refer to [36, Section 2.8].

We consider the domain $\Omega = (-1, 0) \times (-0.5, 0.5)$ with $\Gamma_D = \{-1\} \times (-0.5, 0.5)$, $\Gamma_C = \{0\} \times (-0.5, 0.5)$ and $\Gamma_N = \partial\Omega \backslash (\Gamma_C \cup \Gamma_D)$. We have homogeneous Dirichlet boundary conditions on Γ_D and homogeneous Neumann ones on Γ_N, while the contact can take place on Γ_C. The obstacle is defined by

$$g(x_2) = \begin{cases} -0.01 & |x_2| \leq b, \\ 0.2, & \text{else}, \end{cases}$$

with the constant $b = 0.0625$. We choose Coulomb friction with $\mathscr{F} = 0.1$. The material law is given by Hooke's law under plain strain assumption with modulus of elasticity $E = 3$ and Poisson ration $\nu = 0.25$. The volume force f is set to zero. In [36, Section 2.8], it is shown for the frictionless case in a generalized situation that the contact stress is given by

$$\boldsymbol{\sigma}_{nn}(x_2) = \frac{P}{\pi \left(b^2 - x_2^2\right)^{1/2}}. \tag{25}$$

Here, P is an applied constant load with $P = \int_{\Gamma_C} \boldsymbol{\sigma}_{nn}\, do$. In our setting, P is not known and a reference value has to be determined numerically, which will be discussed in detail in the sequel. The numerical solution of this example is depicted in Fig. 5 for a fine uniformly refined mesh. The von Mises equivalent stress given by Eq. (24) is plotted. We find some minor stress peaks in the left corners of the domain. However, the major ones are seen at the corners of the obstacle. This corresponds to the approximation of the contact stress in normal direction given in Eq. (25). From Eq. (25), we learn that the contact stress in normal direction $\boldsymbol{\sigma}_{nn}$ becomes infinite for $x_2 = \pm b$ and that it is contained in $L^1(\Gamma_C)$ but not in $L^2(\Gamma_C)$. Since we observe sliding nearly on the complete contact boundary especially at the corners of the obstacle, we have $|\sigma_{nt}| = 0.1\sigma_{nn}$ in the sliding regions due to the used friction model and to Coulomb's law. Hence, we also expect $\boldsymbol{\sigma}_{nt}$ in $L^1(\Gamma_C)$ and not in $L^2(\Gamma_C)$. This is substantiated by Fig. 5b, where we plot the $L^1(\Gamma_C)$- and the $L^2(\Gamma_C)$-norm of $\lambda_{n,H}$. We observe convergence of the $L^1(\Gamma_C)$-norm approximately to 0.015596 in comparison to 0.015491 for the frictionless case. In contrast to this, the $L^2(\Gamma_C)$-norm is increasing while refining the mesh. For $\boldsymbol{\lambda}_{t,H}$ we get the same results but scaled by a factor 0.1 approximately.

We consider the quantity of interest

$$J_J(\lambda_n, \boldsymbol{\lambda}_t) = 0.01 \int_{\Gamma_C} \lambda_n(x_2) + \tanh(20x_2)\boldsymbol{\lambda}_t(x_2)\, dx_2,$$

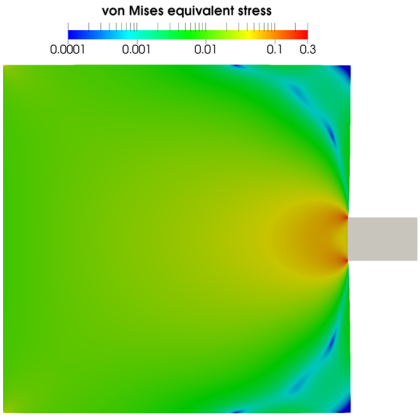

(a) Plot of the von Mises equivalent stress on t he deformed configuration and the obstacle colored in grey on the right

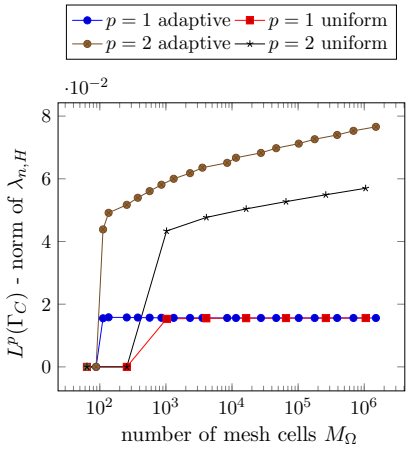

(b) Plot of the $L^p(\Gamma_C)$-norm of $\lambda_{n,H}$

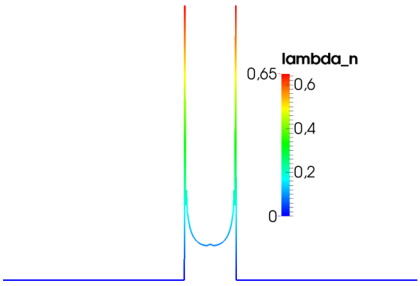

(c) Plot of $I_H^{(1)}\lambda_{n,H}$

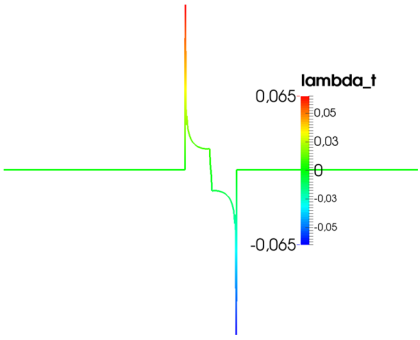

(d) Plot of $I_H^{(1)}\lambda_{t,H}$

Fig. 5 Numerical solution of the second example for $M_\Omega = 1{,}048{,}576$ and $M_C = 512$

where we use the factor $\tanh(20x_2)$ to approximate $|\boldsymbol{\lambda}_t(x_2)|$. Thus J_J is an approximation of the $L^1(\Gamma_C)$-norm of λ_n and $\boldsymbol{\lambda}_t$. We know that the $L^2(\Gamma_C)$-norm of λ_n and $\boldsymbol{\lambda}_t$ is unbounded in contrast to the $L^1(\Gamma_C)$-norm. Furthermore, J_J is closely connected to the applied loads. Thus it is of physical interest on the hand and difficult to estimate on the other one. Consequently, it provides a good test of the presented estimators and algorithms. To calculate the relative error and the effectivity indices, we need $J_J(\lambda_n, \boldsymbol{\lambda}_t)$, which cannot be calculated analytically. Hence, we approximate it numerically. Due to the low regularity, we use the results of the adaptive algorithm and extrapolate them assuming that the adaptive algorithm is converging of order M_Ω^{-1}. We obtain $J_{J,\mathrm{ref}} = 1.6533576749458561 \cdot 10^{-4}$. In Table 5, the results of the adaptive algorithm are shown. We find nearly constant effectivity indices close to 0.9, which is very good for a problem with such a low regularity. The value in the last iteration has to be considered with special care because of the numerical approximation of the reference value. However, they do not converge to 1. It should be remarked that the contact situation is

Table 5 Results of the presented error estimators for J_J using the mesh adaptive algorithm

M_Ω	L	$E_{\text{rel}}(J_J)$	$I_{\text{eff}}(J_J, \eta_p)$	$I_{\text{eff}}(J_J, \eta)$
64	0	$1.00000 \cdot 10^{0}$	13.22686	13.22686
88	1	$1.00000 \cdot 10^{0}$	13.22686	13.22686
112	2	$1.46387 \cdot 10^{-2}$	−0.52308	−0.44869
136	3	$-1.44419 \cdot 10^{-2}$	0.58665	0.55447
256	4	$-1.08569 \cdot 10^{-2}$	0.69491	0.65887
376	5	$-9.35508 \cdot 10^{-3}$	0.81169	0.78018
568	6	$-6.41182 \cdot 10^{-3}$	0.85241	0.82555
856	7	$-4.11795 \cdot 10^{-3}$	0.89752	0.87517
1312	8	$-2.65517 \cdot 10^{-3}$	0.90526	0.88938
2320	9	$-1.50482 \cdot 10^{-3}$	0.91241	0.89377
3568	10	$-9.80850 \cdot 10^{-4}$	0.93485	0.92073
8440	11	$-3.70377 \cdot 10^{-4}$	0.88253	0.86587
11,488	12	$-2.70763 \cdot 10^{-4}$	0.91532	0.90313
27,376	13	$-1.12485 \cdot 10^{-4}$	0.89444	0.87967
46,600	14	$-6.53826 \cdot 10^{-5}$	0.90520	0.89263
102,064	15	$-2.99167 \cdot 10^{-5}$	0.89473	0.88136
177,904	16	$-1.70812 \cdot 10^{-5}$	0.90396	0.89193
389,200	17	$-7.79114 \cdot 10^{-6}$	0.89035	0.87758
686,728	18	$-4.35260 \cdot 10^{-6}$	0.89147	0.87998
1,500,400	19	$-1.95186 \cdot 10^{-6}$	0.86124	0.84929

not resolved in the first two iterations, since the meshes are too coarse. This situation is succesfully solved by the adaptive algorithm based on the presented error estimator, because it includes the additional terms measuring the error in the contact and frictional conditions. The adaptive mesh for $L = 8$ is depicted in Fig. 6a. We observe strong refinements at the corners of the obstacle and in the middle of the contact zone, where $\boldsymbol{\lambda}_t$ changes its sign leading to transition from sliding to sticking and back. Some minor refinements are carried out in the corners, where the Dirichlet and Neumann boundary come together. This is, what is expected from the adaptive meshes. The convergence of the adaptive algorithm is considered in Fig. 6b. We find convergence of order $\mathcal{O}(M_\Omega^{-1/2})$ for uniform refinement and regain the optimal order of convergence $\mathcal{O}(M_\Omega^{-1})$ by the adaptive approach. All in all, the presented estimator and the adaptive algorithm also works well in this situation, where the assumptions are violated.

5.3 Third example: Model adaptivity

In this section, we develop a model adaptive algorithm based on the model hierarchy $\mathscr{H}$ from Table 1 as well as the model error estimator $\eta_m = -\Delta(\mathbf{w}_h)(\mathbf{z}_h)$ defined in Sect. 4. In this section, we neglect the discretization error. The core part of the model adaptive algorithm is detailed in the following algorithm:

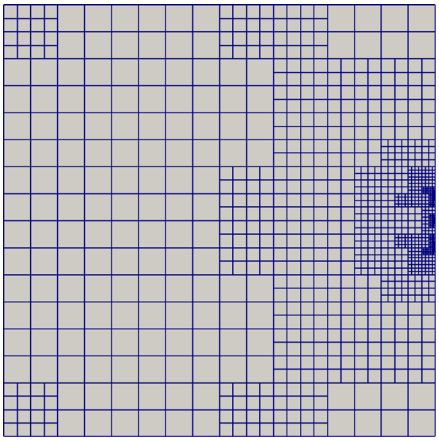

(a) Adaptive mesh for $L = 8$

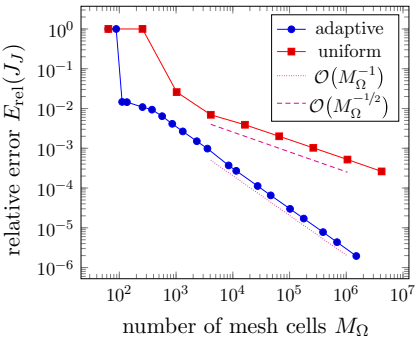

(b) Convergence of the uniform and the adaptive algorithm

Fig. 6 Results of the mesh adaptive algorithm

Algorithm 1 (Model choosing)

Choose $\mathscr{R}_M \subseteq \mathscr{E}_C$ and $\mathscr{C}_M \subseteq \mathscr{E}_C$, the subsets of boundary cells on which the model should be refined and coarsened, respectively.
for all $E \in \mathscr{R}_M$ **do**
  if $s_E = s_0$ **then**
    if $|s_1(\lambda_{n,H}) - s_3(\lambda_{n,H})| < |s_2(\lambda_{n,H}) - s_3(\lambda_{n,H})|$ **then**
      Set $s_E = s_1$.
    else
      Set $s_E = s_2$.
    end if
  end if
  if $s_E = s_1$ **or** $s_E = s_2$ **then**
    Set $s_E = s_3$.
  end if
end for
for all $E \in \mathscr{C}_M$ **do**
  if $s_E = s_3$ **then**
    if $|s_1(\lambda_{n,H}) - s_3(\lambda_{n,H})| < |s_2(\lambda_{n,H}) - s_3(\lambda_{n,H})|$ **then**
      Set $s_E = s_1$.
    else
      Set $s_E = s_2$.
    end if
  end if
  if $s_E = s_1$ **or** $s_E = s_2$ **then**
    Set $s_E = s_0$.
  end if
end for

Here, we do not linearly choose the model but have three levels of models. On Level 1 is the frictionless contact model s_0. The second level consists of Tresca friction s_1 and Coulomb friction s_2. Finally, the friction law of Betten s_3 establishes the third level, see also Fig. 1b. The idea behind this approach is the interpretation of the laws of Tresca and Coulomb as the limiting cases of the one of Betten. The choice of the current model on the second level is based on a comparison of the predicted friction bounds of the friction laws on level 2 to the prediction using s_3, which is an approximation of the expected model error after the enhancement of the model. To choose the subsets $\mathscr{R}_M \subseteq \mathscr{E}_C$ and $\mathscr{C}_M \subseteq \mathscr{E}_C$, standard marking strategies can be used. Here, we apply a fixed fraction strategy with respect to the cells, i.e. we refine the model on `reffrac` percent of the cells on the contact boundary with the largest error. Furthermore, we coarsen the model on `coarsenfrac` percent of the cells with the smallest error. It should be remarked that we only consider those cells on Γ_C in the marking strategy, where the error is numerically larger than zero. In this section, we set `reffrac` $= 6.25\%$ and `coarsenfrac` $= 0\%$.

The model adaptive algorithm works in the following way. In the first iteration, $L = 0$, we set $s \equiv s_0$, i.e. we solve a frictionless contact problem. Then we estimate the model error and modify the model distribution by the approach outlined above. This method is called local. We will see in the numerical experiments that this approach works but has several shortcomings. The most important one is that the dual tangential Lagrange multiplier may be badly resolved leading to inaccurate a posteriori error estimates. To overcome these ones, we add a global model enhancement step to the adaptive algorithm. After the first step, which uses a frictionless contact model, we perform in the second step, $L = 1$, a model enhancement on each cell, where the model error is numerically larger than zero. Afterwards, the algorithm works as in the local approach. We call this ansatz global.

The example, which we consider in this section, is based on the same domain, subdivision of the boundary, and material law as in Sect. 5.1. The volume force f is set to zero. The gap function g is given by $g(y) = 0.1\,(y-1)\,(y+1)$. We choose the frictional parameters $C_T = 0.1$, $\mathscr{F} = 0.4$, and $n = 3$, cf. Table 1. The reference solution $\mathbf{w}_h^r = \left(\mathbf{u}_h^r, \lambda_{n,H}^r, \boldsymbol{\lambda}_{t,H}^r\right)$ with respect to the reference friction model $s^r = s_3$ is illustrated in Fig. 7, where we show the von Mises equivalent stress according to Eq. (24) with $\sigma_e = 1$. From the shape of $\lambda_{n,H}^r$ and $\boldsymbol{\lambda}_{t,H}^r$, we expect a model distribution with Tresca friction in most parts of the contact zone. Only near to the boundary of the contact zone, the laws of Coulomb or Betten should be used.

We consider the quantity of interest

$$J_{m,e}\left(\mathbf{w}\right) = \int_{\Gamma_C} \boldsymbol{\lambda}_t \mathbf{u}_t \, do,$$

which corresponds to the dissipated energy in this example and is of great physical importance. Furthermore, it is also difficult to treat from a numerical point of view, because it is only nonzero on sliding areas of the contact boundary and strongly depends on the accurate determination of this area. In order to test the model adaptive algorithm, we work on a fixed uniformly refined mesh with $M_\Omega = 393{,}216$ cells.

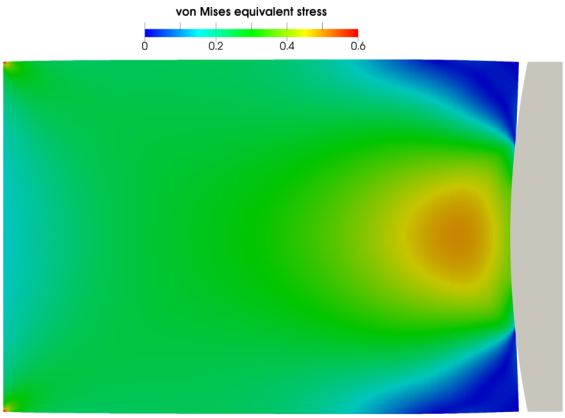

(a) Plot of the von Mises equivalent stress on the deformed configuration and the obstacle colored in grey on the right

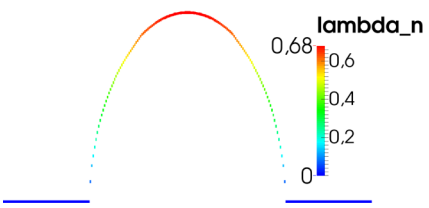

(b) Plot of $\lambda_{n,H}^r$

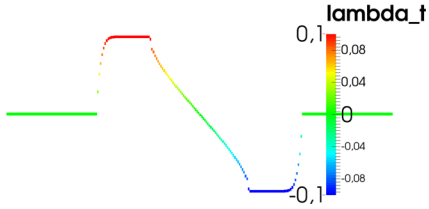

(c) Plot of $\lambda_{t,H}^r$

Fig. 7 Numerical solution of the third example for $M_\Omega = 393{,}216$ and $M_C = 256$

Choosing $s \equiv s^r$ on Γ_C, we calculate a reference primal and dual solution, which is used to determine errors, remainder terms and so on. We obtain

$$J_{m,e}^r := J_{m,e}\left(\mathbf{w}_h^r\right) = 3.9989365363916116 \cdot 10^{-5}.$$

In Table 6, the results of the model adaptive approach using the technique named local are listed. We observe a relative error larger than 20% in the first seven iterations. Afterwards the relative error is fast decreased. This means that we need a lot of iterations to obtain an appropriate local modelling. The second import point lies in the fact that the error is enormously underestimated by the error estimator leading to very large effectivity indices. Looking at the numerical performance, we notice that the needed number of Newton steps and also the steps of the inner solver are significantly reduced after step eight.

We analyse the reasons behind the observed behavior of the algorithm now. The numerical effort, which we have seen, is due to the model distribution, cf. Table 7. In step eight of the algorithm, all decisive parts of the contact boundary are resolved and only the sticking region in the middle with low frictional stresses near to zero is remaining. Once this state is reached, we only have small changes in the numerical solution. Consequently, the solving algorithm performs well using the initial values of

Table 6 Model adaptive results in the third example using the local approach for $J_{m,e}$

L	$E_{\text{rel}}\left(J_{m,e}\right)$	$I_{\text{eff}}\left(J_{m,e}, \eta_m\right)$	$\text{iter}_{\text{Newton}}$	$\text{iter}_{\text{GMRES}}$	$\text{iter}_{\text{dual}}$
0	$1.00000 \cdot 10^{0}$	19.33126	9	344	1
1	$-5.12141 \cdot 10^{-1}$	165.76797	10	642	134
2	$-4.68458 \cdot 10^{-1}$	−10.52985	5	232	132
3	$-1.12041 \cdot 10^{0}$	−110.79093	11	799	133
4	$-1.20949 \cdot 10^{0}$	−944.35280	10	743	129
5	$-9.78867 \cdot 10^{-1}$	1500.89058	8	507	130
6	$-3.68361 \cdot 10^{-1}$	283.61716	9	670	129
7	$-1.91201 \cdot 10^{-1}$	220.47639	8	675	134
8	$-2.29865 \cdot 10^{-3}$	−11.87505	11	1184	135
9	$-1.21771 \cdot 10^{-3}$	−1505.70969	2	93	120
10	$-9.09943 \cdot 10^{-5}$	−2010.64058	2	89	72
11	$-9.82382 \cdot 10^{-7}$	−1965.93382	2	87	71
12	$2.27845 \cdot 10^{-12}$	36.73013	2	81	67
Sum			89	6146	1387

Table 7 Model distribution in the third example using the local approach for $J_{m,e}$

L	Model distribution
0	
1	
2	
3	
4	
5	
6	
7	
8	
9	
10	
11	
12	

the last iteration. This observation is also the reason for the error reduction beginning in step eight. Another point is the small refinement fraction, which leads to a slow improvement of the model distribution.

Table 8 Remainder terms in the third example using the local approach for $J_{m,e}$

L	$\widetilde{\eta}_m$	$-\widetilde{\Delta}(\mathbf{w})(e_{\mathbf{z}}^r)$	$-\frac{1}{2}\widetilde{\Delta}(e_{\mathbf{w}}^r, e_{\mathbf{z}}^r)$	$\widetilde{\mathscr{R}}_c^m$
0	$5.17297 \cdot 10^{-2}$	$2.00733 \cdot 10^{-1}$	$-1.11169 \cdot 10^{-1}$	$-4.75752 \cdot 10^{-3}$
1	$-3.08951 \cdot 10^{-3}$	$2.82081 \cdot 10^{-1}$	$-1.53295 \cdot 10^{-1}$	$-1.33066 \cdot 10^{-3}$
2	$4.44886 \cdot 10^{-2}$	$2.08921 \cdot 10^{-1}$	$-1.18630 \cdot 10^{-1}$	$-6.06609 \cdot 10^{-4}$
3	$1.01128 \cdot 10^{-2}$	$2.32007 \cdot 10^{-1}$	$-1.23651 \cdot 10^{-1}$	$6.17819 \cdot 10^{-4}$
4	$1.28076 \cdot 10^{-3}$	$1.96131 \cdot 10^{-1}$	$-1.00131 \cdot 10^{-1}$	$-6.22628 \cdot 10^{-4}$
5	$-6.52191 \cdot 10^{-4}$	$8.39544 \cdot 10^{-2}$	$4.09325 \cdot 10^{-1}$	$1.35517 \cdot 10^{-4}$
6	$-1.29880 \cdot 10^{-3}$	$2.44526 \cdot 10^{-2}$	$4.59640 \cdot 10^{-1}$	$8.05912 \cdot 10^{-8}$
7	$-8.67218 \cdot 10^{-4}$	$8.10744 \cdot 10^{-3}$	$6.20878 \cdot 10^{-1}$	$4.92545 \cdot 10^{-8}$
8	$1.93569 \cdot 10^{-4}$	$7.69892 \cdot 10^{-4}$	$9.92726 \cdot 10^{-3}$	0
9	$8.08731 \cdot 10^{-7}$	$3.77294 \cdot 10^{-4}$	$-1.88647 \cdot 10^{-4}$	0
10	$4.52564 \cdot 10^{-8}$	$2.77550 \cdot 10^{-5}$	$-1.38775 \cdot 10^{-5}$	0
11	$4.99702 \cdot 10^{-10}$	$3.16235 \cdot 10^{-7}$	$-1.58118 \cdot 10^{-7}$	0
12	$6.20321 \cdot 10^{-14}$	0	0	0

Table 9 Further remainder terms in the third example using the local approach for $J_{m,e}$

L	$\widetilde{\eta}_m$	$\widetilde{\mathscr{R}}_{\chi,1}^m$	$\widetilde{\mathscr{R}}_{\chi,2}^m$	$\widetilde{\mathscr{R}}_Q^m$
0	$5.17297 \cdot 10^{-2}$	0	$-8.60661 \cdot 10^{-4}$	$8.64324 \cdot 10^{-1}$
1	$-3.08951 \cdot 10^{-3}$	0	$3.54203 \cdot 10^{-3}$	$-6.40049 \cdot 10^{-1}$
2	$4.44886 \cdot 10^{-2}$	$-9.58987 \cdot 10^{-2}$	$-7.48296 \cdot 10^{-3}$	$-4.99250 \cdot 10^{-1}$
3	$1.01128 \cdot 10^{-2}$	$-1.14458 \cdot 10^{-1}$	$-1.68355 \cdot 10^{-3}$	$-1.12336 \cdot 10^{0}$
4	$1.28076 \cdot 10^{-3}$	$-3.34929 \cdot 10^{-2}$	$1.45877 \cdot 10^{-4}$	$-1.27280 \cdot 10^{0}$
5	$-6.52191 \cdot 10^{-4}$	$3.05771 \cdot 10^{-2}$	$4.54251 \cdot 10^{-6}$	$-1.50221 \cdot 10^{0}$
6	$-1.29880 \cdot 10^{-3}$	$2.20096 \cdot 10^{-2}$	$4.29122 \cdot 10^{-4}$	$-8.73594 \cdot 10^{-1}$
7	$-8.67218 \cdot 10^{-4}$	$1.00008 \cdot 10^{-2}$	$1.44846 \cdot 10^{-4}$	$-8.29465 \cdot 10^{-1}$
8	$1.93569 \cdot 10^{-4}$	$1.09697 \cdot 10^{-5}$	$-9.50257 \cdot 10^{-7}$	$-1.31994 \cdot 10^{-2}$
9	$8.08731 \cdot 10^{-7}$	0	$-2.13701 \cdot 10^{-7}$	$-1.40696 \cdot 10^{-3}$
10	$4.52564 \cdot 10^{-8}$	0	$-3.64489 \cdot 10^{-9}$	$-1.04913 \cdot 10^{-4}$
11	$4.99702 \cdot 10^{-10}$	0	$-5.61574 \cdot 10^{-11}$	$-1.14094 \cdot 10^{-6}$
12	$6.20321 \cdot 10^{-14}$	0	0	$2.21641 \cdot 10^{-12}$

It remains to clarify the very bad effectivity indices. To this end we take a look on the remainder terms, cf. Proposition 1. The results are listed in Tables 8 and 9, where the tilde marks that the terms are weighted by $J_{m,e}^r$. For comparison, we also give the estimated error. It should be remarked that the term $\widetilde{\mathscr{R}}_Q^m$ is not calculated based on it definition but on the error identity (17), because the involved higher directional derivatives are numerically very difficult to compute. This only leads to problems in the last iteration, where the error is dominated by numerical effects and is numerically

Table 10 Error between the reference and the model adaptive tangential multipliers in the L^2- and the L^∞-norm weighted by $J^r_{m,e}$ for the local approach

L	$\|\boldsymbol{\lambda}^r_{t,H} - \boldsymbol{\lambda}_{t,H}\|^{-J^r_{m,e}}_{0,\Gamma_C}$	$\|\boldsymbol{\lambda}^r_{t,H} - \boldsymbol{\lambda}_{t,H}\|^{-J^r_{m,e}}_{\infty,\Gamma_C}$	$\|\boldsymbol{\xi}^r_{t,H} - \boldsymbol{\xi}_{t,H}\|^{-J^r_{m,e}}_{0,\Gamma_C}$	$\|\boldsymbol{\xi}^r_{t,H} - \boldsymbol{\xi}_{t,H}\|^{-J^r_{m,e}}_{\infty,\Gamma_C}$
0	$1.95856 \cdot 10^3$	$2.50066 \cdot 10^3$	$3.10500 \cdot 10^3$	$2.08031 \cdot 10^4$
1	$1.75250 \cdot 10^3$	$2.50066 \cdot 10^3$	$3.12922 \cdot 10^3$	$2.08691 \cdot 10^4$
2	$1.63868 \cdot 10^3$	$2.50066 \cdot 10^3$	$3.24098 \cdot 10^3$	$2.09102 \cdot 10^4$
3	$1.36059 \cdot 10^3$	$2.50066 \cdot 10^3$	$3.26269 \cdot 10^3$	$2.08937 \cdot 10^4$
4	$1.09574 \cdot 10^3$	$2.50066 \cdot 10^3$	$3.33867 \cdot 10^3$	$2.09072 \cdot 10^4$
5	$9.62587 \cdot 10^2$	$2.50066 \cdot 10^3$	$3.17988 \cdot 10^3$	$2.15533 \cdot 10^4$
6	$5.98689 \cdot 10^2$	$1.63758 \cdot 10^3$	$3.43033 \cdot 10^3$	$2.23747 \cdot 10^4$
7	$4.91608 \cdot 10^2$	$1.63758 \cdot 10^3$	$3.54735 \cdot 10^3$	$2.24351 \cdot 10^4$
8	$2.37544 \cdot 10^2$	$1.69193 \cdot 10^3$	$2.42920 \cdot 10^3$	$2.10702 \cdot 10^4$
9	$2.15493 \cdot 10^2$	$1.05337 \cdot 10^3$	$3.19952 \cdot 10^2$	$1.55314 \cdot 10^3$
10	$1.24543 \cdot 10^2$	$7.16344 \cdot 10^2$	$1.86163 \cdot 10^2$	$1.08301 \cdot 10^3$
11	$1.04418 \cdot 10^1$	$8.49499 \cdot 10^1$	$1.51450 \cdot 10^1$	$1.23208 \cdot 10^2$
12	$2.10765 \cdot 10^{-9}$	$1.08137 \cdot 10^{-8}$	$1.25512 \cdot 10^{-8}$	$9.92692 \cdot 10^{-8}$

speaking zero. What we see here is that the error estimator η_m is dominated by the remainder terms $-\Delta(\mathbf{w})\left(e^r_{\mathbf{z}}\right)$, $-\frac{1}{2}\bar{\Delta}\left(e^r_{\mathbf{w}}, e^r_{\mathbf{z}}\right)$, and $\mathscr{R}^m_Q$, while the other remainder terms $\mathscr{R}^m_c$, $\mathscr{R}^m_{\chi,1}$, and $\mathscr{R}^m_{\chi,2}$ are considerably smaller or even vanishing. It should be remarked that we have listed values smaller than 10^{-15} as zero here. Now the question arises, why these three remainder terms are not of higher order as one would expect. The answer is found in Table 10, where we see that the error with respect to the decisive values $\boldsymbol{\lambda}_{t,H}$ and $\boldsymbol{\xi}_{t,H}$ is approximately constant up to iteration number ten. Then it is fast decreasing. But it reaches only in the last iteration appropriate values. Because the remainder terms $-\Delta(\mathbf{w})\left(e^r_{\mathbf{z}}\right)$, $-\frac{1}{2}\bar{\Delta}\left(e^r_{\mathbf{w}}, e^r_{\mathbf{z}}\right)$, and $\mathscr{R}^m_Q$ are mainly depending on these errors, they also stay large. The major factor for the large error with respect to $\boldsymbol{\lambda}_{t,H}$ and $\boldsymbol{\xi}_{t,H}$ lies in the model distribution shown in Table 7, where in the middle of the contact zone frictionless contact is used up to the last iteration. This behavior is expected in view of the quantity of interest $J_{m,e}$, because the tangential displacement $\mathbf{u}_t$ and therewith also $\boldsymbol{\lambda}_t\mathbf{u}_t$ is zero there nevertheless a friction model is used or not. However, the Lagrange multipliers $\boldsymbol{\lambda}_{t,H}$ and $\boldsymbol{\xi}_{t,H}$ are not well approximated leading to the bad estimation of the model error.

The observations of the last paragraph motivate the model adaptive strategy named global, where we conduct a global model enhancement step in the beginning. The results are listed in Table 11, where we observe a fast reduction of the error and a very accurate estimation of the error except of the first and the last iteration, where the inaccuracy in the last step arises from numerical errors, because the error is smaller than the stopping tolerance of the used solvers. The resulting model distributions, cf. Table 12, are similar to the ones in Table 7. The only difference is the use of Tresca's law in the middle of the contact zone from the beginning. The remainder terms are

Table 11 Model adaptive results in the third example using the global approach for $J_{m,e}$

L	$E_{\text{rel}}\left(J_{m,e}\right)$	$I_{\text{eff}}\left(J_{m,e}, \eta_m\right)$	$\text{iter}_{\text{Newton}}$	$\text{iter}_{\text{GMRES}}$	$\text{iter}_{\text{dual}}$
0	$1.00000 \cdot 10^{0}$	19.33126	9	344	1
1	$1.64373 \cdot 10^{-2}$	0.99798	14	1187	137
2	$4.01897 \cdot 10^{-4}$	0.99965	3	147	144
3	$1.36270 \cdot 10^{-6}$	1.00001	3	117	128
4	$9.96663 \cdot 10^{-10}$	1.02364	2	60	68
5	$1.02213 \cdot 10^{-12}$	16.47748	2	44	56
Sum			33	1899	534

Table 12 Model distribution in the third example using the global approach for $J_{m,e}$

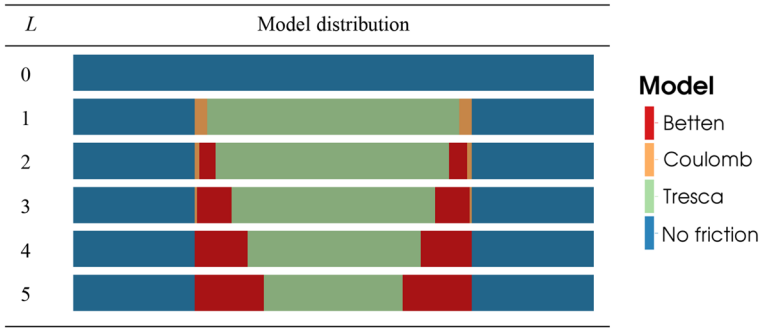

Table 13 Remainder terms in the third example using the global approach for $J_{m,e}$, $\widetilde{\mathscr{R}}^m_{\chi,1}$ is zero for all L as well as $\widetilde{\mathscr{R}}^m_c$ equals $-4.75752 \cdot 10^{-3}$ for $L = 0$ and is zero afterwards

L	$\widetilde{\eta}_m$	$-\widetilde{\Delta}\left(\mathbf{w}\right)\left(e^r_{\mathbf{z}}\right)$	$-\frac{1}{2}\widetilde{\Delta}\left(e^r_{\mathbf{w}}, e^r_{\mathbf{z}}\right)$	$\widetilde{\mathscr{R}}^m_{\chi,2}$	$\widetilde{\mathscr{R}}^m_Q$
0	$5.17297 \cdot 10^{-2}$	$2.00733 \cdot 10^{-1}$	$-1.11169 \cdot 10^{-1}$	$-8.60661 \cdot 10^{-4}$	$8.64324 \cdot 10^{-1}$
1	$1.64705 \cdot 10^{-2}$	$3.71207 \cdot 10^{-4}$	$-2.04889 \cdot 10^{-4}$	$-1.99633 \cdot 10^{-4}$	$6.10165 \cdot 10^{-8}$
2	$4.02038 \cdot 10^{-4}$	$3.57002 \cdot 10^{-7}$	$-1.79140 \cdot 10^{-7}$	$-3.18559 \cdot 10^{-7}$	$4.30094 \cdot 10^{-11}$
3	$1.36268 \cdot 10^{-6}$	$5.20209 \cdot 10^{-11}$	$-2.60118 \cdot 10^{-11}$	$-6.07970 \cdot 10^{-12}$	$-3.11405 \cdot 10^{-13}$
4	$9.73648 \cdot 10^{-10}$	0	0	0	$2.30150 \cdot 10^{-11}$
5	$6.20321 \cdot 10^{-14}$	0	0	0	$9.60100 \cdot 10^{-13}$

now really of higher order, see Table 13. Only in the last two iterations $\mathscr{R}^m_Q$ becomes dominant, because numerical effects pollute its calculation. We observe, that the error with respect to the decisive values $\boldsymbol{\lambda}_{t,H}$ and $\boldsymbol{\xi}_{t,H}$ is rapidly decreasing using the global strategy in contrast to the local one, cf. Table 14.

Another question, which is addressed here, is the possible gain of model adaptive methods. To this end, we compare the numerical effort for solving the discrete systems. To simplify the comparison, we do not use the complex solution algorithm

Table 14 Error between the reference and the model adaptive tangential multipliers in the L^2- and the L^∞-norm weighted by $J^r_{m,e}$ for the global approach

L	$\|\lambda^r_{t,H} - \lambda_{t,H}\|^{-J^r_{m,e}}_{0,\Gamma_C}$	$\|\lambda^r_{t,H} - \lambda_{t,H}\|^{-J^r_{m,e}}_{\infty,\Gamma_C}$	$\|\xi^r_{t,H} - \xi_{t,H}\|^{-J^r_{m,e}}_{0,\Gamma_C}$	$\|\xi^r_{t,H} - \xi_{t,H}\|^{-J^r_{m,e}}_{\infty,\Gamma_C}$
0	$1.95856 \cdot 10^3$	$2.50066 \cdot 10^3$	$3.10500 \cdot 10^3$	$2.08031 \cdot 10^4$
1	$3.65171 \cdot 10^1$	$2.12218 \cdot 10^2$	$1.41776 \cdot 10^1$	$7.49034 \cdot 10^1$
2	$9.55712 \cdot 10^{-1}$	$7.69382 \cdot 10^0$	$4.05469 \cdot 10^{-1}$	$2.17961 \cdot 10^0$
3	$5.72818 \cdot 10^{-3}$	$4.28184 \cdot 10^{-2}$	$7.50040 \cdot 10^{-3}$	$5.51168 \cdot 10^{-2}$
4	$2.65464 \cdot 10^{-6}$	$2.32711 \cdot 10^{-5}$	$3.32915 \cdot 10^{-6}$	$2.90435 \cdot 10^{-5}$
5	$1.76888 \cdot 10^{-9}$	$1.38249 \cdot 10^{-8}$	$1.16721 \cdot 10^{-8}$	$9.43635 \cdot 10^{-8}$

proposed in [10,24] here, but we solve the Schur complement system directly using a restarted GMRES method with a diagonal preconditioner. In this case, the iteration count of the GMRES method is an appropriate measure for the solving effort. The arising inner systems with respect to the stiffness matrix in every GMRES step are solved by a direct solver using a Cholesky factorization, which is determined in advance because the stiffness matrix stays constant over the whole calculation. We need 33 Newton steps with in total 3, 261 GMRES steps to solve the reference problem, where we use the law of Betten globally. To calculate the reference dual solution, we need 141 steps of the restarted GMRES method with diagonal preconditioning. As listed in Table 11, we need in total 33 Newton steps for solving all problems of the model adaptive approach. Therein, 1, 899 GMRES steps are applied. Even, if we add the 534 GMRES steps for solving the dual problems, these are 828 GMRES steps less. The additional overhead for the error estimation is negligible, because we only have to perform one integration over the contact boundary per iteration.

To substantiate the efficiency and accuracy of the model adaptive approach, we also consider a second quantity of interest, which is completely different to $J_{m,e}$. It is given by

$$J_{m,d}(\mathbf{u}) := \int_\Omega \omega_2(x)\,|\mathbf{u}|^2\,dx,$$

where $\omega_2(x) = 0.5\left(\tanh(20(0.5 - |x - (-2.5, 0)^\top|)) + 1\right)$ is a cut off function with respect to the disc $B_{0.5}\left((-2.5, 0)^\top\right)$. Here, we can expect a small influence of the frictional modeling on the quantity of interest, which is illustrated by the small initial error, cf. Table 15. Using the global approach, we get an accurate error estimation and a rapidly decreasing error as for the quantity of interest $J_{m,e}$. And again, we see a bad effectivity index in the last iteration due to numerical pollution. Here, we need 1, 047 GMRES steps less in the whole model adaptive approach, mainly arising from the simpler dual problem. The model distribution, depicted in Table 16, is almost the same as for the quantity of interest $J_{m,e}$. However, we arrive at an relative error of approximately 10^{-10} in the third step, where the reference model is used in a much smaller region. This is, what one would expect for the considered quantity of interest.

Table 15 Model adaptive results in the third example using the global approach for $J_{m,d}$

L	$E_{\text{rel}}(J_{m,d})$	$I_{\text{eff}}(J_{m,d}, \eta_m)$	$\text{iter}_{\text{Newton}}$	$\text{iter}_{\text{GMRES}}$	$\text{iter}_{\text{dual}}$
0	$-1.63284 \cdot 10^{-4}$	159.77757	9	344	33
1	$-2.04258 \cdot 10^{-5}$	1.02659	14	1187	131
2	$-3.08325 \cdot 10^{-7}$	1.00017	3	145	76
3	$-1.70134 \cdot 10^{-10}$	0.99972	3	117	68
4	$-4.62794 \cdot 10^{-14}$	−0.72619	2	58	55
Sum			31	1851	363

Table 16 Model distribution in the third example using the global approach for $J_{m,d}$

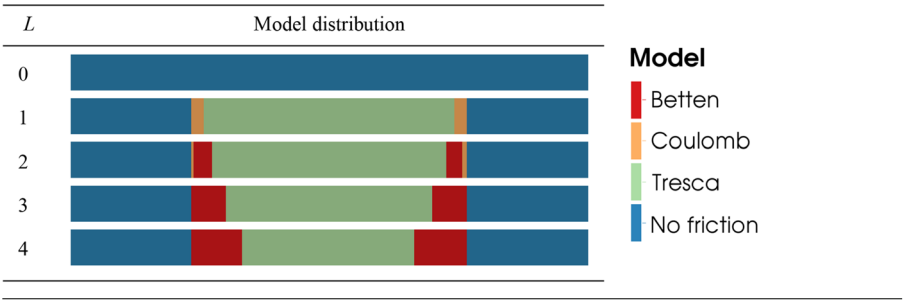

5.4 Fourth example: Mesh and model adaptivity

In this section, we test the mesh and model adaptive algorithm by a nonsmooth example. We pick up the domain and the boundary data of the second example describe in Sect. 5.2. The obstacle is given by

$$g(y) = \tan(\alpha)\,|y| - 0.02 \qquad \text{with} \qquad \alpha = \frac{\pi}{36}.$$

The frictionless contact of an obstacle of this type with an elastic half space is discussed in [36, Section 5.2]. There, the analytic contact stress distribution

$$\sigma_{nn}(x_2) = \frac{E\cot(\alpha)}{2\pi} \log\left[\frac{a + \left(a^2 - x_2^2\right)^{1/2}}{a - \left(a^2 - x_2^2\right)^{1/2}}\right] = \frac{E\cot(\alpha)}{\pi} \cosh^{-1}\left(\frac{a}{x_2}\right)$$

is derived, where a denotes the width of the active contact zone. We see that the contact stress goes to zero, if one approaches the boundary of the active contact zone, and that it has a singularity in 0, i.e. in the middle of the contact zone. Furthermore, we obtain

$$\int_{\Gamma_C} \sigma_{nn}\, do = aE\cot(\alpha).$$

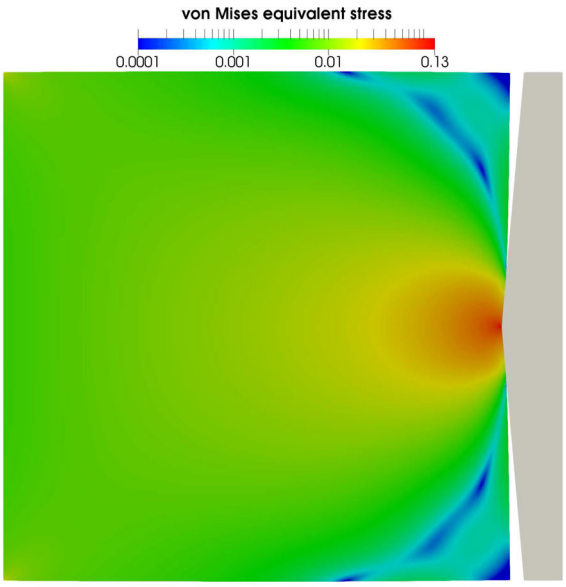

(a) Plot of the von Mises equivalent stress on the deformed con - figuration and the obstacle colored in grey on the right

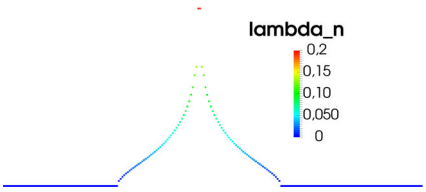

(b) Plot of $\lambda_{n,H}$

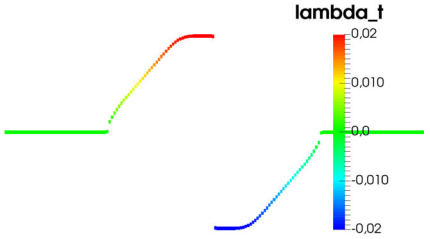

(c) Plot of $\boldsymbol{\lambda}_{t,H}$

Fig. 8 Numerical solution of the fourth example for $M_\Omega = 1{,}048{,}576$ and $M_C = 512$

We choose the material parameters $E = 1$ and $\nu = 0.25$ as well as the frictional parameters $C_T = 0.02$, $\mathscr{F} = 0.4$, and $n = 3$, see Table 1 for the notation. The numerical solution is illustrated for a fine uniformly refined mesh in Fig. 8, where the von Mises equivalent stress following Eq. (24) with $\sigma_e = 1$ is plotted. We observe stress peaks at the tip of the wedge and in the corners, where the boundary conditions changes from Dirichlet to Neumann type. Consequently, we expect adaptive mesh refinements in these points. Furthermore, the boundary of the active contact zone should be strongly refined. The plot of $\lambda_{n,H}$ reveals the singularity on the tip of the wedge, where $\boldsymbol{\lambda}_{t,H}$ changes its sign. From the plot of $\boldsymbol{\lambda}_{t,H}$, we expect the use of Tresca's friction law in the middle of the contact zone as well as of Coulomb's or Betten's law at the boundary.

Here, we compare three different approaches: One based on uniform mesh refinement with Betten's friction law, one using adaptive mesh refinement utilizing Betten's friction law, and a model and mesh adaptive one. In the last approach, an equilibration

strategy up to a constant $c_e \geq 1$ is employed between the discretization and the model error. Until the first model enhancement, we set $c_e = 1000$ and perform a global model refinement step. Afterwards, we reduce c_e and choose $c_e = 10$, i.e. the discretization and the model error should be of the same order of magnitude. To shorten the notation, we set

$$\eta_{pd}^m := \eta_m + \eta \qquad \text{and} \qquad \eta_p^m := \eta_m + \eta_p.$$

We consider the quantity of interest

$$J_{W,\lambda}(\mathbf{w}) = \int_{\Gamma_C} -0.001 \tanh(20x_2)\boldsymbol{\lambda}_t + 0.001\lambda_n + 0.1\boldsymbol{\lambda}_t \mathbf{u}_t \, do,$$

which consists of a weighted sum of an approximation of the L^1-norm of $\boldsymbol{\lambda}_t$, the L^1-norm of λ_n, and of the dissipated energy. Here, we have a difficult quantity of interest concentrated on the contact variables. The reference value to calculate errors and effectivity indices is calculated as in Sect. 5.2 and we obtain

$$J_{W,\lambda}(\mathbf{w}) \approx 1.0245635776184553 \cdot 10^{-5}.$$

In Tables 17 and 18, the results of the model and mesh adaptive algorithm are listed. The effectivity indices are on finer meshes in the range of 1.15, which is excellent for this type of problem and comparable to the results for the example discussed in Sect. 5.2. We also give the wall time of the computation up to finishing the current iteration in percentage of the wall time of calculating the numerical solution on a uniformly refined mesh with $M_\Omega = 1,048,576$ cells, where we observe an relative error $E_{\text{rel}}(J_W)$ of $5.215 \cdot 10^{-5}$. Thus, we arrive at an error, which is about 50 times smaller, by the model and mesh adaptive approach in less than one third of the wall time including an accurate error estimation. The model distribution depicted in Table 18 is at first sight astonishing, since it does not meet expectations. The reason lies in the fact that in the global model enhancement step only Coulomb's law is chosen due to the contact stress distribution in this step. The results of the mesh adaptive approach are given in Table 19. They almost agree with the results of the model and mesh adaptive algorithm. However, we need 6 iterations less to achieve almost the same accuracy with almost the same number of mesh elements. Taking a look on the adaptive meshes depicted in Fig. 9 reveals that the structure of the adaptive meshes also coincides. It is remarkable that the model and mesh adaptive needs less wall time, 31.06% to 35.08%, in spite of the higher iteration count. The accordance of the two adaptive approaches is further substantiated by the convergence plot in Fig. 10, where the two graphs coincide nearly after the first iterations. They outperform obviously the uniform approach by far. A short comment on the jumping of the error plot in the first iterations is in order: The first jump of the error upward is due to a change of sign in the error. A second effect on coarse meshes comes into play after an adaptive mesh refinement step following a model enhancement one. By changing the mesh, the results on the border of the active contact set are significantly influenced implying a possible bad choice of the friction model. This bad choice is corrected in

Table 17 Results of the mesh and model adaptive algorithm for the quantity of interest $J_{W,\lambda}$

M_Ω	L	$E_{\text{rel}}\left(J_{W,\lambda}\right)$	$I_{\text{eff}}\left(J_{W,\lambda}, \eta_p^m\right)$	$I_{\text{eff}}\left(J_{W,\lambda}, \eta_{pd}^m\right)$	Wall time (%)
64	0	$2.48568 \cdot 10^{-1}$	6.55438	62.76759	0.00
64	1	$1.25069 \cdot 10^{-1}$	1.73085	3.10429	0.00
88	2	$-1.50805 \cdot 10^{-1}$	35.42453	35.22117	0.00
112	3	$-6.12244 \cdot 10^{-2}$	−6.78108	−4.05300	0.00
208	4	$-1.38183 \cdot 10^{-2}$	−1.55629	−1.13188	0.00
208	5	$-2.59729 \cdot 10^{-3}$	0.45037	2.24576	0.00
280	6	$-1.05344 \cdot 10^{-2}$	1.12840	1.08499	0.00
280	7	$-8.44962 \cdot 10^{-3}$	1.16375	1.32843	0.00
736	8	$-2.41636 \cdot 10^{-3}$	0.99806	0.93770	0.01
736	9	$-2.20098 \cdot 10^{-3}$	0.99743	0.96576	0.01
2440	10	$-7.28187 \cdot 10^{-4}$	1.16693	1.15004	0.01
7648	11	$-3.37022 \cdot 10^{-4}$	1.34136	1.49279	0.05
22,312	12	$-1.22755 \cdot 10^{-4}$	1.07848	1.09406	0.12
22,312	13	$-7.71421 \cdot 10^{-5}$	1.13096	1.16028	0.17
83,836	14	$-2.24692 \cdot 10^{-5}$	1.08836	1.11318	0.51
83,836	15	$-1.99230 \cdot 10^{-5}$	1.10077	1.12939	0.65
176,284	16	$-1.01709 \cdot 10^{-5}$	1.13701	1.14751	1.32
587,152	17	$-3.22243 \cdot 10^{-6}$	1.15804	1.16419	4.56
1,944,688	18	$-1.00690 \cdot 10^{-6}$	1.14391	1.14916	31.06

the next model enhancement step leading to a large decrease of the error. This effect arises more often in the calculations to the second considered quantity of interest, see Fig. 11b.

Finally, we consider a second quantity of interest, which is given by

$$J_{W,\mathbf{u}}(\mathbf{u}) = 0.0005 \int_\Omega \left[\tanh\left(20\left(0.25 - |x - a|\right)\right) + 1\right]\left[|\mathbf{u}|^2 - \mathbf{u}_1 + \mathbf{u}_2\right] dx$$

with $a = (-0.625, 0.125)^\top$. Here, we are interested in the displacement in the disc of radius 0.25 around the point a, which we approximate by a smooth function. We expect that the effects due to contact and friction have less influence on the quantity of interest than in the foregoing one. The numerically determined reference value is given by

$$J_{W,\mathbf{u}}(\mathbf{u}) \approx 7.673943612476585 \cdot 10^{-7}.$$

To shorten the presentation, we focus on the mesh and model adaptive approach. The mesh adaptive one gives similar results just like in the foregoing calculation. The detailed results of the mesh and model adaptive algorithm are listed in Tables 20 and

Table 18 Model distribution in the fourth example for the quantity of interest $J_{W,\lambda}$

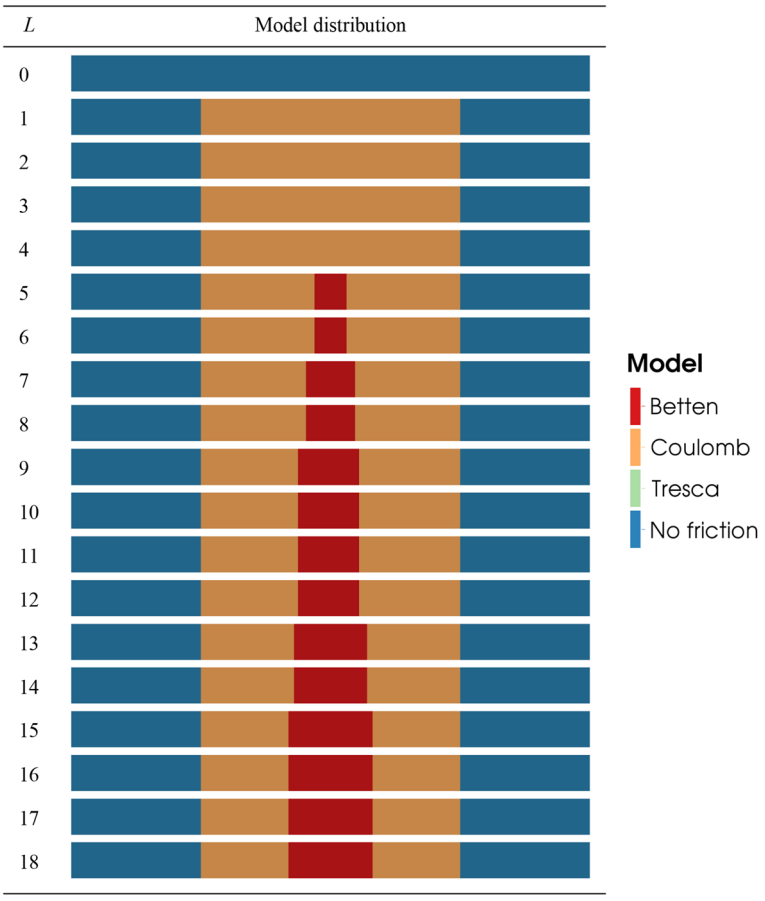

21. We find excellent effectivity indices in the range of 1 on finer meshes, where the last iteration is perturbed by the numerically determined reference value. We need less than 25% of the wall time of the uniform approach with $M_\Omega = 1{,}048{,}576$ to perform the complete model and mesh adaptive algorithm, leading to an error, which is a magnitude smaller, cf. Fig. 11b. In the model distribution, see Table 21, we find significant difference compared to the foregoing calculation. The first model enhancement is conducted in the seventh step compared to the first one. Furthermore, we find the expected model distribution: Tresca's law in the middle, Coulomb's law at the boundary of the contact zone, and Betten's law between them. A short comment concerning the comparison of the mesh and model adaptive algorithm to the mesh adaptive one is in order. The mesh adaptive algorithm needs 22.76% of the wall time of the uniform approach with an error similar to the one of the mesh and model adaptive algorithm. The performance of the mesh and model adaptive algorithm mainly depends

Table 19 Results of the mesh adaptive algorithm for the quantity of interest $J_{W,\lambda}$

M_Ω	L	$E_{\text{rel}}\left(J_{W,\lambda}\right)$	$I_{\text{eff}}\left(J_{W,\lambda}, \eta_p\right)$	$I_{\text{eff}}\left(J_{W,\lambda}, \eta\right)$	Wall time (%)
64	0	$1.25069 \cdot 10^{-1}$	1.73084	3.10427	0.00
88	1	$-1.50805 \cdot 10^{-1}$	35.42287	34.80175	0.00
112	2	$-1.56346 \cdot 10^{-2}$	1.22312	−1.01051	0.00
208	3	$-2.11472 \cdot 10^{-3}$	0.40677	2.92888	0.00
280	4	$-8.24509 \cdot 10^{-3}$	1.17202	1.34236	0.00
736	5	$-2.15609 \cdot 10^{-3}$	0.99704	0.92938	0.01
2392	6	$-6.87787 \cdot 10^{-4}$	1.17538	1.13931	0.01
7600	7	$-2.91460 \cdot 10^{-4}$	1.39701	1.72390	0.03
22,528	8	$-7.39779 \cdot 10^{-5}$	1.13851	1.16866	0.11
84,472	9	$-1.97694 \cdot 10^{-5}$	1.10244	1.13059	0.43
176,536	10	$-1.01376 \cdot 10^{-5}$	1.13777	1.14806	1.12
587,728	11	$-3.19374 \cdot 10^{-6}$	1.15990	1.16592	4.82
1,947,544	12	$-9.77713 \cdot 10^{-7}$	1.14901	1.15430	35.08

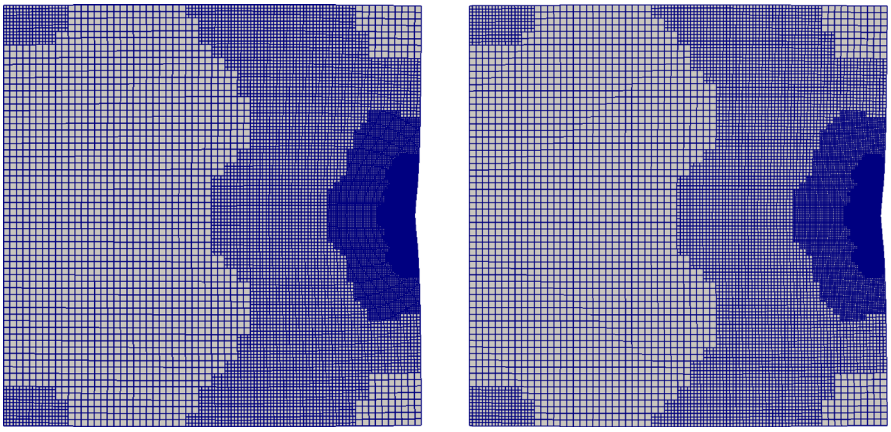

(a) Mesh adaptive algorithm, $L = 8$ **(b)** Mesh and model adaptive algorithm, $L = 12$

Fig. 9 Adaptive meshes in the mesh adaptive as well as in the mesh and model adaptive algorithm in the fourth example for the quantity of interest $J_{W,\lambda}$

on the question, if the model adaptive steps are carried out in the early stages of the adaptive algorithm, where they do not imply a large effort, or in the later stages, where the additional effort compared to the mesh adaptive algorithm is larger. All in all, the mesh and model adaptive algorithm as well as the mesh adaptive one lead to nearly identical results using a comparable wall time. Taking the additional effort of the mesh and model adaptive algorithm into account clearly visible by the higher number of adaptive iterations, this result shows the potential of the model adaptive approach.

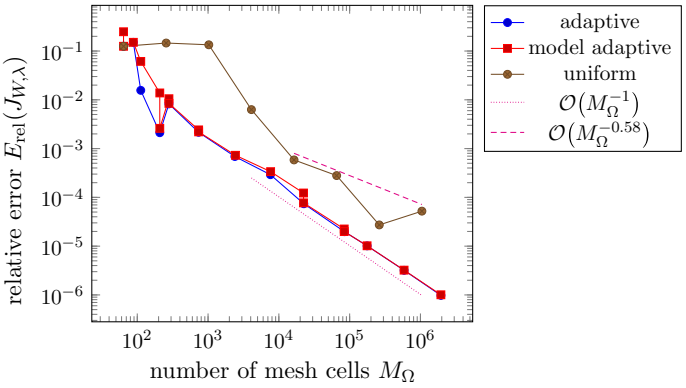

Fig. 10 Comparison of the convergence properties of the different approaches in the fourth example for the quantity of interest $J_{W,\lambda}$

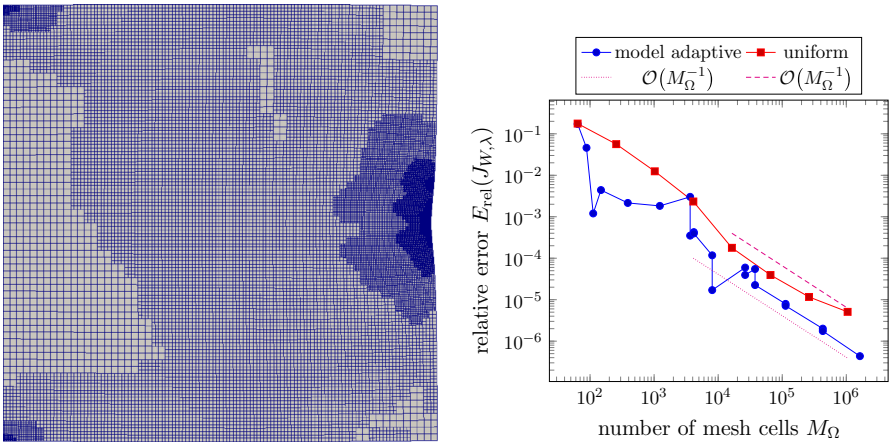

(a) Adaptive mesh, $L = 13$ **(b)** Convergence results

Fig. 11 Adaptive mesh in the mesh and model adaptive algorithm and convergence results in the fourth example for the quantity of interest $J_{W,\mathbf{u}}$

6 Conclusions and outlook

We have derived goal oriented a posteriori error estimates with respect to the discretization as well as model error for discretizations of frictional contact problems in this article. The presented approach leads to accurate estimates even using higher order reconstruction, although it is not asymptotically exact. Furthermore, it is based

Table 20 Results of the mesh and model adaptive algorithm for the quantity of interest $J_{W,\mathbf{u}}$

M_Ω	L	$E_{\text{rel}}\left(J_{W,\mathbf{u}}\right)$	$I_{\text{eff}}\left(J_{W,\mathbf{u}}, \eta_p^m\right)$	$I_{\text{eff}}\left(J_{W,\mathbf{u}}, \eta_{pd}^m\right)$	Wall time (%)
64	0	$1.72642 \cdot 10^{-1}$	3.00284	8.60724	0.00
88	1	$-4.60109 \cdot 10^{-2}$	−6.62090	3.74950	0.00
112	2	$-1.20104 \cdot 10^{-3}$	0.12480	0.05963	0.00
148	3	$4.40116 \cdot 10^{-3}$	−1.05815	−0.68818	0.00
388	4	$-2.15290 \cdot 10^{-3}$	0.58717	0.46851	0.00
1228	5	$1.82707 \cdot 10^{-3}$	−1.61089	−1.41665	0.01
3652	6	$3.01930 \cdot 10^{-3}$	−8.14365	−7.39158	0.01
3652	7	$-3.50418 \cdot 10^{-4}$	0.95891	0.82398	0.03
4168	8	$-4.25549 \cdot 10^{-4}$	1.15699	1.13607	0.04
4168	9	$-3.95865 \cdot 10^{-4}$	1.15960	1.13708	0.04
8068	10	$-1.17377 \cdot 10^{-4}$	0.95370	0.92130	0.07
8068	11	$-1.70178 \cdot 10^{-5}$	0.70890	0.60195	0.08
26,368	12	$5.95043 \cdot 10^{-5}$	0.99061	1.00439	0.19
26368	13	$3.94487 \cdot 10^{-5}$	0.96457	0.97133	0.26
37,624	14	$5.48018 \cdot 10^{-5}$	1.01664	1.02401	0.36
37,624	15	$-2.25305 \cdot 10^{-5}$	0.98129	0.96065	0.46
112,840	16	$-7.92119 \cdot 10^{-6}$	1.02711	1.01617	0.90
112,840	17	$-7.11743 \cdot 10^{-6}$	1.02995	1.02046	1.26
429,688	18	$-2.00424 \cdot 10^{-6}$	1.01468	1.00707	3.73
429,688	19	$-1.75265 \cdot 10^{-6}$	1.01537	1.00562	5.39
1,630,696	20	$-4.34912 \cdot 10^{-7}$	0.95201	0.94408	24.43

on a linear dual problem and directly measures the error in the frictional contact conditions, which is necessary for the estimation of the model error. However, it is not clear, whether the remainder terms are of higher order or not. Numerical results substantiate the assumption that they are of higher order. However, a precise analysis is a topic of further research. A further content is the extension to more complex contact problems. Some results on multibody contact problems are discussed in [24, Chapter 5]. Especially in dynamic contact problems, the precise consideration of the error in the contact conditions is needed to accurately resolve impact phenomena.

Table 21 Model distribution in the fourth example for the quantity of interest $J_{W,\mathbf{u}}$

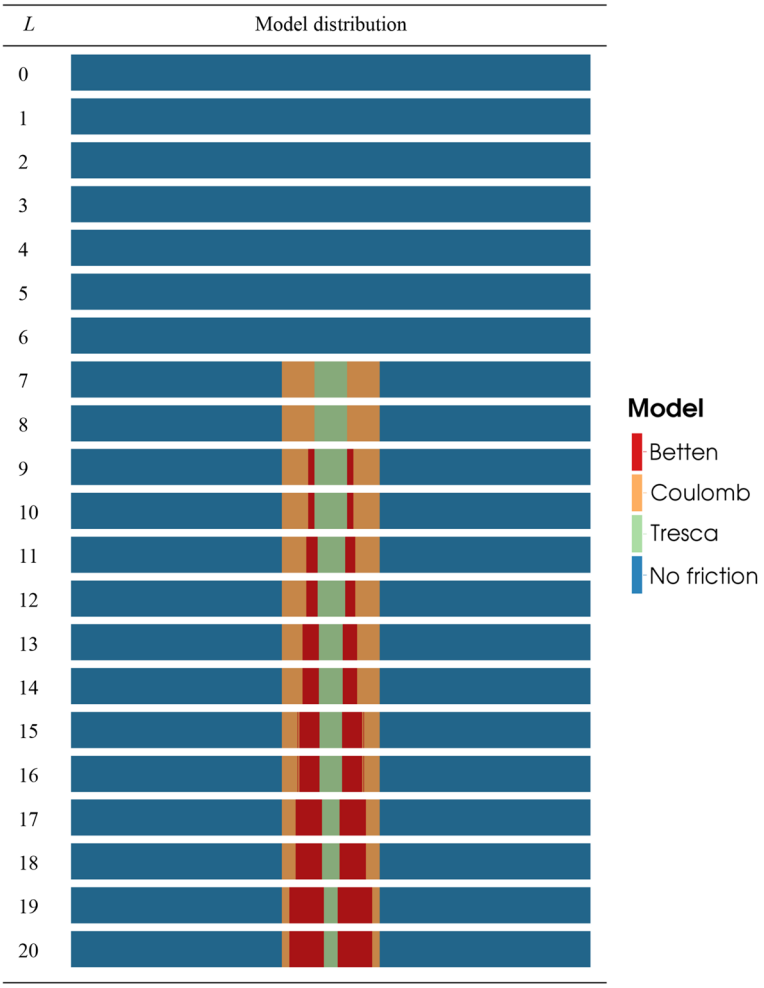

Acknowledgements The author gratefully acknowledges the financial support by the German Research Foundation (DFG) within the subproject A5 of the transregional collaborative research centre (Transregio) 73 "Sheet-Bulk-Metal-Forming".

References

1. Actis, R.L., Szabo, B.A., Schwab, C.: Hierarchic models for laminated plates and shells. Comp. Methods Appl. Mech. Engrg. **172**, 79–107 (1999)
2. Ainsworth, M., Oden, J., Lee, C.: Local a posteriori error estimators for variational inequalities. Numer. Methods Partial Differ. Equ. **9**, 23–33 (1993)

3. Bangerth, W., Rannacher, R.: Adaptive finite element methods for differential equations. Lectures in Mathematics, ETH Zürich. Birkhäuser, Basel (2003)
4. Bartels, S., Carstensen, C.: Averaging techniques yield reliable a posteriori finite element error control for obstacle problems. Numer. Math. **99**(2), 225–249 (2004)
5. Becker, R., Rannacher, R.: An optimal control approach to a posteriori error estimation in finite element methods. Acta Numerica **10**, 1–102 (2001)
6. Betten, J.: Bemerkungen zum Versuch von Hohenemser. ZAMM **55**, 149–158 (75)
7. Beyer, F., Blum, H., Kumor, D., Rademacher, A., Willner, K., Schneider, T.: Experimental and simulative investigations of tribology in sheet-bulk-metal-forming. Key Engrg. Mat. **639**, 283–290 (2015)
8. Billade, N., Vemaganti, K.: Hierarchical models of thin elastic structures: Overview and recent adcances in error estimation and adaptivity. Comp. Methods Appl. Mech. Engrg. **196**, 3508–3523 (2007)
9. Blum, H., Braess, D., Suttmeier, F.T.: A cascadic multigrid algorithm for variational inequalities. Comput. Vis. Sci. **7**(3–4), 153–157 (2004)
10. Blum, H., Frohne, H., Frohne, J., Rademacher, A.: Semi-smooth Newton methods for mixed FEM discretizations of higher-order for frictional, elasto-plastic two-body contact problems. Comput. Method. Appl. Mech. Eng. **309**, 131–151 (2016)
11. Blum, H., Schroeder, A., Suttmeier, F.: A posteriori estimates for FE-solutions of variational inequalities. In: F. Brezzi, et al. (eds.) Numerical mathematics and advanced applications. Proceedings of ENUMATH 2001, the 4th European conference, Ischia, July 2001, pp. 669–680. Springer, Berlin (2003)
12. Blum, H., Suttmeier, F.T.: An adaptive finite element discretisation for a simplified Signorini problem. Calcolo **37**(2), 65–77 (2000)
13. Bohinc, U.: Adaptive analysis of plate structures. Ph.D. thesis, L'Ecole Normale Supérieure de Cachan (2011)
14. Bowden, F.P., Tabor, T.: The Friction and Lubrication of Solids. Clarendon Press, Oxford (2001)
15. Braack, M., Ern, A.: A posteriori control of modeling errors and discretization errors. Multiscale Model. Simul. **1**(2), 221–238 (2003)
16. Braack, M., Taschenberger, N.: A posteriori control of modeling and discretization errors for quasi periodic solutions. J. Numer. Math. **22**(2), 87–108 (2014)
17. Braess, D.: A posteriori error estimators for obstacle problems - another look. Numer. Math. **101**(3), 415–421 (2005)
18. Braess, D., Carstensen, C., Hoppe, R.: Error reduction in adaptive finite element approximations of elliptic obstacle proplems. J. Comput. Math. **27**, 148–169 (2009)
19. Braess, D., Carstensen, C., Hoppe, R.H.: Convergence analysis of a conforming adaptive finite element method for an obstacle problem. Numer. Math. **107**(3), 455–471 (2007)
20. Chen, Z., Nochetto, R.H.: Residual type a posteriori error estimates for elliptic obstacle problems. Numer. Math. **84**(4), 527–548 (2000)
21. Dörsek, P., Melenk, J.: Adaptive hp-FEM for the contact problem with Tresca friction in linear elasticity: The primal-dual formulation and a posteriori error estimation. Appl. Numer. Math. **60**(7), 689–704 (2010)
22. Duvaut, G., Lions, J.L.: Inequalities in Mechanics and Physics. Grundlehren der mathematischen Wissenschaften. Springer, Berlin (1976)
23. Eck, C., Jarusek, J., Krbec, M.: Unilateral Contact Problems: Variational Methods and Existence Theorems. CRC Press, Boca Raton (2005)
24. Frohne, H.: Finite Elemente Methoden höherer Ordnung für reibungsbehaftete, elasto-plastische Mehrkörperkontaktprobleme - Fehlerkontrolle, adaptive Methoden und effiziente Lösungsverfahren. Ph.D. thesis, Technische Universität Dortmund (2018)
25. Große-Wöhrmann, A., Blum, H., Stiemer, M.: A posteriori control of modelling errors in linear elasticity. Proc. Appl. Math. Mech. **10**, 647–648 (2010)
26. Haslinger, J.: Mixed formulation of elliptic variational inequalities and its approximation. Appl. Math. **26**, 462–475 (1981)
27. Haslinger, J., Dostál, Z., Kučera, R.: On a splitting type algorithm for the numerical realization of contact problems with coulomb friction. Comput. Methods Appl. Mech. Eng. **191**(21–22), 2261–2281 (2002)
28. Haslinger, J., Sassi, T.: Mixed finite element approximation of 3D contact problems with given friction: error analysis and numerical realization. Math. Mod. Numer. Anal. **38**, 563–578 (2004)

29. Hauer, F.: Die elasto-plastische Einglättung rauer Oberflächen und ihr Einfluss auf die Reibung in der Umformtechnik. Ph.D. thesis, Friedrich-Alexander-Universität Erlangen-Nürnberg (2014)
30. Hild, P., Nicaise, S.: A posteriori error estimations of residual type for Signorini's problem. Numer. Math. **101**(3), 523–549 (2005)
31. Hintermüller, M., Ito, K., Kunisch, K.: The primal-dual active set strategy as a semi-smooth newton method. SIAM J. Optim. **13**(3), 865–888 (2003)
32. Hoppe, R., Kornhuber, R.: Adaptive multilevel methods for obstacle problems. SIAM J. Numer. Anal. **31**, 301–323 (1994)
33. Hüeber, S.: Discretization techniques and efficient algorithms for contact problems. Ph.D. thesis, Universität Stuttgart (2008)
34. Hüeber, S., Mair, M., Wohlmuth, B.: A priori error estimates and an inexact primal-dual active set strategy for linear and quadratic finite elements applied to multibody contact problems. Appl. Numer. Math. **54**(3–4), 555–576 (2005)
35. Johnson, C.: Adaptive finite element methods for the obstacle problem. Math. Models Meth. Appl. Sci. **2**, 483–487 (1992)
36. Johnson, K.: Contact Mechanics. Cambridge University Press, Cambridge (1985)
37. Kikuchi, N., Oden, J.: Contact problems in elasticity: A study of variational inequalities and finite element methods. SIAM Studies in Applied Mathematics. SIAM, Society for Industrial and Applied Mathematics, Philadelphia (1988)
38. Kleemann, H.: Adaptive FEM für Mehrkörperkontaktprobleme. Ph.D. thesis, Technische Universität Dortmund (2011)
39. Kornhuber, R., Krause, R.: Adaptive multigrid methods for Signorini's problem in linear elasticity. Comput. Vis. Sci. **4**(1), 9–20 (2001)
40. Krause, R., Veeser, A., Walloth, M.: An efficient and reliable residual-type a posteriori error estimator for the Signorini problem. Numer. Math. **130**, 151–197 (2015)
41. Mirabella, L., Nobile, F., Veneziani, A.: An a posteriori error estimator for model adaptivity in electrocardiology. Comp. Methods Appl. Mech. Eng. **200**, 2727–2737 (2011)
42. Nochetto, R., Siebert, K., Veeser, A.: Pointwise a posteriori error control for elliptic obstacle problems. Numer. Math. **95**, 163–195 (2003)
43. Oden, J.T., Vemaganti, K.: Estimation of local modeling error and goal-oriented modeling of heterogeneous materials; Part I: Error estimates and adaptive algorithms. J. Comput. Phys. **164**, 22–47 (2000)
44. Oden, J.T., Vemaganti, K.: Estimation of local modeling error and goal-oriented modeling of heterogeneous materials; Part II: A computational environment for adaptive modeling of heterogeneous elastic solids. Comput. Methods Appl. Mech. Eng. **190**, 3–25 (2001)
45. Paraschivoiu, M., Peraire, J., Patera, A.T.: A posteriori finite element bounds for linear-functional outputs of elliptic partial differential equations. Comput. Methods Appl. Mech. Eng. **150**(1–4), 289–312 (1997)
46. Prudhomme, S., Oden, J.: On goal-oriented error estimation for elliptic problems: application to the control of pointwise errors. Comput. Methods Appl. Mech. Eng. **176**(1–4), 313–331 (1999)
47. Rademacher, A.: NCP function-based dual weighted residual error estimators for Signorini's problem. SIAM J. Sci. Comput. **38**, A1743–A1769 (2016)
48. Rademacher, A., Schröder, A.: Dual weighted residual error control for frictional contact problems. Comput. Methods Appl. Math. **15**, 391–413 (2015)
49. Richter, T., Wick, T.: Variational localizations of the dual-weighted residual estimator. J. Comput. Appl. Math. **279**, 192–208 (2015)
50. Schmaltz, S., Landkammer, P., Beyer, F., Kumor, D., Rademacher, A., Blum, H., Steinmann, P., Willner, K.: Vorstellung eines simulationsbenchmarks für die blechmassivumformung. In: M. Merklein, B.A. Behrens, A.E. Tekkaya (eds.) 2. Workshop Blechmassivumformung, pp. 53–68. Meisenbach, Bamberg (2013)
51. Schröder, A.: Error control in h- and hp-adaptive FEM for Signorini's Problem. J. Numer. Math. **17**(4), 299–318 (2009)
52. Schröder, A., Blum, H., Rademacher, A., Kleemann, H.: Mixed FEM of higher order for contact Problems with friction. Int. J. Numer. Anal. Model. **8**(2), 302–323 (2011)
53. Schröder, A., Rademacher, A.: Goal-oriented error control in adaptive mixed FEM for Signorini's Problem. Comput. Methods Appl. Mech. Eng. **200**(1–4), 345–355 (2011)
54. Shaw, M.C.: The role of friction in deformation processing. Wear **6**, 140–158 (1963)

55. Siebert, K., Veeser, A.: A unilaterally constrained quadratic minimization with adaptive finite elements. SIAM J. Optim. **18**, 260–289 (2007)
56. Stein, E., Ohnimus, S.: Anisotropic discretization- and model-error estimation in solid mechanics by local neumann problems. Comput. Methods Appl. Mech. Eng. **176**, 363–385 (1999)
57. Stein, E., Rüter, M., Ohnimus, S.: Implicit upper bound error estimates for combined expansive model and discretization adaptivity. Comput. Methods Appl. Mech. Eng. **200**, 2626–2638 (2011)
58. Suttmeier, F.: Numerical Solution of Variational Inequalities by Adaptive Finite Elements. Advances in Numerical Mathematics. Vieweg-Teubner, Wiesbaden (2008)
59. Veeser, A.: Efficient and reliable a posteriori error estimators for elliptic obstacle problems. SIAM J. Numer. Anal. **39**, 146–167 (2001)
60. Walloth, M.: Adaptive numerical simulation of contact problems: Resolving local effects at the contact boundary in space and time. Ph.D. thesis, Rheinischen Friedrich-Wilhelms-Universität Bonn (2012)
61. Weiss, A., Wohlmuth, B.I.: A posteriori error estimator and error control for contact problems. Math. Comp. **78**(267), 1237–1267 (2009)
62. Wohlmuth, B.I.: An a posteriori error estimator for two-body contact problems on non-matching meshes. J. Sci. Comput. **33**(1), 25–45 (2007)
63. Wohlmuth, B.I.: Variationally consistent discretization schemes and numerical algorithms for contact problems. Acta Numerica **20**, 569–734 (2011)
64. Wohlmuth, B.I., Krause, R.H.: Monotone multigrid methods on nonmatching grids for nonlinear multibody contact problems. SIAM J. Sci. Comput. **25**(1), 324–347 (2003)
65. Wriggers, P.: Computational Contact Mechanics. Wiley, Chichester (2002)
66. Wriggers, P.: Nonlinear Finite Element Methods. Springer, Berlin Heidelberg (2008)